Sensor and Simulation Notes

Note 200

June 1974

Performance of an Admittance Sheet Plus Coplanar Flanges as a Matched Termination of a Two-Dimensional Parallel-Plate Transmission Line II. Sloped Admittance Sheet

by

A. D. Varvatsis and M. I. Sancer[*]
Tetra Tech, Inc.
Pasadena, California

Abstract

The reflections of a monochromatic TEM wave or a TEM step-pulse from a sloped RL admittance sheet terminating the transmission line are calculated. To minimize these reflections and thus obtain an optimum matching we use the value for R obtained elsewhere and determine L by a parametric study for a number of inclination angles. The effect of sloping the termination in the presence of flanges is examined and their contribution to the time-history of the reflected fields is evaluated.

Sensor and Simulation Notes

Note 200

June 1974

Performance of an Admittance Sheet Plus Coplanar Flanges as a Matched
Termination of a Two-Dimensional Parallel-Plate Transmission Line
II. Sloped Admittance Sheet

by

A. D. Varvatsis and M. I. Sancer[*]
Tetra Tech, Inc.
Pasadena, California

Abstract

The reflections of a monochromatic TEM wave or a TEM step-
pulse from a sloped RL admittance sheet terminating the transmission
line are calculated. To minimize these reflections and thus obtain an
optimum matching we use the value for R obtained elsewhere and deter-
mine L by a parametric study for a number of inclination angles. The
effect of sloping the termination in the presence of flanges is examined
and their contribution to the time-history of the reflected fields is
evaluated.

I.   Introduction

This note is a continuation of SSN 163 [1] in which the termination plane
was perpendicular to the axis of the two-dimensional parallel-plate trans-
mission line. In the present note the termination admittance is a sloped
distributed RL sheet and the R, L parameters should be chosen such that
the reflections of an incident TEM monochromatic wave or a TEM step-
pulse are a minimum. The value of the resistance R has been found to
be equal to $Z_o \sin \xi$ [2] where Z_o is the free space characteristic im-
pedance (377Ω) and ξ the inclination angle. The inductance L will be
determined by a parametric study as it was done in ref. 1.

A sloped termination allows multiple reflections off the admittance sheet
(for $\xi < 60^o$) (Figs. 4, 5 and 6) and consequently the total field reflected
back into the region between the parallel plates could be decreased by
making the inclination angle ξ smaller than 60° (see section V for a dis-
cussion). The smallest inclination angle we considered in this note was
30°. This angle is sufficiently small to allow for the effect of multiple
reflections, but not too small to require excessive computer time. Our
method of calculating reflections requires the knowledge of a sufficient
number of field aperture expansion coefficients and this number increases
rapidly with decreasing ξ due to resonances (see section III).

To facilitate the mathematical formulation and numerical calculations,
infinitely conducting flanges coplanar to the admittance sheet were con-
sidered (Fig. 1). In actuality, the termination for the transmission line
in the ATLAS design does not include flanges, and one should be careful
in interpreting the numerical results in order to separate the effect of
the flanges. In section V we explore this matter and also the effect of
sloping the termination. We find that in the presence of flanges the ini-
tial reflection (before multiple reflections occur) increases with decreasing
ξ and is fairly insensitive to the choice of L (for $\xi > 45^o$) which are
unwanted features. We speculate that in the absence of flanges the initial
reflection is sensitive to the choice of L and it can be reduced by selecting

an appropriate value for L and also by sloping the termination plane. It is also found that for the same values of parameters L and ξ the presence of flanges versus absence inhibits initial reflections. In the same section V we determine the optimum L, in the presence of flanges, for each angle ξ considered in this note (75°, 60^{0}, 45°, 30°), and we speculate about the corresponding values for L in the absence of flanges and also about the magnitude of the reflection coefficients for the TEM mode.

In section II we formulate and solve the problem by expressing the reflection coefficients of the TEM and TM modes (in the region between the parallel plates where they can be defined) in terms of suitable aperture expansion coefficients. The fields within the triangular region (Fig. 3) are also investigated and the "reflection" coefficients of the in-homogeneous TEM and TM modes in this region are given in terms of integrals of the aperture fields. In section III the method for obtaining the numerical results (and the importance of the resonances in the calculation of the reflection coefficients) is discussed, and in section IV a detailed description of the plots of the reflected fields in both the frequency and time domain with the inductance L as a parameter are presented.

II. Formulation and Solution

We start by recalling two integral relationships derived in SSN 163 [Ref. 1].

$$\int_2^1 \left(\frac{\partial G_I}{\partial n} H_{Iy} + i\omega \epsilon_o G_I E_s \right) ds_1 = H_{Iy} - H_o \qquad (1)$$

$$-\int_2^1 i\omega \epsilon_o G_{II} E_s \, ds_1 = H_{IIy} \qquad (2)$$

The geometry is depicted in Fig. 1 , E_s is the aperture electric field, H_{Iy}, H_{IIy} are the total magnetic fields in regions I and II, H_o is the incident TEM magnetic field, and G_I, G_{II} are Green's functions defined as follows

$$\left(\frac{\partial^2}{\partial x^2} + \frac{\partial^2}{\partial y^2} \right) G_I = \delta(x - x') \, \delta(z - z') \qquad (3)$$

$$\frac{\partial G_I}{\partial x} = 0 \quad \text{on the plates} \qquad (4)$$

$$\left(\frac{\partial^2}{\partial x^2} + \frac{\partial^2}{\partial y^2} \right) G_{II} = \delta(x - x') \, \delta(z - z') \qquad (5)$$

$$\frac{\partial G_{II}}{\partial n} = \text{on the termination plane .} \qquad (6)$$

The form of G_I we subsequently use refers to a Green's function satisfying Eqs. 3 and 4 throughout the infinite domain within two parallel plates. Its application, however, is restricted within region I (Fig. 1). This is valid, because Green's second identity, the application of which led to Eq. 1, does not impose any restrictions on the form of the functions outside the domain of integration.

4

Referring to Fig. 2 , Eqs. 1 and 2 can be rewritten as follows

$$
H_I(x_1, z_1) - H_o = \int_{-h_1/2}^{h_1/2} \left\{ \left[\frac{\partial}{\partial z_1'} G_I(x_1, z_1; x_1', z_1') \Big|_{z_1' = 0} \right] H_I(x_1', z_1' = 0) \right.
$$

$$
\left. - i\omega \epsilon_o G_I(x_1, z_1; x_1', z_1' = 0) \, E(x_1', z_1' = 0) \right\} dx_1' \tag{7}
$$

$$
H_{II}(x_1, z_1) = \int_{-h_1/2}^{h_1/2} i\omega \epsilon_o E(x_1', z_1' = 0) \, G_{II}(x_1, z_1; x_1', z_1' = 0) \, dx_1' \tag{8}
$$

where $H_I = H_{Iy}$, $H_{II} = H_{IIy}$, $E = E_{x_1} = -E_s$, $h_1 = h/\sin \xi$,

primed variables are integration variables, and

$$
x_1 = x \sin \xi - z \cos \xi \tag{9}
$$

$$
z_1 = x \cos \xi + z \sin \xi \tag{10}
$$

$$
x = x_1 \sin \xi + z_1 \cos \xi \tag{11}
$$

$$
z = -x_1 \cos \xi + z_1 \sin \xi \tag{12}
$$

$$
x^* = x \tag{13}
$$

$$
z^* = z + (\tfrac{1}{2}) h \cot \xi \tag{14}
$$

In SSN 163 where ξ was equal to $\pi/2$, we calculated the reflected TEM and TM fields for the case of an incident TEM wave characterized by a wave number k_o and a TEM step pulse. In the present note the incident wave is again a TEM wave or a TEM step pulse, and we still want to calculate the reflected TEM and TM fields. These TEM and TM fields can only be defined in the region $z^* < 0$ (Fig. 3). The form of the fields within the triangular region will be examined later.

For $z^* < 0$ and assuming an incident TEM electric field $E_o = e^{ik_o z^*}$ we have

$$E_x = e^{ik_o z^*} + \Gamma_o e^{-ik_o z^*} + \sum_{n=1}^{\infty} \Gamma_n \cos \frac{2n\pi x}{h} e^{-i\gamma_n z^*} \tag{15}$$

$$H_y = (1/Z_o) e^{ik_o z^*} - (\Gamma_o/Z_o) e^{-ik_o z^*} - \sum_{n=1}^{\infty} (\Gamma_n/Z_n) \cos \frac{2n\pi x}{h} e^{-i\gamma_n z^*} \tag{16}$$

$$E_z = \sum_{n=1}^{\infty} i(2n\pi/\gamma_n h) \Gamma_n \sin (2n\pi x/h) e^{-i\gamma_n z^*} \tag{17}$$

where Γ_o and Γ_n's are coefficients to be determined, $Z_n = \gamma_n/\omega \epsilon_o$, and γ_n is defined by the relationship

$$\gamma_n^2 = k_o^2 - (2n\pi/h)^2$$

with $\quad \gamma_n = \left[k_o^2 - (2n\pi/h)^2 \right]^{\frac{1}{2}} \quad$ for $\quad k_o > 2n\pi/h, \quad$ and

$$\gamma_n = i \left[(2n\pi/h)^2 - k_o^2 \right]^{\frac{1}{2}} \quad \text{for} \quad k_o < 2n\pi/h$$

to ensure evanescent reflected waves. (For $a > 0$, $a^{\frac{1}{2}}$ is the positive square root.) Equation 7 is valid throughout region I, which includes the triangular region. For $z^* < 0$, Eq. 7 should reduce to Eq. 16. To prove this we must evaluate $[(\partial/\partial z_1') G_I]|_{z_1' = 0}$. G_I satisfying Eqs. 3 and 4 can be shown to have the form

$$G_I(x, z; x', z') = (1/2ihk_o) e^{ik_o |z - z'|} + \sum_{n=1}^{\infty} (1/i\gamma_n h) \cos (2n\pi x/h)$$
$$\cos (2n\pi x'/h) e^{i\gamma_n |z - z'|} \tag{18}$$

For points to the left of the $z^* = 0$ plane, i.e. in the region with $z < -(\frac{1}{2}) h \cot \xi$, we have $|z - z'| = z' - z$ since z', for points on the termination plane,

6

ranges from $(-\frac{1}{2})h \cot \xi$ to $(\frac{1}{2})h \cot \xi$. Thus Eq. 18 can be rewritten as

$$G_I(x, z; x', z') = (1/2ihk_o) e^{-ik_o z + ik_o z'}$$

$$+ \sum_{n=1}^{\infty} (1/i\gamma_n h) \cos (2n\pi x/h) \cos (2n\pi x'/h) e^{-i\gamma_n z + i\gamma_n z'} \qquad (19)$$

and

$$[\partial G_I / \partial z_1']_{z_1' = 0} = \left\{ (1/2ihk_o) e^{-ik_o z} (ik_o)(\partial z'/\partial z_1') e^{ik_o z'} \right.$$

$$+ \sum_{n=1}^{\infty} - (1/i\gamma_n h) \cos (2n\pi x/h)(2n\pi/h) \sin (2n\pi x'/h)(\partial x'/\partial z_1') e^{-i\gamma_n z + i\gamma_n z'}$$

$$\left. + \sum_{n=1}^{\infty} (1/i\gamma_n h) \cos (2n\pi x/h) \cos (2n\pi x'/h) e^{-i\gamma_n z + i\gamma_n z'} (i\gamma_n)(\partial z'/\partial z_1') \right\} z_1' = 0$$

or

$$[\partial G_I / \partial z_1']_{z_1' = 0} = \sin \xi \left\{ (1/2h) e^{-ik_o z - ik_o x_1' \cos \xi} \right.$$

$$\left. + \sum_{n=1}^{\infty} (1/h) \cos (2n\pi x/h) \cos (2n\pi x_1'/h_1) e^{-i\gamma_n z - i\gamma_n x_1' \cos \xi} \right\}$$

$$+ \sum_{n=1}^{\infty} (-2n\pi/\gamma_n h^2) \cos \xi \cos (2n\pi x/h) \sin (2n\pi x_1'/h_1) e^{-i\gamma_n z - i\gamma_n x_1' \cos \xi} \qquad (20)$$

If we insert Eq. 19, evaluated at $z_1' = 0$, and Eq. 20 into Eq. 7, we obtain,

$$H_I(x, z) - H_o = e^{-ik_o z} \left[(1/2h) \int_{-h_1/2}^{h_1/2} [\sin \xi \, H_I - (1/Z_o) E] e^{-ik_o x_1' \cos \xi} dx_1' \right]$$

$$+ \sum_{n=1}^{\infty} \cos (2n\pi x/h) e^{-i\gamma_n z} \left[(1/h) \int_{-h_1/2}^{h_1/2} [\sin \xi \, H_I - (1/Z_n) E] e^{-i\gamma_n x_1' \cos \xi} \right.$$

7

$$\cos(2n\pi x_1'/h_1)\,dx_1' - (2n\pi/\gamma_n h^2)\cos\xi \int\limits_{-h_1/2}^{h_1/2} H_I\, e^{-i\gamma_n x_1'\cos\xi}$$

$$\left.\sin(2n\pi x_1'/h_1)\,dx_1'\right] \tag{21}$$

If we use Eq. 14, Eq. 21 can be rewritten as

$$H_I(x^*, z^*) = (1/Z_o)\, e^{ik_o z^*} - (\Gamma/Z_o)\, e^{-ik_o z^*} - \sum_{n=1}^{\infty}(\Gamma_n/Z_n)\cos(2n\pi x^*/h)\, e^{-i\gamma_n z^*} \tag{22}$$

where

$$\Gamma = -e^{(i/2)k_o h\cot\xi}\left[(1/2h)\int\limits_{-h_1/2}^{h_1/2}(\sin\xi\, Z_o H_I - E)\, e^{-ik_o x_1'\cos\xi}\,dx_1'\right] \tag{21a}$$

$$\Gamma_n = -e^{(i/2)\gamma_n h\cot\xi}\left[(1/h)\int\limits_{-h_1/2}^{h_1/2}(\sin\xi\, Z_n H_I - E)\, e^{-i\gamma_n x_1'\cos\xi}\cos(2n\pi x_1'/n_1)\,dx_1'\right.$$

$$\left. + (-2n\pi/h^2\omega\epsilon_o)\cos\xi \int\limits_{-h_1/2}^{h_1/2} H_I\, e^{-i\gamma_n x_1'\cos\xi}\sin(2n\pi x_1'/h_1)\,dx_1'\right]\quad n = 1, 2, 3,\ldots \tag{22a}$$

Equations 21a and 22a provide explicit expressions for the reflection co-
efficients in terms of the aperture fields H_I, E. These fields will be cal-
culated shortly, following a brief discussion of the fields within the trian-
gular region (see Fig. 3).

To evaluate the magnetic field at a point P within the triangular region
we will employ Eq. 7. To calculate G_I and $\partial G_I/\partial z_1'$ at $z_1' = 0$ we use
Eq. 18 in the two regions of interest, $z > z'$ and $z < z'$. For $z < z'$,

$\partial G_I / \partial z_1'$ at $z_1' = 0$ is given by Eq. 20. For $z > z'$ it is straightforward to obtain the result

$$[\partial G_I / \partial z_1']_{z_1' = 0} = - \sin \xi \left\{ (1/2h) e^{ik_o z + ik_o x_1' \cos \xi} \right.$$

$$+ \sum_{n=1}^{\infty} (1/h) \cos (2n\pi x/h) \cos (2n\pi x_1'/h_1) e^{i\gamma_n z + i\gamma_n x_1' \cos \xi}$$

$$+ \sum_{n=1}^{\infty} (-2n\pi / \gamma_n h^2) \cot \xi \cos (2n\pi x/h) \sin (2n\pi x_1'/h_1) e^{i\gamma_n z + i\gamma_n x_1' \cos \xi} \left. \right\} \quad (23)$$

We can now evaluate the magnetic field at P with the aid of Eq. 7:

$$H_I = H_o + \int_{-h_1/2}^{(-z/\cos \xi)} \left(H_I \frac{\partial G_I}{\partial z_1'} - i\omega \epsilon_o G_I E \right) dx_1'$$

$$+ \int_{(-z/\cos \xi)}^{h_1/2} \left(H_I \frac{\partial G_I}{\partial z_1'} - i\omega \epsilon_o G_I E \right) dx_1' \quad (24)$$

The range of integration for the first integral corresponds to $z' > z$ whereas the second integral corresponds to $z' < z$. If we use the appropriate expressions for the Green's function and its derivative, Eq. 24 yields,

$$H_I(P) = (1/Z_o) e^{ik_o z^*} + H_1 + H_2 \quad (25)$$

where

$$H_1 = - [\Gamma(z)/Z_o] e^{-ik_o z^*} - \sum_{n=1}^{\infty} [\Gamma_n(z)/Z_n] \cos (2n\pi x^*/h) e^{-i\gamma_n z^*} \quad (26)$$

$$H_2 = [\Gamma^\dagger(z)/Z_o] e^{ik_o z^*} + \sum_{n=1}^{\infty} [\Gamma_n^\dagger(z)/Z_n] \cos (2n\pi x^*/h) e^{i\gamma_n z^*} \quad (27)$$

9

and

$$\Gamma(z) = -e^{(i/2)k_o h \cot \xi} \left[(1/2h) \int_{-h_1/2}^{(-z/\cos\xi)} (\sin\xi\, Z_o H_I - E)\, e^{-ik_o x_1' \cos\xi}\, dx_1' \right] \qquad (28)$$

$$\Gamma_n(z) = -e^{(i/2)\gamma_n h \cot\xi} \left[(1/h) \int_{-h_1/2}^{(-z/\cos\xi)} (\sin\xi\, Z_n H_I - E)\, e^{-i\gamma_n x_1' \cos\xi} \cos(2n\pi x_1'/h_1)\, dx_1' \right.$$

$$\left. + (-2n\pi/h^2 \omega\epsilon_o)\cot\xi \int_{-h_1/2}^{(-z/\cos\xi)} H_I\, e^{-i\gamma_n x_1' \cos\xi} \sin(2n\pi x_1'/h_1)\, dx_1' \right], \quad n \geq 1 \qquad (29)$$

$$\Gamma^{\dagger}(z) = -e^{(-i/2)k_o h \cot\xi} \left[(1/2h) \int_{(-z/\cos\xi)}^{h_1/2} (\sin\xi\, Z_o H_I - E)\, e^{i\gamma_n x_1' \cos\xi}\, dx_1' \right] \qquad (30)$$

$$\Gamma_n^{\dagger}(z) = -e^{(-i/2)\gamma_n h \cot\xi} \left[(1/h) \int_{(-z/\cos\xi)}^{h_1/2} (\sin\xi\, Z_n H_I - E)\, e^{i\gamma_n x_1' \cos\xi} \cos(2n\pi x_1'/h_1)\, dx_1' \right.$$

$$\left. + (-2n\pi/h^2 \omega\epsilon_o)\cot\xi \int_{(-z/\cos\xi)}^{h_1/2} H_I\, e^{i\gamma_n x_1' \cos\xi} \sin(2n\pi x_1'/h_1)\, dx_1' \right], \quad n \geq 1 \qquad (31)$$

Thus at any point within the triangular region we have TEM and TM modes travelling in both directions with "reflection" coefficients that are functions of position. We can call these modes inhomogeneous TEM and TM modes. Notice that at $z = -(\frac{1}{2}) h \cot\xi$, i.e. $z^* = 0$

10

$$\Gamma(z = -\tfrac{1}{2}h \cot \xi) = \Gamma, \qquad \Gamma_n(z = -\tfrac{1}{2}h \cot \xi) = \Gamma_n \qquad (32)$$

and

$$\Gamma^\dagger(z = -\tfrac{1}{2}h \cot \xi) = 0, \qquad \Gamma_n^\dagger(z = -\tfrac{1}{2}h \cot \xi) = 0 \qquad (33)$$

where Γ, Γ_n are given by Eqs. 21a and 22b respectively.

Equations 33 ensure that there is nothing peculiar about "reflected" TEM and TM modes travelling in the positive z direction within the triangular region.

Next we proceed to derive two coupled integral equations, for the aperture fields H_I and E, the solution of which will allow us to evaluate the reflection coefficients given by Eqs. 21a and 22a.

First, we use integral relationships 7 and 8 and allow the observation point (x_1, z_1) to approach the termination plane. Because of the presence of the derivative of G_I in Eq. 7, the integral is equal to $\tfrac{1}{2}H_I(x_1, z_1)$ plus the same integral evaluated in the principal value sense. Equation 8, however, remains unchanged in form.

$$H_I(x_1, z_1 = 0) = 2H_o(x_1, z_1 = 0) + 2\fint_{-h_1/2}^{h_1/2} \left(H_I \frac{\partial G_I}{\partial z_1'} - i\omega \epsilon_o E G_I \right) dx_1' \qquad (34)$$

$$H_{II}(x_1, z_1 = 0) = \int_{-h_1/2}^{h_1/2} i\omega \epsilon_o E G_{II} \, dx_1' \qquad (35)$$

Next we invoke the boundary condition across the admittance sheet $(z_1 = 0)$,

$$Z(-\hat{z}_1 \times \underline{H}_I + \hat{z}_1 \times \underline{H}_{II}) = E \, \hat{x}_1$$

11

or
$$Z(H_I - H_{II}) = E \tag{36}$$

Using Eq. 35 we can substitute H_{II} in Eq. 36 to obtain

$$E = ZH_I - i\omega\epsilon_o Z \int_{-h_1/2}^{h_1/2} EG_{II} \, dx_1' \tag{37}$$

Equations 34 and 37 are two coupled integral equations the solution of which will determine H_I and E.

For $\xi = \pi/2$, there is a simple relationship between the aperture fields, i.e. Eqs. 15 and 16 evaluated at $z^* = 0$. Thus

$$E = 1 + \Gamma + \sum_{n=1}^{\infty} \Gamma_n \cos(2n\pi x/h) \tag{38}$$

$$\left. \vphantom{\sum} \right\} \quad \xi = \pi/2$$

$$H_I = (1/Z_o)(1 - \Gamma) - \sum_{n=1}^{\infty} (\Gamma_n/Z_n) \cos(2n\pi x/h) \tag{39}$$

Combining Eq. 37 with Eqs. 38 and 39 allows us to calculate the expansion coefficients for the aperture electric field as it was done in SSN 163 [Ref. 1]. For $\xi = \pi/2$, these expansion coefficients coincide with the reflection coefficients.

For $\xi < \pi/2$, however, no simple relationship exists between the expansion coefficients of the aperture fields. The relationship we will use is integral equation 34. We write the aperture fields in terms of sine and cosine expansions.

$$E(x_1, 0) = \sum_{m=0}^{\infty} C_m \cos(2m\pi x_1/h_1) + \sum_{m=0}^{\infty} C_m' \sin(2m\pi x_1/h_1) \tag{40}$$

$$Z_o H_I(x_1, 0) = \sum_{m=0}^{\infty} D_m \cos(2m\pi x_1/h_1) + \sum_{m=0}^{\infty} D_m' \sin(2m\pi x_1/h_1) \tag{41}$$

12

where $\qquad\qquad C_0' = D_0' = 0.$

Before we use Eqs. 40 and 41 in Eq. 34 we evaluate $\partial G_I / \partial z_1'$ (at $z_1' = 0$, $z_1 = 0$) first. For this purpose, we rewrite Eq. 18 as

$$G_I(x_1, z_1; x_1', z_1') = (1/2ik_0 h)\, e^{ik_0 \left| (x_1' - x_1) \cos \xi + (z_1 - z_1') \sin \xi \right|}$$

$$+ \sum_{n=1}^{\infty} (1/i\gamma_n h) \cos \frac{2n\pi}{h} (x_1 \sin \xi + z_1 \cos \xi) \cos \frac{2n\pi}{h} (x_1' \sin \xi + z_1' \cos \xi)$$
$$e^{i\gamma_n \left| (x_1' - x_1) \cos \xi + (z_1 - z_1') \sin \xi \right|} \qquad (42)$$

If we use the relationship

$$\left[\frac{\partial}{\partial x} |a - bx| \right]_{x=0} = - \frac{a}{|a|} b, \qquad a \neq 0 \quad (\xi < \pi/2) \qquad (43)$$

we obtain from Eq. 42

$$\frac{\partial}{\partial z_1'} G(x_1, z_1; x_1', z_1') \Big|_{z_1 = z_1' = 0} = - \frac{\sin \xi}{2h} \frac{x_1' - x_1}{|x_1' - x_1|} e^{ik_0 |x_1' - x_1| \cos \xi}$$

$$- \sum_{n=1}^{\infty} \frac{\sin \xi}{h} \frac{x_1' - x_1}{|x_1' - x_1|} \cos \frac{2n\pi x_1}{h_1} \cos \frac{2n\pi x_1'}{h_1} e^{i\gamma_n |x_1' - x_1| \cos \xi}$$

$$- \sum_{n=1}^{\infty} \frac{2n\pi}{h^2} \frac{\cos \xi}{i\gamma_n} \cos \frac{2n\pi x_1}{h_1} \sin \frac{2n\pi x_1'}{h_1} e^{i\gamma_n |x_1' - x_1| \cos \xi} \qquad (44)$$

When $x_1'/h_1 = x_1/h_1 \pm \epsilon$, where ϵ is an arbitrarily small quantity, the third term in Eq. 44 can be shown to have an integrable singularity, whereas the first two terms, combined, exhibit a delta-function singularity. To see this we recall that

$$(\tfrac{1}{2}) \delta (x_1 - x_1') = \tfrac{1}{2}h_1 + \sum_{n=1}^{\infty} (1/h) \cos (2n\pi x_1/h_1) \cos (2n\pi x_1'/h_1) \qquad (45)$$

and we rewrite Eq. 44 as

13

$$\left[\frac{\partial G_I}{\partial z_1'}\right]_{z_1' = 0, \, z_1 = 0} = (x_1' - x_1)/|x_1' - x_1| \left\{ \sum_{n=1}^{\infty} (1/h_1) \cos (2n\pi x_1/h_1) \right.$$

$$\cos (2n\pi x_1'/h_1) \left[e^{i\gamma_n |x_1' - x_1| \cos \xi} - e^{ik_o |x_1' - x_1| \cos \xi} \right] + (\tfrac{1}{2}) \, \delta \, (x_1 - x_1')$$

$$e^{ik_o |x_1' - x_1|) \cos \xi} \left. \right\} - \sum_{n=1}^{\infty} (2n\pi \cos \xi /i\gamma_n h^2) \cos (2n\pi x_1/h_1) \sin (2n\pi x_1'/h_1)$$

$$e^{i\gamma_n |x_1' - x_1| \cos \xi} \tag{46}$$

As we mentioned earlier, the integral in Eq. 34 should be evaluated as a principal value integral about $x_1' = x_1$. Thus, the delta-function contributions are zero. However, because of the factor $(x_1' - x_1)/|x_1' - x_1|$ in front of Eq. 46, we must divide the integration range into $(-h_1/2, x_1)$ and $(x_1, h_1/2)$, and consequently the delta-function contributions cancel out even if we treat the integral in the ordinary sense. The representation of $\partial G/\partial z_1'$ given by Eq. 46 is also very convenient for accurate numerical calculations.

We are now in a position to use Eqs. 40 and 41 in Eqs. 34 and 37 in order to derive an infinite system of equations for the expansion coefficients C_m, C_m', D_m and D_m'. To that effect Eq. 37 can be rewritten as,

$$\sum_{m=0}^{\infty} \left[C_m \cos \frac{2m\pi x_1}{h_1} + C_m' \sin \frac{2m\pi x_1}{h_1} \right]$$

$$= (Z/Z_o) \sum_{m=0}^{\infty} \left[D_m \cos \frac{2m\pi x_1}{h_1} + D_m' \sin \frac{2m\pi x_1}{h_1} \right]$$

$$- \frac{\omega \epsilon_o Z}{2} \int_{-h_1/2}^{h_1/2} H_o^{(1)} (k_o |x_1' - x_1|) \sum_{\ell=0}^{\infty} \left[C_\ell \cos \frac{2\ell \pi x_1'}{h_1} + C_\ell' \sin \frac{2\ell \pi x_1'}{h_1} \right] dx_1' \tag{47}$$

14

where $G_{II}(x_1, 0; x_1', 0) = (-i/2)H_o^{(1)}(k_o|x_1' - x_1|)$ and $H^{(1)}(u)$ is the Hankel function of the first kind, and Eq. 34 as

$$(1/Z_o)\sum_{m=0}^{\infty}\left[D_m \cos\frac{2m\pi x_1}{h_1} + D_m' \text{ sm } \frac{2m\pi x_1}{h_1}\right] = (2/Z_o) e^{ik_o(\frac{1}{2}h\cot\xi - x_1\cos\xi)}$$

$$+ (2/Z_o)\int_{-h_1/2}^{x_1}\sum_{\ell=0}^{\infty}\left[D_\ell \cos\frac{2\ell\pi x_1'}{h_1} + D_\ell' \sin\frac{2\ell\pi x_1'}{h_1}\right]\left\{\sum_{n=1}^{\infty}\frac{1}{h_1}\cos\frac{2n\pi x_1}{h_1}\right.$$

$$\cos\frac{2n\pi x_1'}{h_1}\left[e^{i\gamma_n(x_1 - x_1')\cos\xi} - e^{ik_o(x_1 - x_1')\cos\xi}\right]$$

$$\left. -\sum_{n=1}^{\infty}\frac{2n\pi}{h^2}\frac{\cos\xi}{i\gamma_n}\cos\frac{2n\pi x_1'}{h_1}\sin\frac{2n\pi x_1'}{h_1}e^{i\gamma_n(x_1 - x_1')\cos\xi}\right\}dx_1'$$

$$- (2/Z_o)\int_{x_1}^{h_1/2}\sum_{\ell=0}^{\infty}\left[D_\ell \cos\frac{2\ell\pi x_1'}{h_1} + D_\ell' \sin\frac{2\ell\pi x_1'}{h_1}\right]\left\{\sum_{n=1}^{\infty}\frac{1}{h_1}\cos\frac{2n\pi x_1}{h_1}\right.$$

$$\cos\frac{2n\pi x_1'}{h_1}\left[e^{i\gamma_n(x_1' - x_1)\cos\xi} - e^{ik_o(x_1' - x_1)\cos\xi}\right]$$

$$\left. +\sum_{n=1}^{\infty}\frac{2n\pi}{h^2}\frac{\cos\xi}{i\gamma_n}\cos\frac{2n\pi x_1}{h_1}\sin\frac{2n\pi x_1'}{h_1}e^{i\gamma_n(x_1' - x_1)\cos\xi}\right\}dx_1'$$

$$-2i\omega\epsilon_o\int_{-h_1/2}^{x_1}\sum_{\ell=0}^{\infty}\left[C_\ell \cos\frac{2\ell\pi x_1'}{h_1} + C_\ell' \sin\frac{2\ell\pi x_1'}{h_1}\right]\left\{(1/2ik_o h) e^{ik_o(x_1 - x_1')\cos\xi}\right.$$

15

$$+\sum_{n=1}^{\infty} (1/i\gamma_n h) \cos \frac{2n\pi x_1}{h_1} \cos \frac{2n\pi x_1'}{h_1} e^{i\gamma_n(x_1 - x_1') \cos \xi} \Bigg\} dx_1'$$

$$-2i\omega \epsilon_o \int_{x_1}^{h_1/2} \sum_{\ell=0}^{\infty} \left[C_\ell \cos \frac{2\ell\pi x_1'}{h_1} + C_\ell' \sin \frac{2\ell\pi x_1'}{h_1} \right] \Bigg\{ (1/2ik_o h) e^{ik_o(x_1' - x_1) \cos \xi}$$

$$+\sum_{n=1}^{\infty} (1/i\gamma_n h) \cos \frac{2n\pi x_1}{h_1} \cos \frac{2n\pi x_1'}{h_1} e^{i\gamma_n(x_1' - x_1) \cos \xi} \Bigg\} dx_1' \tag{48}$$

Using the orthogonality properties of the trigonometric functions, Eq. 47 yields

$$2C_m - 2(Z/Z_o) D_m + \epsilon_m \sum_{\ell=0}^{\infty} K_{\ell m} C_\ell = 0 \tag{49}$$

$$C_m' - (Z/Z_o) D_m' + \sum_{\ell=0}^{\infty} R_{\ell m} C_\ell' = 0 \tag{50}$$

where $\epsilon_m = 1$ for $m = 0$, $\epsilon_m = 2$ for $m \neq 0$, and

$$K_{\ell m} = \frac{Zk_o h}{4Z_o \sin \xi} \int_{-1}^{1}\int_{-1}^{1} H_o^{(1)} \left[(k_o h/2)|u - u'|\right] \cos(m\pi u) \cos(\ell\pi u') \, du \, du' \tag{51}$$

$$R_{\ell m} = \frac{Zk_o h}{4Z_o \sin \xi} \int_{-1}^{1}\int_{-1}^{1} H_o^{(1)} \left[(k_o h/2)|u - u'|\right] \sin(m\pi u) \sin(\ell\pi u') \, du \, du' \tag{52}$$

A simple transformation can reduce the double integrals into single ones. The details can be found in Appendix III of SSN 163 [Ref. 1].

If we call $Zk_o h/4Z_o \sin \xi = \alpha$ we have the following results

16

$$K_{\ell m} = \frac{\alpha}{\pi} \int_0^2 dy\, H_o^{(1)}(k_o h\, y/2\, \sin\xi)\, (-1)^{\ell+m+1} \left[\frac{\sin \ell\pi y + \sin m\pi y}{\ell + m}\right.$$

$$\left. + \frac{\sin \ell\pi y - \sin m\pi y}{\ell - m}\right] \qquad \ell \neq m \tag{53}$$

$$K_{mm} = -\alpha \int_0^2 dy\, H_o^{(1)}(k_o h\, y/2\, \sin\xi) \left[\frac{1}{\pi\ell}\sin \ell\pi y + (y-2)\cos \ell\pi y\right] \quad m \neq 0 \tag{54}$$

$$K_{oo} = -2\alpha \int_0^2 dy\, (2-y)\, H_o^{(1)}(k_o h\, y/2\, \sin\xi) \tag{55}$$

$$R_{\ell m} = \frac{\alpha}{\pi} \int_0^2 dy\, H_o^{(1)}(k_o h\, y/2\, \sin\xi)\, (-1)^{\ell+m} \left[\frac{\sin \ell\pi y + \sin m\pi y}{\ell + m}\right.$$

$$\left. - \frac{\sin \ell\pi y - \sin m\pi y}{\ell - m}\right] \qquad \ell \neq m \tag{56}$$

$$R_{mm} = \alpha \int_0^2 dy\, H_o^{(1)}(ky/2\, \sin\xi) \left[\frac{1}{\ell\pi}\sin \ell\pi y - (y-2)\cos \ell\pi y\right] \qquad m \neq 0 \tag{57}$$

$$R_{\ell o} = R_{o\ell} = 0 \quad \text{for any } \ell \tag{58}$$

Applying the orthogonality properties of the trigonometric functions on Eq. 48 we obtain

$$(2/\epsilon_m)\, D_m + \sum_{\ell=0}^{\infty} (S_{1\ell m} D_\ell + S_{2\ell m} D_\ell' + S_{3\ell m} C_\ell + S_{4\ell m} C_\ell') = 2I_{cm} \tag{59}$$

$$D_m' + \sum_{\ell=0}^{\infty} (S_{5\ell m} D_\ell + S_{6\ell m} D_\ell' + S_{7\ell m} D_\ell + S_{8\ell m} C_\ell') = 2I_{sm} \tag{60}$$

where

$$S_{1\ell m} = -\sum_{n=1}^{\infty} \left\{ \left[I_2(\gamma_n) - I_2(k_o) - I_2'(\gamma_n) + I_2'(k_o)\right] - (2n\pi/ik_o h)\, p_n \cot\xi\, (I_9 + I_9') \right\}$$

17

$$S_{2\ell m} = -\sum_{n=1}^{\infty}\left\{\left[I_6(\gamma_n) - I_6(k_o) - I_6'(\gamma_n) + I_6'(k_o)\right] - (2n\pi/ik_o h)\, p_n \cot \xi\, (I_{11} + I_{11}')\right\}$$

$$S_{3\ell m} = (1/2\,\sin \xi)\left[I_1 + I_1' + \sum_{n=1}^{\infty} 2\,p_n\left[I_2(\gamma_n) + I_2'(\gamma_n)\right]\right]$$

$$S_{4\ell m} = (1/2\,\sin \xi)\left[I_5 + I_5' + \sum_{n=1}^{\infty} 2\,p_n\left[I_6(\gamma_n) + I_6'(\gamma_n)\right]\right]$$

$$S_{5\ell m} = -\sum_{n=1}^{\infty}\left\{\left[I_4(\gamma_n) - I_4(k_o) - I_4'(\gamma_n) + I_4'(k_o)\right] - (2n\pi/ik_o h)\, p_n \cot \xi\, (I_{10} + I_{10}')\right\}$$

$$S_{6\ell m} = -\sum_{n=1}^{\infty}\left\{\left[I_8(\gamma_n) - I_8(k_o) - I_8'(\gamma_n) + I_8'(k_o)\right] - (2n\pi/ik_o h)\, p_n \cot \xi\, (I_{12} + I_{12}')\right\}$$

$$S_{7\ell m} = (1/2\,\sin \xi)\left[I_3 + I_3' + \sum_{n=1}^{\infty} 2\,p_n\left[I_4(\gamma_n) + I_4'(\gamma_n)\right]\right]$$

$$S_{8\ell m} = (1/2\,\sin \xi)\left[I_7 + I_7' + \sum_{n=1}^{\infty} 2\,p_n\left[I_8(\gamma_n) + I_8'(\gamma_n)\right]\right]$$

$$I_{cm} = e^{(i/2)k_o h \cot \xi} \int_{-1}^{+1} e^{(-i/2)k_o hu \cot \xi}\, \cos m\pi u \, du$$

$$I_{sm} = e^{(i/2)k_o h \cot \xi} \int_{-1}^{+1} e^{(-i/2)k_o hu \cot \xi}\, \sin m\pi u \, du$$

where $p_n = k_o/\gamma_n$ and

$$I_1 = I_2(\alpha = k_o,\ n = 0) \qquad\qquad (61)$$

$$I_2(\alpha) = \int_{-1}^{+1} du \int_{-1}^{+1} e^{(i/2)\alpha h(u-u')\cot \xi}\, \cos(\ell\pi u')\cos(n\pi u)\cos(n\pi u')\cos(m\pi u)\, du' \qquad (62)$$

18

$$I'_1 = I'_2 \, (\alpha = k_o, \ n = 0) \tag{63}$$

$$I'_2(\alpha) = \int_{-1}^{+1} du \int_{u}^{1} e^{(-i/2)\alpha h(u-u')} \cot \xi \, \cos(\ell \pi u') \cos(n\pi u) \cos(n\pi u') \cos(m\pi u) \, du'$$

$$I_3 = I_4 \, (\alpha = k_o, \ n = 0) \tag{64}$$

$$I_4(\alpha) = \int_{-1}^{+1} du \int_{-1}^{u} e^{(-i/2)\alpha h(u-u')} \cot \xi \, \cos(\ell \pi u') \cos(n\pi u) \cos(n\pi u') \sin(m\pi u) \, du'$$

$$I'_3 = I'_4 \, (\alpha = k_o, \ n = 0) \tag{65}$$

$$I'_4(\alpha) = \int_{-1}^{+1} du \int_{u}^{1} e^{(-i/2)\alpha h(u-u')} \cot \xi \, \cos(\ell \pi u') \cos(n\pi u) \cos(n\pi u') \cos(m\pi u) \, du' \tag{66}$$

$$I_5 = I_6 \, (\alpha = k_o, \ n = 0) \tag{67}$$

$$I_6(\alpha) = \int_{-1}^{+1} du \int_{-1}^{u} e^{(i/2)\alpha h(u-u')} \cot \xi \, \sin(\ell \pi u') \cos(n\pi u) \cos(n\pi u') \cos(m\pi u) \, du' \tag{68}$$

$$I'_5 = I'_6 \, (\alpha = k_o, \ n = 0) \tag{69}$$

$$I'_6(\alpha) = \int_{-1}^{+1} du \int_{u}^{1} e^{(-i/2)\alpha h(u-u')} \cot \xi \, \sin(\ell \pi u') \cos(n\pi u) \cos(n\pi u') \cos(m\pi u) \, du' \tag{70}$$

$$I_7 = I_8 \, (\alpha = k_o, \ n = 0) \tag{71}$$

$$I_8(\alpha) = \int_{-1}^{+1} du \int_{-1}^{u} e^{(i/2)\alpha h(u-u')} \cot \xi \, \sin(\ell \pi u') \cos(n\pi u) \cos(n\pi u') \sin(m\pi u) \, du' \tag{72}$$

$$I'_7 = I'_8 \, (\alpha = k_o, \ n = 0) \tag{73}$$

$$I'_8(\alpha) = \int_{-1}^{+1} du \int_{u}^{1} e^{(-i/2)\alpha h(u-u')} \cot \xi \, \sin(\ell \pi u') \cos(n\pi u) \cos(n\pi u') \sin(m\pi u) \, du' \tag{74}$$

$$I_9 = \int_{-1}^{+1} du \int_{-1}^{u} e^{(i/2)\alpha h(u-u')} \cot \xi \, \cos(\ell \pi u') \cos(n\pi u) \sin(n\pi u') \cos(m\pi u) \, du' \tag{75}$$

19

$$I'_9 = \int_{-1}^{+1} du \int_u^1 e^{(-i/2)\alpha h(u-u')\cot\xi} \cos(\ell\pi u')\cos(n\pi u)\sin(n\pi u')\cos(m\pi u)\,du' \qquad (76)$$

$$I_{10} = \int_{-1}^{+1} du \int_{-1}^u e^{(i/2)\alpha h(u-u')\cot\xi} \cos(\ell\pi u')\cos(n\pi u)\sin(n\pi u')\sin(m\pi u)\,du' \qquad (77)$$

$$I'_{10} = \int_{-1}^{+1} du \int_u^1 e^{(-i/2)\alpha h(u-u')\cot\xi} \cos(\ell\pi u')\cos(n\pi u)\sin(n\pi u')\sin(m\pi u)\,du' \qquad (78)$$

$$I_{11} = \int_{-1}^{+1} du \int_{-1}^u e^{(i/2)\alpha h(u-u')\cot\xi} \sin(\ell\pi u')\cos(n\pi u)\sin(n\pi u')\cos(m\pi u)\,du' \qquad (79)$$

$$I'_{11} = \int_{-1}^{+1} du \int_u^1 e^{(-i/2)\alpha h(u-u')\cot\xi} \sin(\ell\pi u')\cos(n\pi u)\sin(n\pi u')\cos(m\pi u)\,du' \qquad (80)$$

$$I_{12} = \int_{-1}^{+1} du \int_{-1}^u e^{(i/2)\alpha h(u-u')\cot\xi} \sin(\ell\pi u')\cos(n\pi u)\sin(n\pi u')\sin(m\pi u)\,du' \qquad (81)$$

$$I'_{12} = \int_{-1}^{+1} du \int_u^1 e^{(-i/2)\alpha h(u-u')\cot\xi} \sin(\ell\pi u')\cos(n\pi u)\sin(n\pi u')\sin(m\pi u)\,du' \qquad (82)$$

It is easy to show that the following relationships are true,

$$I_2(\alpha) = I'_2(\alpha)$$

$$I_4(\alpha) + I'_4(\alpha) = 0$$

$$I_6(\alpha) + I'_6(\alpha) = 0$$

$$I_8(\alpha) = I'_8(\alpha)$$

$$I_9 + I'_9 = 0$$

$$I_{10} = I'_{10}$$

20

$$I_{11} = I'_{11}$$

$$I_{12} + I'_{12} = 0$$

Using the above relationships and also Eqs. 49, 50, 59 and 60 we arrive at the following infinite system of algebraic equations for the expansion coefficients.

$$2C_m - 2(Z/Z_o) D_m + \epsilon_m \sum_{\ell=0}^{\infty} K_{\ell m} C_\ell = 0 \tag{83}$$

$$C'_m - (Z/Z_o) D'_m + \sum_{\ell=0}^{\infty} R_{\ell m} C'_\ell = 0 \tag{84}$$

$$(2/\epsilon_m) D_m + \sum_{\ell=0}^{\infty} S_{2\ell m} D'_\ell + \sum_{\ell=0}^{\infty} S_{3\ell m} C_\ell = 2I_{cm} \tag{85}$$

$$D'_m + \sum_{\ell=0}^{\infty} S_{5\ell m} D_\ell + \sum_{\ell=0}^{\infty} S_{8\ell m} C'_\ell = 2I_{sm} \tag{86}$$

where $K_{\ell m}$, $R_{\ell m}$ are given by Eqs. 53 through 58 and

$$S_{2\ell m} = -2 \sum_{n=1}^{\infty} \left\{ [I_6(\gamma_n) - I_6(k_o)] - (2n\pi/ik_o h) \, p_n \cot \xi \, I_{11} \right\} \tag{87}$$

$$S_{3\ell m} = (1/\sin \xi) \left[I_1 + \sum_{n=1}^{\infty} 2p_n I_2(\gamma_n) \right] \tag{88}$$

$$S_{5\ell m} = -2 \sum_{n=1}^{\infty} \left\{ [I_4(\gamma_n) - I_4(k_o)] - (2n\pi/ik_o h) \, p_n \cot \xi \, I_{10} \right\} \tag{89}$$

$$S_{8\ell m} = (1/\sin \xi) \left[I_7 + \sum_{n=1}^{\infty} 2p_n I_8(\gamma_n) \right] \tag{90}$$

The integrals involved in the above expressions have already been defined (Eqs. 61 through 82) and can be calculated explicitly.

21

Z is the termination impedance and is given by

$$Z = R - i\omega L = Z_o \sin \xi - i\omega L \tag{90}$$

To conform with Ref.   we rewrite Eq. 91 as

$$Z = Z_o \sin \xi \left[1 - i (k_o h) \beta (\xi) \right] \tag{92}$$

where

$$\beta(\xi) = \frac{cL}{Z_o h \sin \xi} \tag{93}$$

Parameter $\beta(\xi)$ is thus a normalized inductance and a parametric study on β, for a given ξ, will determine the optimum L.

Once we solve the system of Eqs. 83 through 86, we are in a position to calculate the reflection coefficients of the electric field for the TEM and TM modes given by Eqs. 21a and 22a. For convenience we rewrite Eqs. 21a and 22a in terms of the expansion coefficients C's and D's.

$$\Gamma = - (1/4 \sin \xi) e^{ir_o/2} \sum_{m=0}^{\infty} \left[(-C_m + \sin \xi \, D_m) J_{10} + (-C'_m + \sin \xi \, D'_m) J_{20} \right] \tag{94}$$

$$\Gamma_n = - (1/2 \sin \xi) e^{ir_n/2} \sum_{m=0}^{\infty} \left\{ \left[-C_m + (\sin \xi /p_n) D_m \right] J_{1n} \right.$$

$$\left. + \left[-C'_m + (\sin \xi /p_n) D'_m \right] J_{2n} - (2n\pi \cos \xi /ik_o h) (D_m J_{3n} + D'_m J_{4n}) \right\} \tag{95}$$

where

$$J_{1n} = -2(A + B) (-1)^{m+n} r_n \sin(r_n/2) \tag{96}$$

$$J_{2n} = 4i \left[A (m + n) \pi + B (m - n) \pi \right] (-1)^{m+n} \sin(r_n/2) \tag{97}$$

$$J_{3n} = 4i \left[A (m + n) \pi - B (m - n) \pi \right] (-1)^{m+n} \sin(r_n/2) \tag{98}$$

22

$$J_{4n} = 2(A - B) (-1)^{m + n} r_n \sin (r_n/2) \tag{99}$$

$$A = \left[4(m + n)^2 \pi^2 - r_n^2\right]^{-1} \tag{100}$$

$$B = \left[4(m - n)^2 \pi^2 - r_n^2\right]^{-1} \tag{101}$$

$$r_n = (k_o h/p_n) \cot \xi \tag{102}$$

$$p_n = k_o/\gamma_n \tag{103}$$

One can easily show that as $\xi \to \pi/2$ the system of Eqs. 83 through 86 reduces to

$$2C_m - 2 (Z/Z_o) D_m + \epsilon_m \sum_{\ell=0}^{\infty} K_{\ell m} C_\ell = 0 \tag{104}$$

$$C_m' - (Z/Z_o) D_m' + \sum_{\ell=0}^{\infty} R_{\ell m} C_\ell' = 0 \tag{105}$$

$$(2/\epsilon_m) D_m + \sum_{\ell=0}^{\infty} S_{3\ell m} C_\ell = 4 \delta_{mo} \tag{106}$$

$$D_m' + \sum_{\ell=0}^{\infty} S_{8\ell m} C_\ell' = 0 \tag{107}$$

which shows that $C_m' = D_m' = 0$ for any m. Also $S_{3\ell m}$ reduces to

$$S_{300} = 2$$
$$S_{3\ell m} = p_m \delta_{\ell m}$$
$$S_{3\ell o} = 0 \qquad \ell \neq 0$$

and Eq. 106 gives

$$\left.\begin{array}{l} D_o + C_o = 2 \\ D_m + p_m C_m = 0 \quad m \neq 0 \end{array}\right\} \tag{108}$$

23

If we combine Eqs. 104 and 108 we arrive at a system of equations for the electric field expansion coefficients C_o, C_m's that is identical to Eqs. 36 of SSN 163. It is now easy to show that Eqs. 94 and 95 reduce to $\Gamma = C_o - 1$, $\Gamma_n = C_n$ as they should.

III. Numerical Results and Plots

The procedure to solve the system of equations (83) through (86) is essentially similar to the one employed in SSN 163 [Ref. 1] and has been explained there in sufficient detail. The present treatment only differs in that it involves more unknown coefficients and also the input terms I_{cm}, I_{sm} are functions at the wavenumber k_o, i.e.

$$I_{cm} = (-1)^m \left[\sin (r_o/2)\right] \left[4r_o/(r_o^2 - 4m^2\pi^2)\right] \tag{109}$$

$$I_{sm} = i(-1)^{m+1} \left[\sin (r_o/2)\right] \left[8m\pi/(r_o^2 - 4m^2\pi^2)\right] \tag{110}$$

where $r_o = k_o h \cot \xi$.

If we rewrite $\sin (r_o/2)$ as $(-1)^m \sin [(1/2)(r_o - 2m\pi)]$, it is easy to see that I_{cm} and iI_{sm} ($m > 0$) exhibit a maximum at $r = 2m\pi$ ($I_{co} = 2$, $I_{cm} = 1$ for $m > 0$, $iI_{sm} = 1$ for $m > 0$). Since our ultimate goal is the calculation of Γ and Γ_n's given by (94) and (95), we understand that for given ξ and $k_o h$ we should know enough aperture expansion coefficients to ensure the series convergence in (94) and (95). The number of required aperture coefficients depends on $k_o h$ (also on ξ) since this determines the integer m that maximizes the input terms. Thus for a given $k_o h$ we should have to progress well beyond the mth order expansion coefficients in order to obtain adequate convergence for the series in (94) and (95). From $k_o h \cot \xi = 2m\pi$ we see that the critical integer m increases with increasing $k_o h$ and decreasing ξ. In this note, as it was done in SSN 163, we calculate the reflected TEM and first four TM modes in both the frequency and time domain. The origin of time is the same for all ξ and corresponds to the instant at which the wavefront of the incident TEM step pulse passes through the $z^* = 0$ plane. This is the same as in SSN 163. Such a choice of the origin of time corresponds to an incident TEM wave with a phase factor $\exp [ik_o z^*]$, which was

25

actually the case in the previous section. The numerical procedure to
Fourier-invert reflection coefficients Γ and Γ_n's into the time domain
is identical to the one employed in SSN 163, and it will not be repeated
here.

IV. Description of the Plots

We have plotted the reflection coefficient of the x-component of the electric field for the TEM and first four TM modes (in the region $z^* < 0$) in both the frequency and time domains with the inclination angle ξ and the normalized inductance $\beta(\xi)$ as parameters. The plots in the frequency domain correspond to a monochromatic TEM incident wave with an electric field of unit amplitude $E_x = e^{-ik_o z^*}$, whereas the time plots correspond to an incident TEM step pulse of unit amplitude $E_x = u(t - z^*/c)$. The $t = 0$ instant marks the passage of the pulse wavefront through the $z^* = 0$ plane (Fig. 2).

Figures 8 through 27 are plots of the absolute values of the reflection coefficients for the TEM and TM modes versus $k_o h$ for four inclination angles $\xi = 70^\circ$, 60°, 45°, 30° with $\beta(\xi)$ as a parameter. For high frequencies the values of the reflection coefficients for various β often differed by a small amount only and have been drawn as having identical values. Figures 28 through 31 are time plots of the x-component of the reflected electric field for the TEM mode versus ct/h for $\xi = 75^\circ$, 60°, 45°, 30° with $\beta(\xi)$ as a parameter. The reflected TEM wave is not attenuated with distance and the plots are the same over any cross section $(z^* = <0$, Fig. 2), provided the appropriate shift in time is taken into account.

Figures 32 through 47 are time plots of the x-component of the reflected electric field for the first four TM modes versus ct/h with $\beta(\xi)$ as parameter. The time history is given over two cross sections, $z^*/h = 0$ and $z^*/h = -1$, to show the attenuation of the reflected TM modes with distance. Most of the attenuation occurs over a distance h and for $\left| z^* \right| > h$ the remaining pulse -- mainly containing the high frequency portion of the frequency spectrum -- suffers little change. (See Ref. 1, 1. 15 for a more detailed discussion.)

Finally, in Figs. 48 and 49 the values of the optimum β and L respectively are plotted versus the inclination angle, and the curves are tentatively extrapolated to include smaller values for ξ.

27

V. Discussion of Results

The reflection of TEM and TM modes into region I (Fig. 1) takes place in various stages. As the incident TEM step pulse arrives at the $z^*=0$ plane it is diffracted by the top edge 1 (Fig. 2). As a result, electromagnetic fields are generated, in both regions I and II, as well as currents on the admittance sheet. Subsequently the TEM pulse wavefront starts sweeping through the termination plane where it is specularly reflected - until the disturbance from the top edge arrives at the point under consideration. This time-delay is equal to $(\delta/c) \tan (\xi/2)$ (Fig. 7) and decreases with decreasing ξ, implying that the steady state is more quickly approached by sloping the admittance sheet. This, of course, ignores the effect of the bottom edge, but this effect gets diminished as ξ decreases. (For $\xi \to 0$ this effect is never felt.) As the TEM pulse arrives at the bottom edge 2 it is once more diffracted and at a time $(h/c) \tan (\xi/2)$ later the disturbance from the top edge also suffers diffraction.

Returning to the reflection of the incident TEM pulse at the termination plane we see that, depending on the magnitude of the inclination angle ξ, we have one or more reflections off the admittance sheet (where some transmission into region II occurs) and also off the bottom plate (where no transmission occurs). (Figs. 4, 5, and 6). Multiple reflections (within the triangular region, Fig. 3) are always possible for $\xi > 60°$. For $45° < \xi < 60°$ we can have up to two reflections off the termination plane (Fig. 4b), for $30° < \xi < 45°$ up to three (Fig. 4d) and for $22.5° < \xi < 30°$ up to four (Fig. 4f). In general, exactly n reflections (for all rays) can be shown to correspond to an inclination angle $\xi = 90/n$. (The number off the bottom plate is equal to n-1.) When n is even all rays follow parallel paths and reverse direction by bouncing off the bottom plate at right angles (Fig. 4c, 5a), whereas for n odd all rays follow parallel paths and reverse direction by bouncing off the admittance sheet (Fig. 4c, 5b). For a given $\xi(<60°)$ the number of reflections n satisfies the inequality $k-1 \leq n \leq k$ where k is the integer nearest but larger than $90/\xi$.

The calculation of the fields reflected into region I and to the left of the $z^* = 0$ plane (Fig. 2) requires the knowledge of the x-component of the total electric field E_x -- generated by the various mechanisms described above -- at any point on the $z^* = 0$ plane. If we expand $E_x(x^*, z^* = 0, t)$ into a series $\sum_{n=0}^{\infty} \Gamma_n(t) \cos(2n\pi x^*/h)$, the reflection coefficients $\Gamma_n(t)$ can easily be determined. The calculation of E_z and H_y is then completed with the aid of Eq. (16) and (17) by appropriate convolution integrals. (In this note we have calculated the reflection coefficients in the frequency domain first and obtained the time-history by Fourier inversion.) As ξ decreases the contributions to the aperture field $E_x(x^*, z^* = 0, t)$ from specular reflections and the lower edge occur at progressively later times. Thus by sloping the admittance sheet the early time history of the reflected fields mainly depends on the diffracting properties of the top edge and the currents induced on the admittance sheet due to the edge diffraction. From this we understand that the presence of the flanges may have an appreciable effect on the early time response and possibly the choice of the optimum inductance L. We will postpone examining this effect until we have discussed the plots pertinent to the problem considered in this note i. e. a termination with co-planar flanges.

First we direct our attention to the time history of the reflected TEM electric field E_{ox} for various inclination angles (Figs. 28 through 31). From these plots it appears that as ξ decreases the initial reflection increases and the optimum value for $\beta(\xi)$ (that minimizes the overall reflection) decreases. Thus we can make the following choices:

Table I

$\xi =$	90°	75°	60°	45°	30°
$\beta =$	1.10	1.10	1.05	.95	.80
$L/\mu_o h =$	1.10	1.06	.91	.67	.40

These numbers are in general agreement with the results in Ref. 2 where Baum studied the same problem but with a different approach. Baum con-

sidered inclination angles as small as $.9^{\circ}$, whereas our smallest angle is 30°. In Figs. 48 and 49 we have plotted β and L respectively versus ξ and tentatively extrapolated the curves to include smaller values for ξ. Thus for $\xi = 18^{\circ}$ our extrapolated value for β is .55 and Baum's average value is approximately the same except for late times. The discrepancy for late times may be due to the fact that Baum's treatment does not account for multiple reflections.

So far we have examined the time history of the reflected TEM electric field and selected the optimum values for the inductance L by minimizing the TEM reflections. If we examine the time histories of the reflected TM electric fields we find that, for a given ξ, smaller values for β correspond to smaller reflections. It is also true that the reflected TM modes decay with distance (Figs. 32 through 47). Only the part of the reflected pulse containing the high frequencies propagates without attenuation, but its amplitude becomes insignificant over a distance h. This decay is due to the fact that for a given mode n frequencies below ω_{on} ($\omega_{on} = 2n\pi c/h$) correspond to evanescent waves. (See Ref. 1, p. 15 for a more complete discussion.) Thus for pulse reflection the choice of L should be based on minimization of TEM reflection. If the incident TEM wave is monochromatic ($\omega = \omega_{o}$) the optimum value for L may be obtained with the aid of Figs. 8 through 27. Notice that if ω_{o} is well below cutoff for all TM modes ($\omega_{o} \ll 2\pi c/h$) the choice of L should be made on the basis of TEM reflection only, since the reflected TM modes decay rapidly with distance.

Next we examine the effect of the conducting flanges on the time response of the reflected fields in order to evaluate the merits of sloping the admittance sheet for the transmission line (no flanges) in the ATLAS design. The problem of terminating a two-parallel plate transmission line by a suitable RL admittance sheet without coplanar flanges has been examined in Ref. 3 for the special case $\xi = 90^{\circ}$. The approach in Ref. 3 is identical to the one employed in Ref. 2 and is based on the comparison of the current induced on a perfect termination, i. e. no reflection, to the current induced on an RL admittance sheet (still assuming no reflections) in order to choose the optimum L ($R = Z_{o} \sin \xi$ by the

30

usual low-frequency argument explained in Ref. 2). The disadvantage
of this method is that knowing an optimum value for L provides no in-
formation as to how good the RL termination really is. In this note our
analysis provides this information by allowing the calculation of the re-
flected fields but the inclusion of coplanar flanges may have an appreciable
effect on the values of the reflected fields and the choice of β. As we
mentioned earlier our values for β are in satisfactory agreement with
the ones obtained by Baum (Ref. 2) despite the fact that his approach was
different from ours. This observation makes us believe that the value
for the optimum β found in Ref. 3 for $\xi = 90^\circ$ is the correct one for the
case of no flanges. This value is approximately equal to .75. Our value
for $\xi = 90^\circ$ is 1.10 and consequently the true values for β as a function
of ξ may be smaller than the ones shown in Table I. To evaluate the
effect of the flanges further, we examine the fields diffracted by the top
edge 1. As ξ decreases the diffracted fields increase, especially in
the region about the termination line 12 (Fig. 1). Thus the increase of
the initial reflection of the TEM fields as ξ decreases (Figs. 28 through
31) depends on the changing diffracting properties of the top edge. This
implies that the initial small reflection for angles close to 90° may be
erroneous in the absence of flanges. From the plots we observe that for
β constant the rate of increase of the maximum initial reflection decreases
as ξ decreases, i.e. the $\xi = 30^\circ$ may be a good approximation for the
actual edge without flanges. It is also interesting to notice that as ξ de-
creases the first maximum becomes more sensitive to changes of β.
This implies that by sloping the admittance sheet one can reduce the in-
itial reflection considerably by choosing a suitable β. For later times
though the subsequent reflection increases with β and the optimum value
for β should minimize the overall reflection. From the above discussion
we understand that the value $\beta \approx .75$ found in Ref. 3 seems compatible
with the decreasing optimum values for β (for the case of coplanar flanges)
as ξ decreases and especially for the case $\xi = 30^\circ$ which simulates the
diffracting properties of the actual edge (for early times). Of course the
sloping of the admittance sheet has an effect, but its contribution cannot
be easily separated. We can also speculate that the initial high reflection

31

expected in the actual situation (no flanges) can be diminished by sloping the admittance sheet and choosing a suitable β.

In conclusion we believe that to minimize the reflections in the absence of flanges it is advisable to slope the admittance sheet. The actual values for β, i.e. in the absence of flanges, are smaller than the ones shown in Table I. For 90°, β should be approximately equal to .75 rather than 1.1. If we write β (without flanges) = $\lambda\beta$ (with flanges), then λ is a function of ξ and increases with decreasing ξ. For $\xi = 90^{\circ}$, $\lambda = .75/1.10 \approx .68$, whereas for $\xi = 30^{\circ}$, λ should be closer to unity, even though we do not know its exact value. The expected magnitude for the x-component of the TEM electric field for $\xi = 30^{\circ}$ should not exceed 5.5% E_o, where E_o is the incident electric field step pulse (Fig. 31, $\beta = .8$).
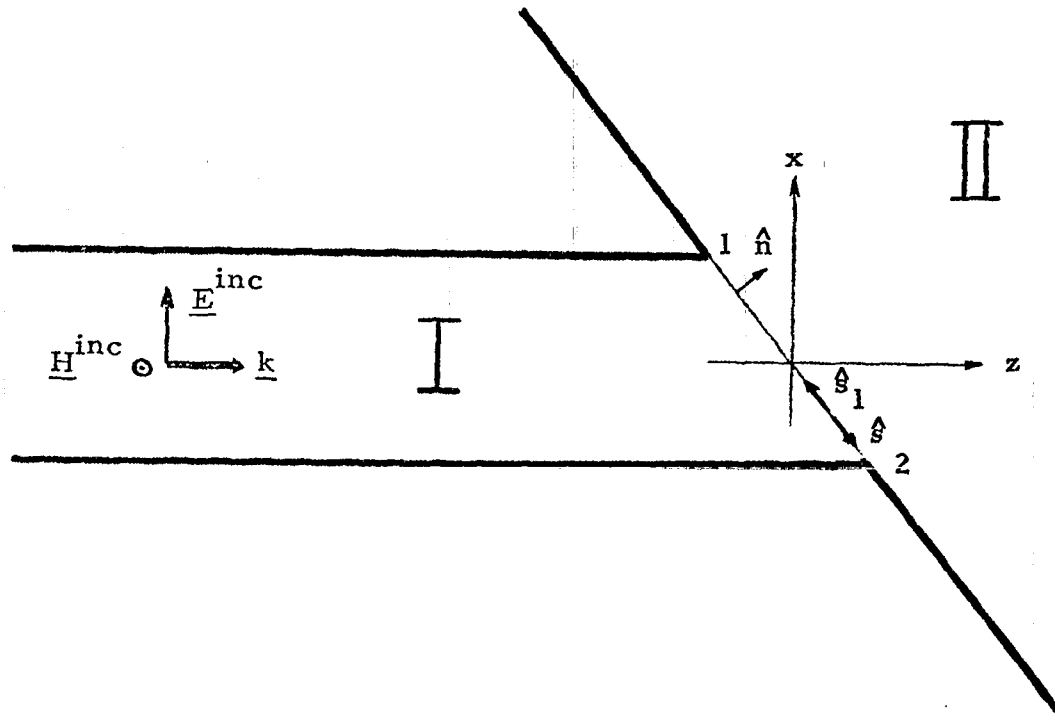
Figure 1: Geometry of the two-dimensional parallel-plate transmission line terminated by a sloped R, L admittance sheet with coplanar flanges.
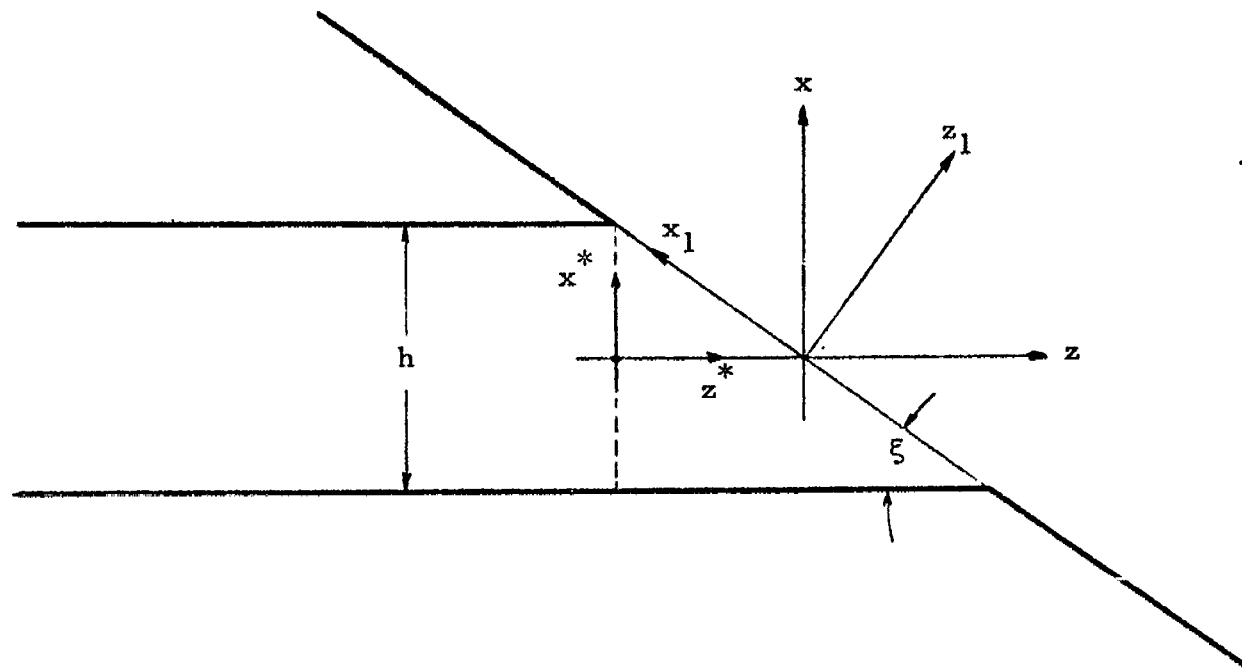
Figure 2: Coordinate systems appropriate in the derivation of integral relationships (7) and (8).
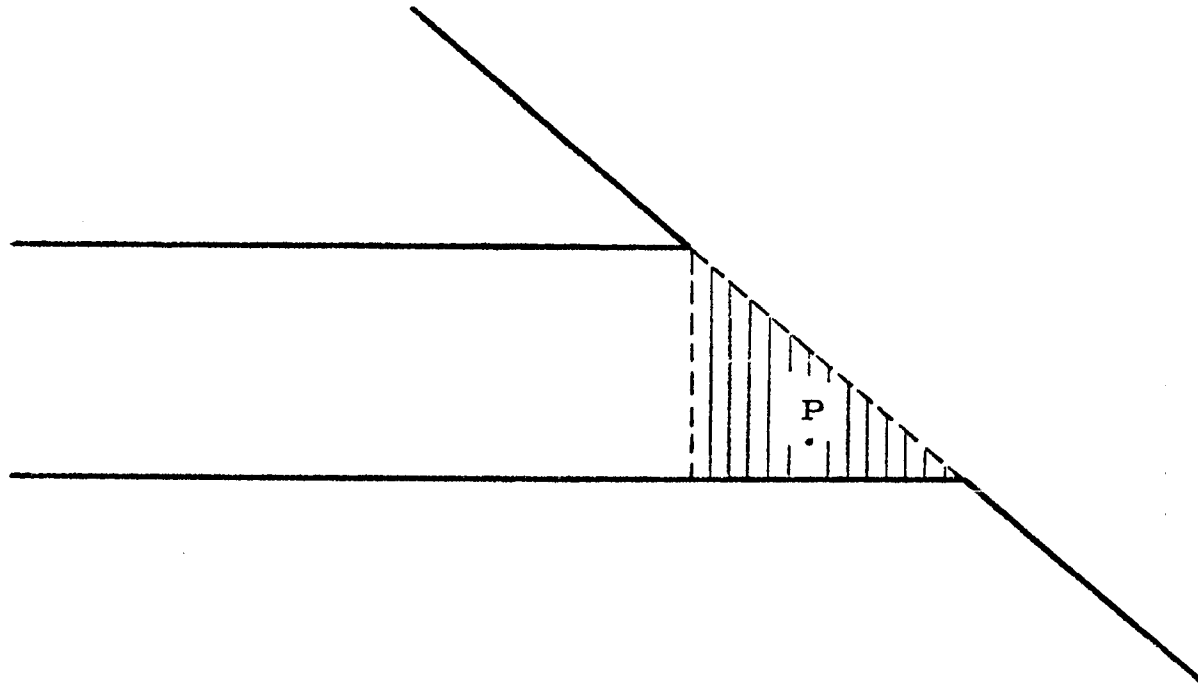
Figure 3: The shaded area is the triangular region where inhomogeneous TEM and TM modes exist.
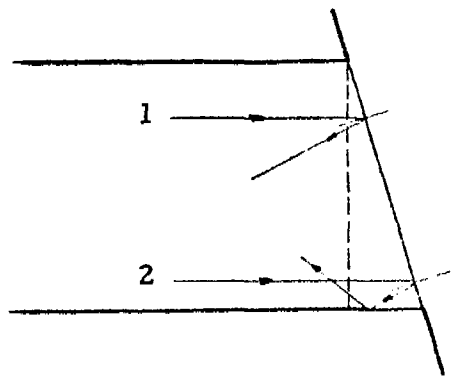
Figure 4a: For $\xi < 60°$ there is only one reflection off the admittance sheet.
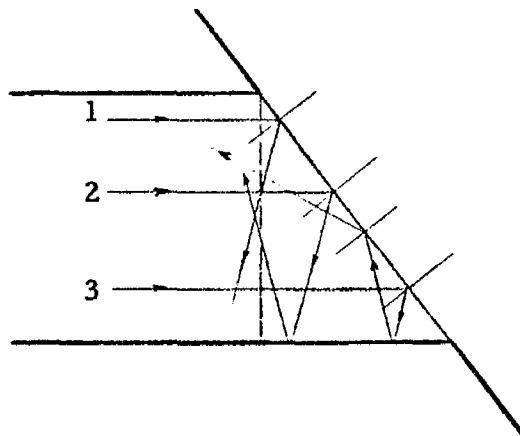
Figure 4b: For $45° < \xi < 60°$ there can be up to two reflections off the admittance sheet (ray 3).
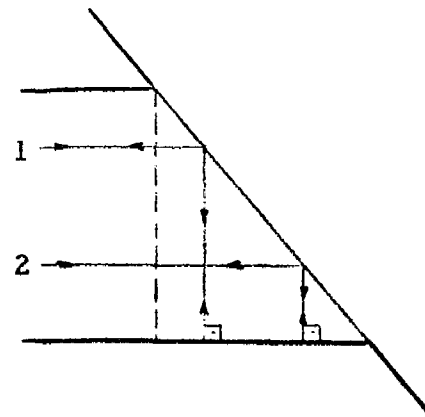
Figure 4c: For $\xi = 45°$ all rays are reflected twice off the admittance sheet.
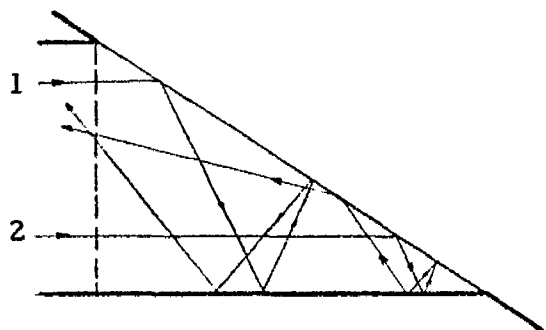
Figure 4d: For $30° < \xi < 45°$ there can be up to three reflections off the admittance sheet (ray 2).
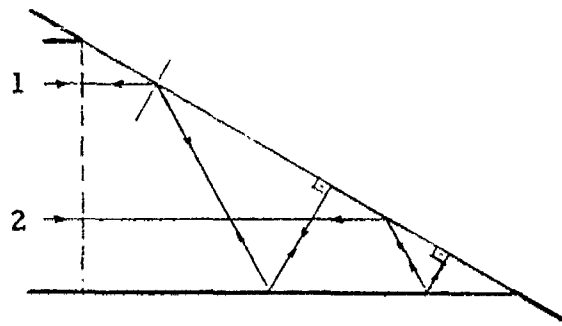
Figure 4e: For $\xi = 30°$ all rays are reflected three times off the admittance sheet.
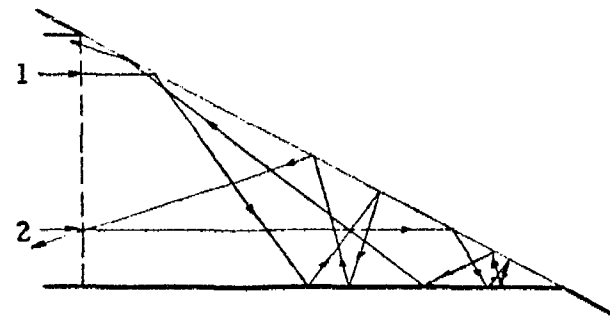
Figure 4f: For $22.5° < \xi < 30°$ there can be up to four reflections off the admittance sheet (ray 2).
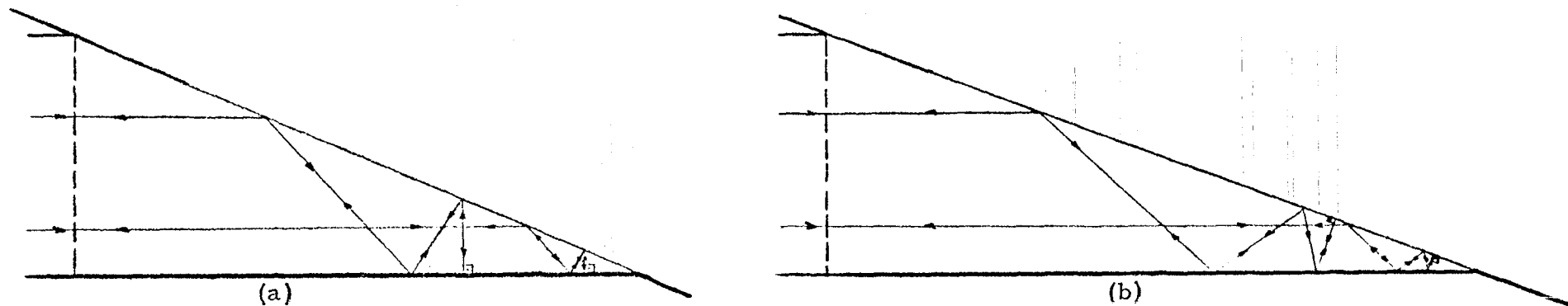
Figure 5: The number of reflections off the admittance sheet is exactly n (integer) when the inclination angle is $90^{\circ}/n$. For n even all rays follow parallel paths and reverse direction by bouncing off the bottom plate at right angles (Fig. 5a, n = 4). For n odd all rays follow parallel paths and reverse direction by bouncing off the admittance sheet at right angles (Fig. 5b, n = 5).
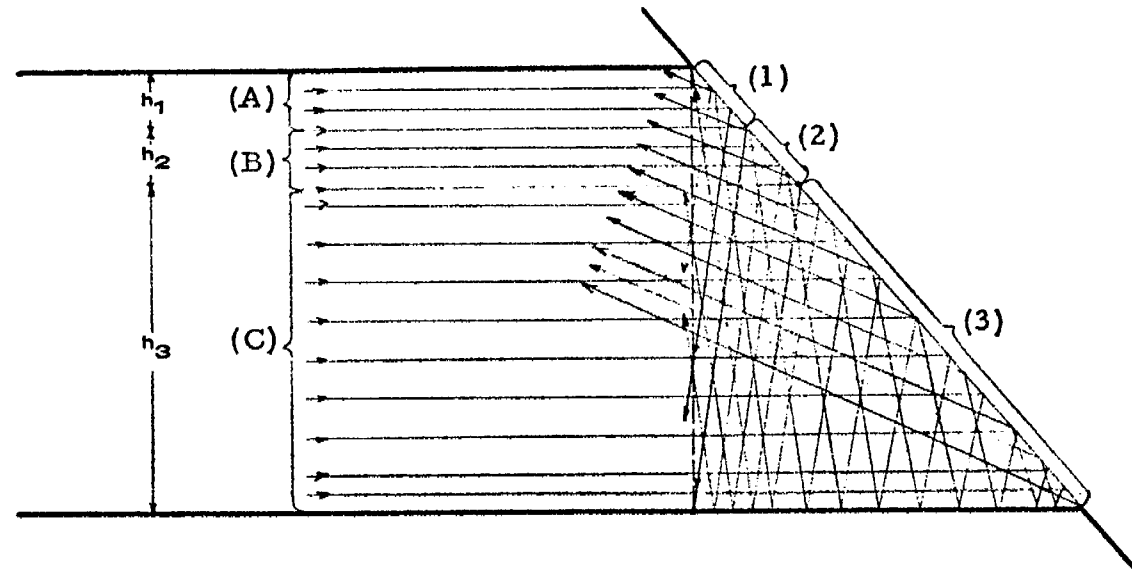
Figure 6: Reflected rays from (1) are directed towards the bottom plate, reflected rays from (2) towards the upper plate, whereas rays (C) are reflected off (3) and then once more off the entire admittance sheet and are directed towards the upper plate.
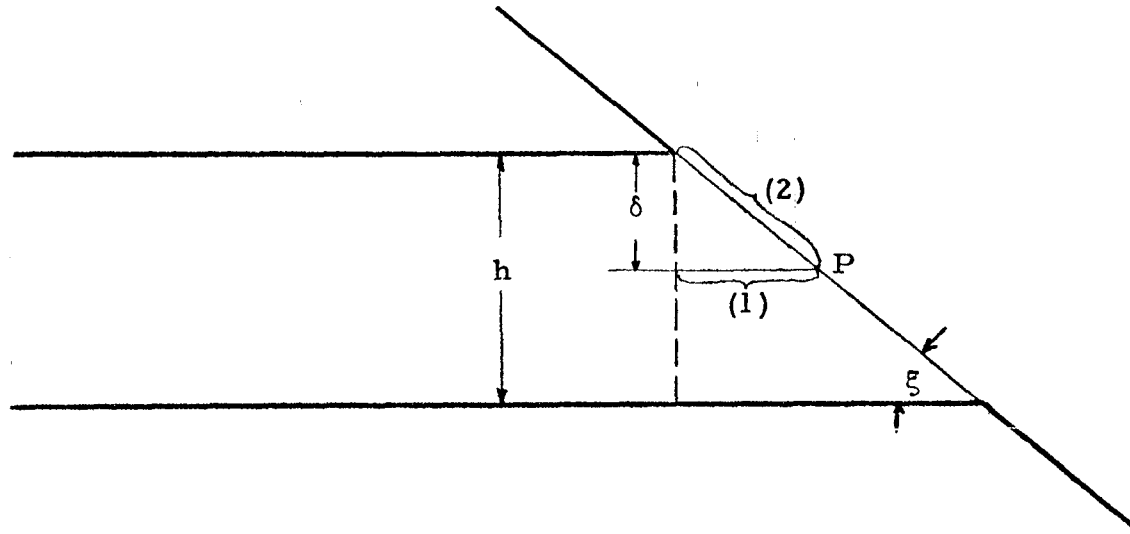
Figure 7: The disturbance from the top edge arrives at P later than the wavefront of the incident TEM step-pulse. The time-delay is $[(2)-(1)]/c = (\delta/c) \tan(\xi/2)$.
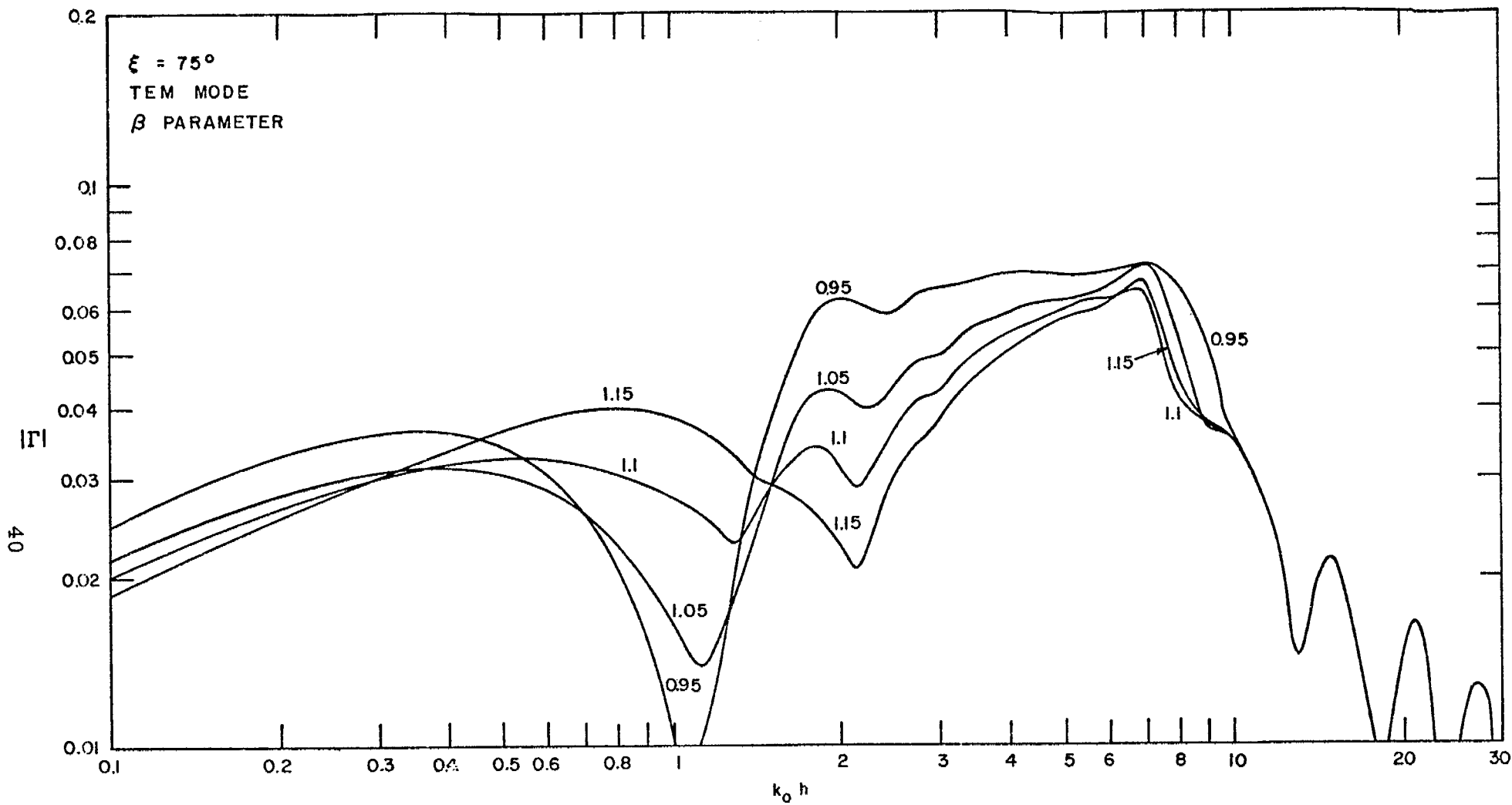
FIGURE 8
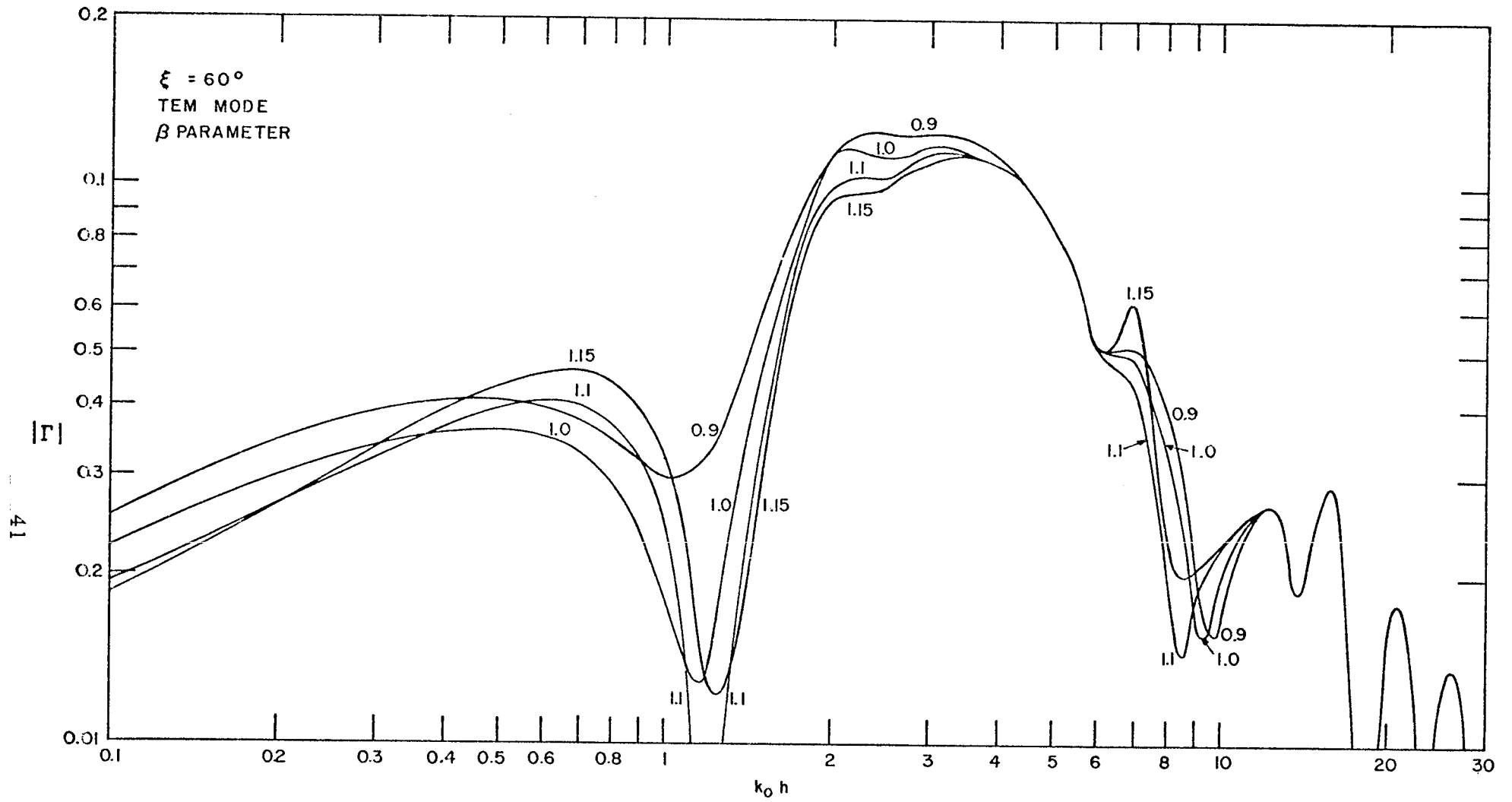
FIGURE 9
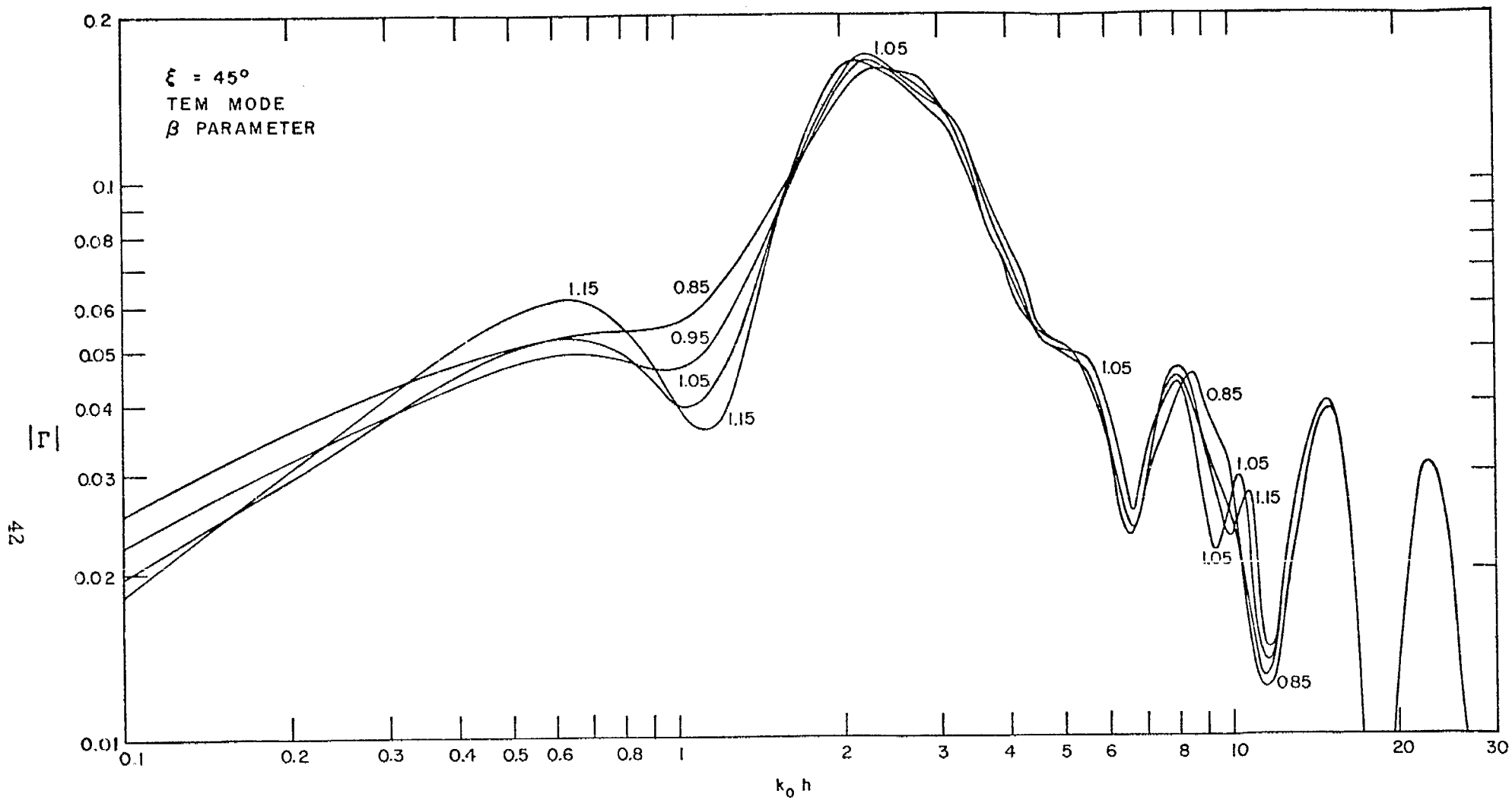
FIGURE 10
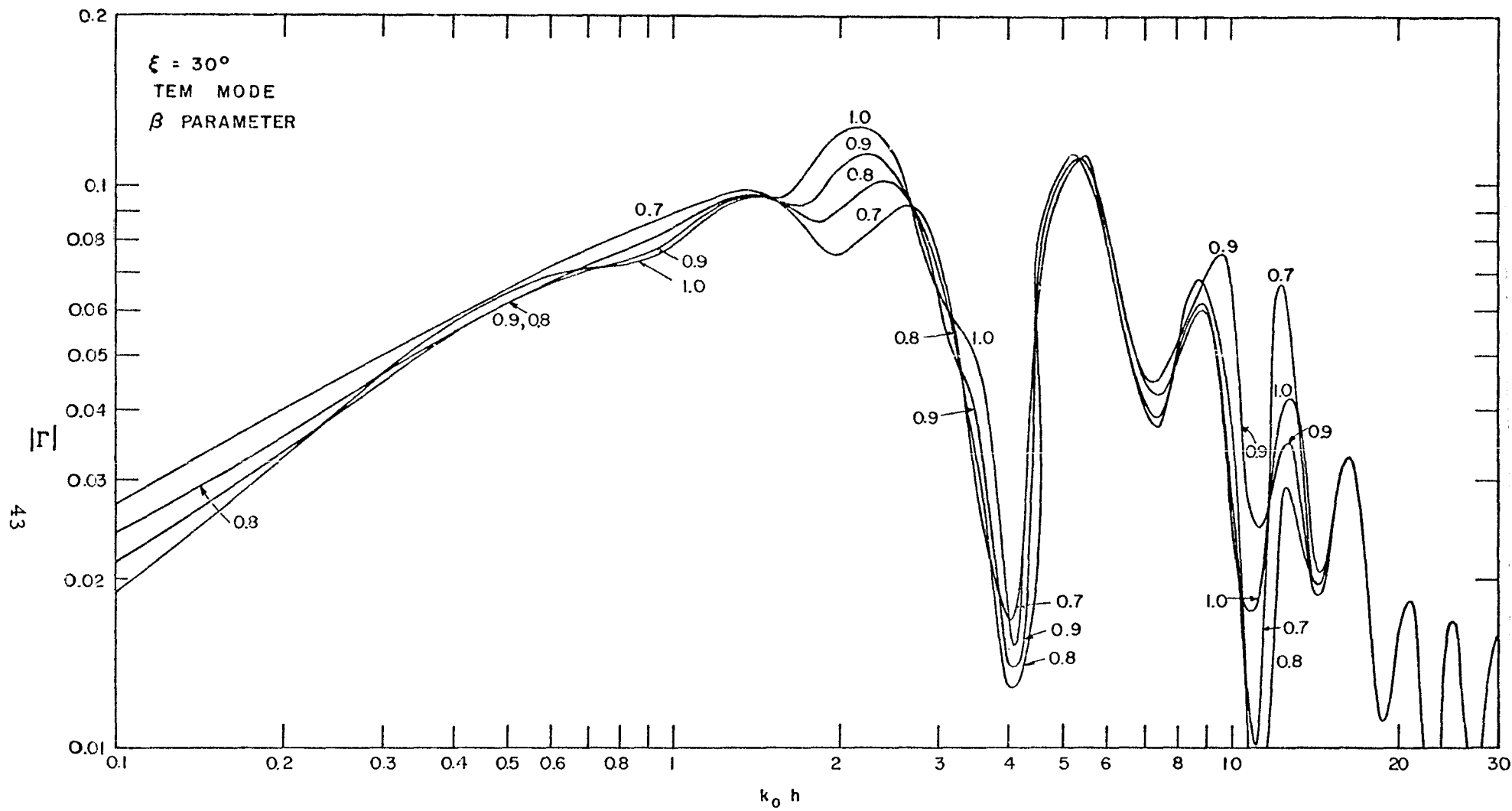
FIGURE 11
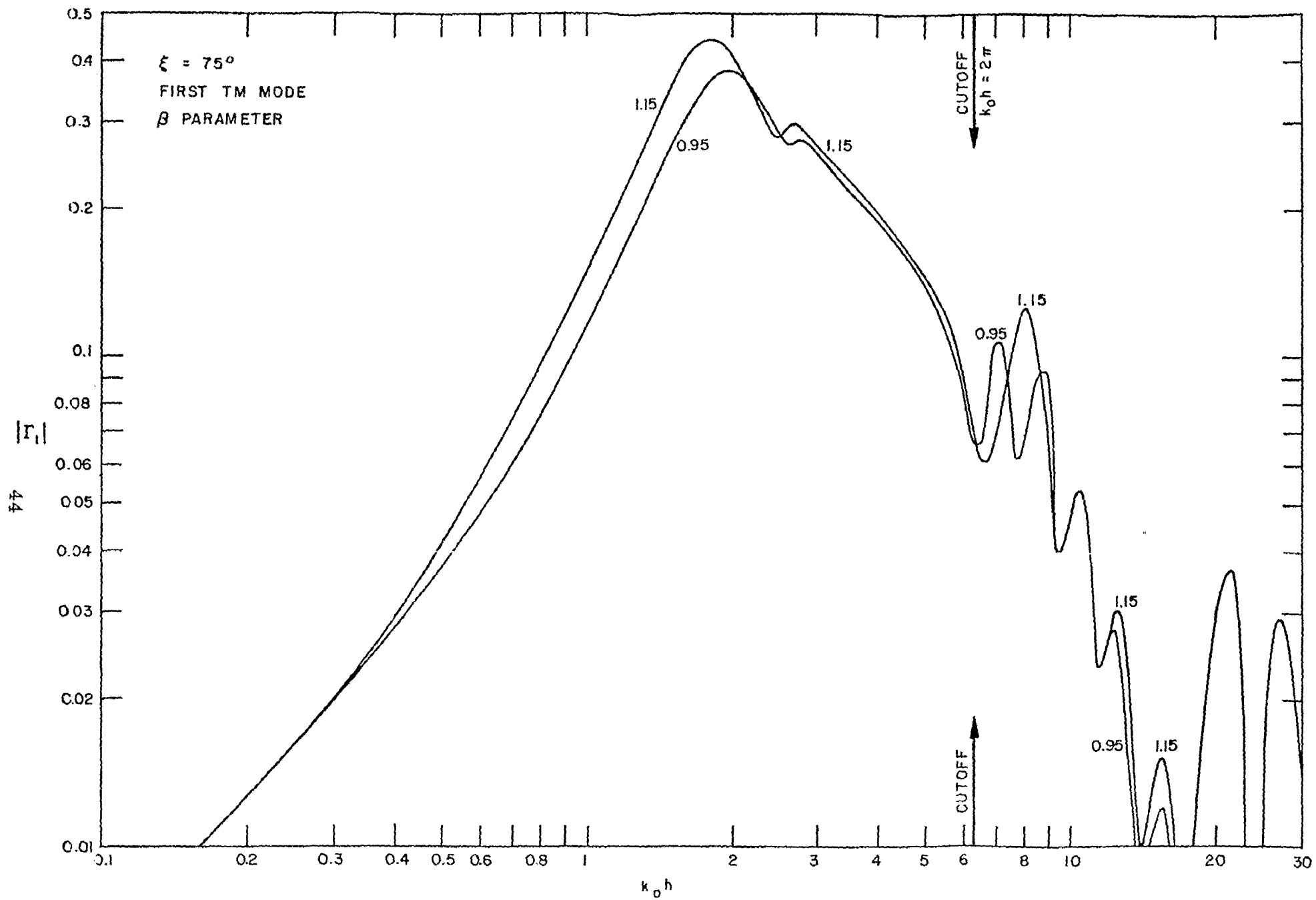
FIGURE 12

FIGURE 13

45
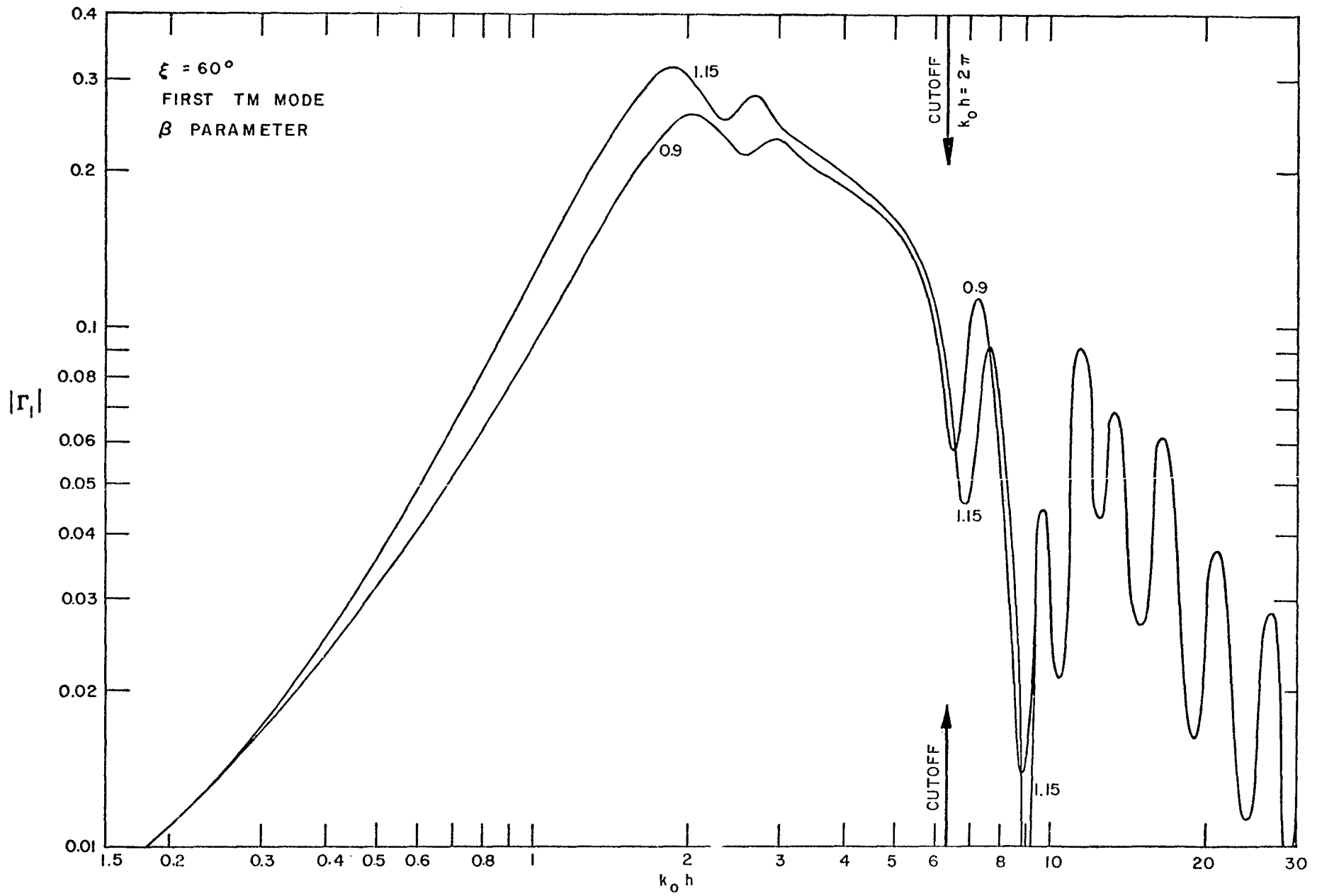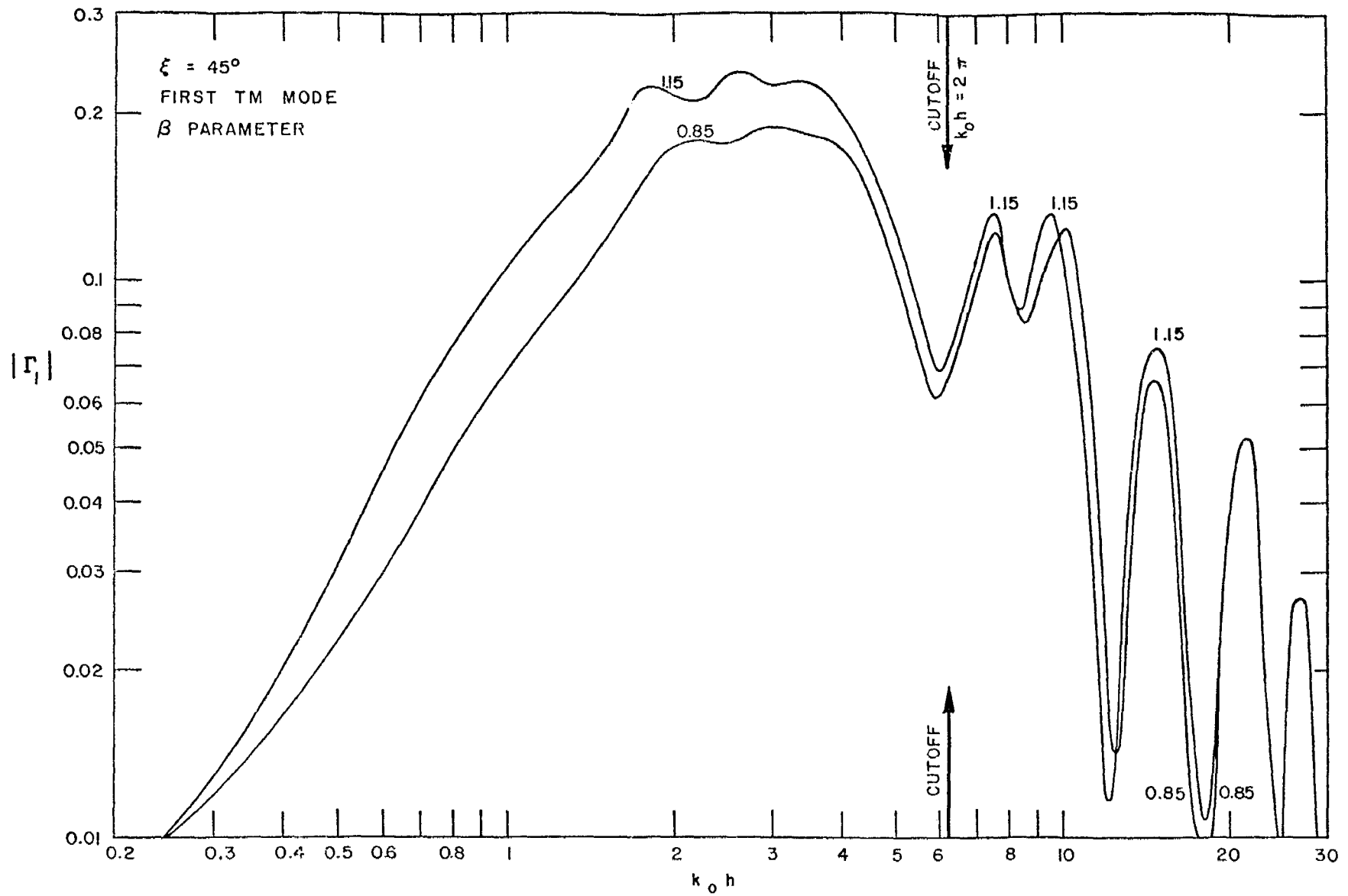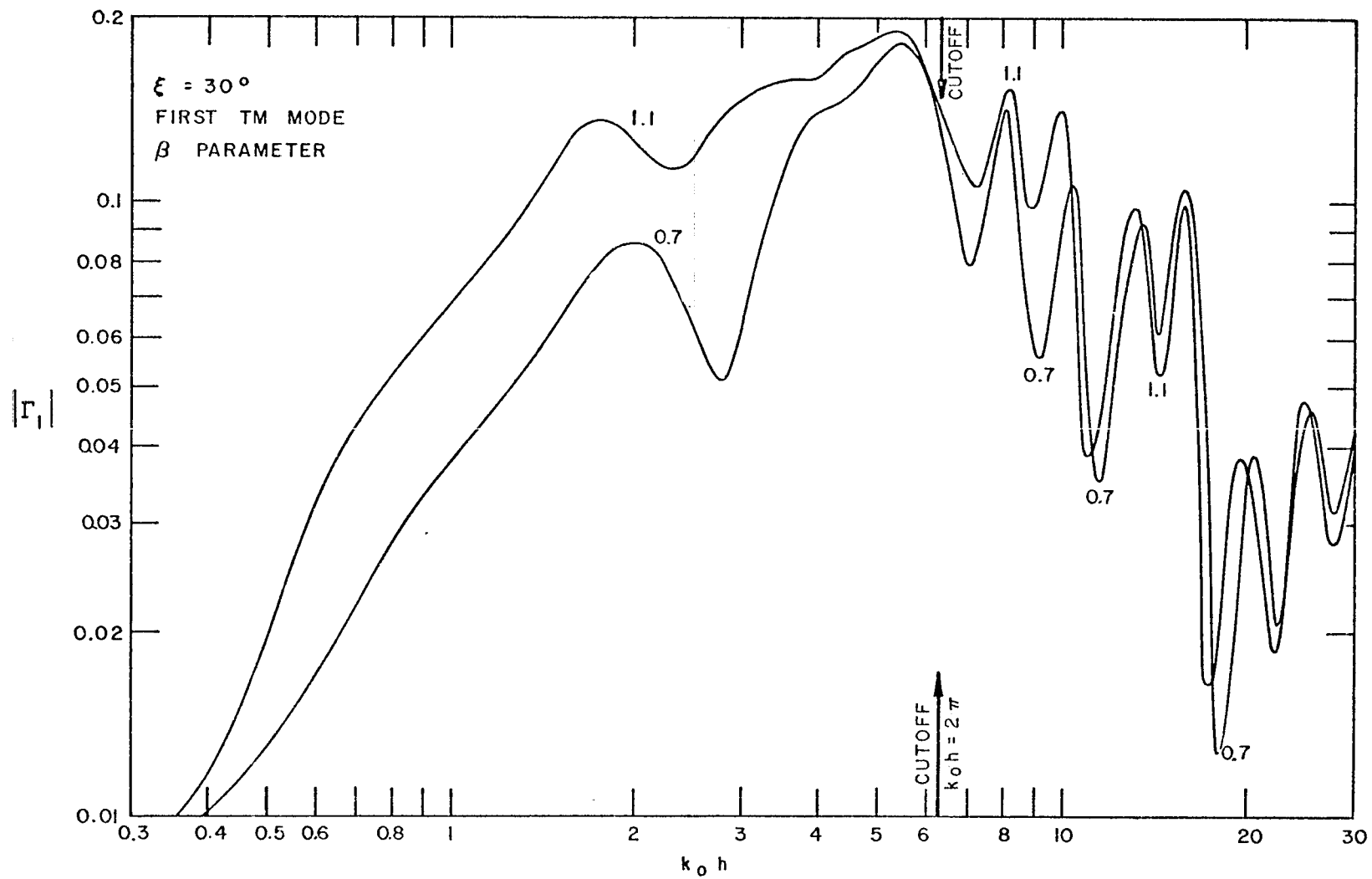
FIGURE 14

FIGURE 15
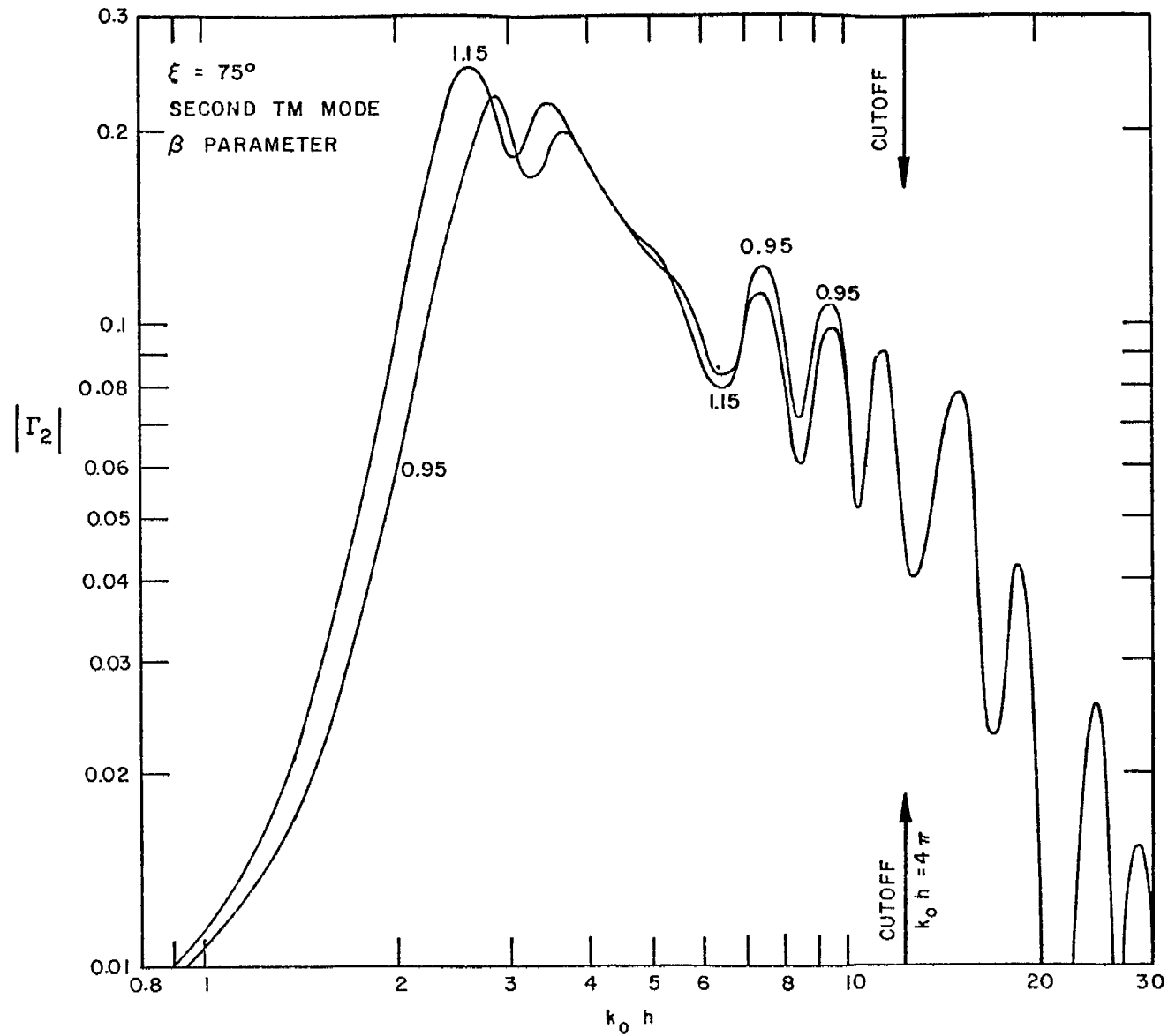
FIGURE 16
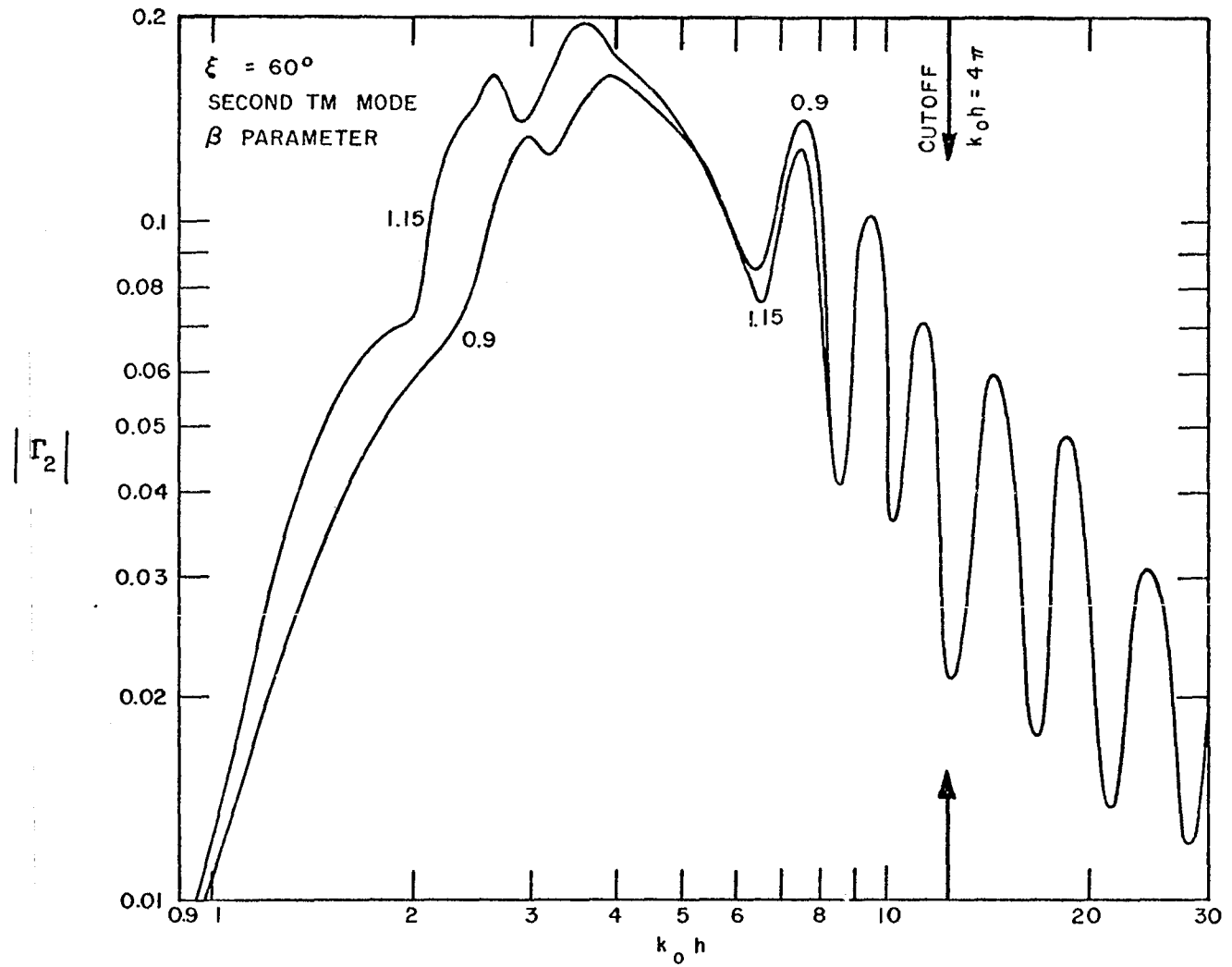
FIGURE 17
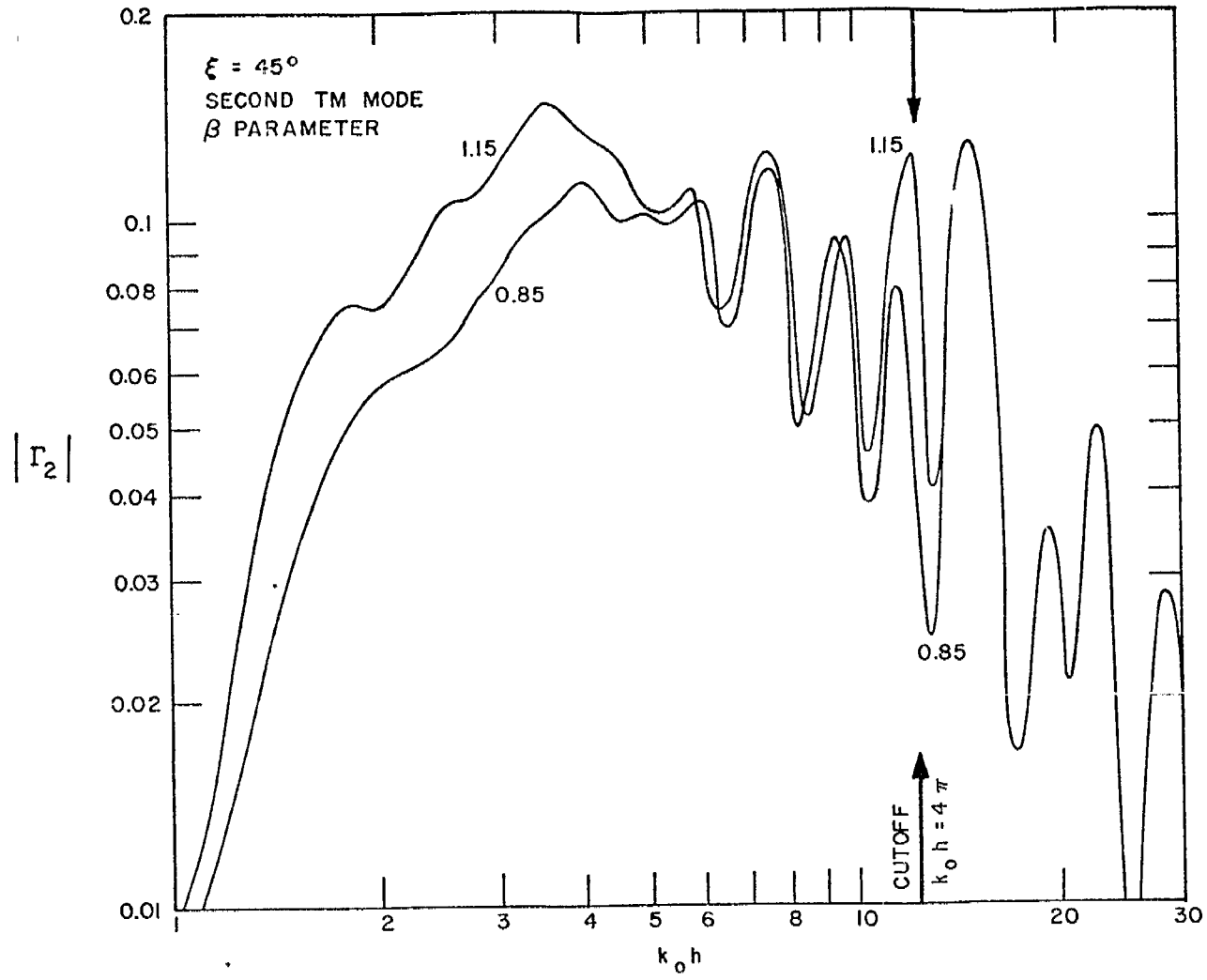
FIGURE 18
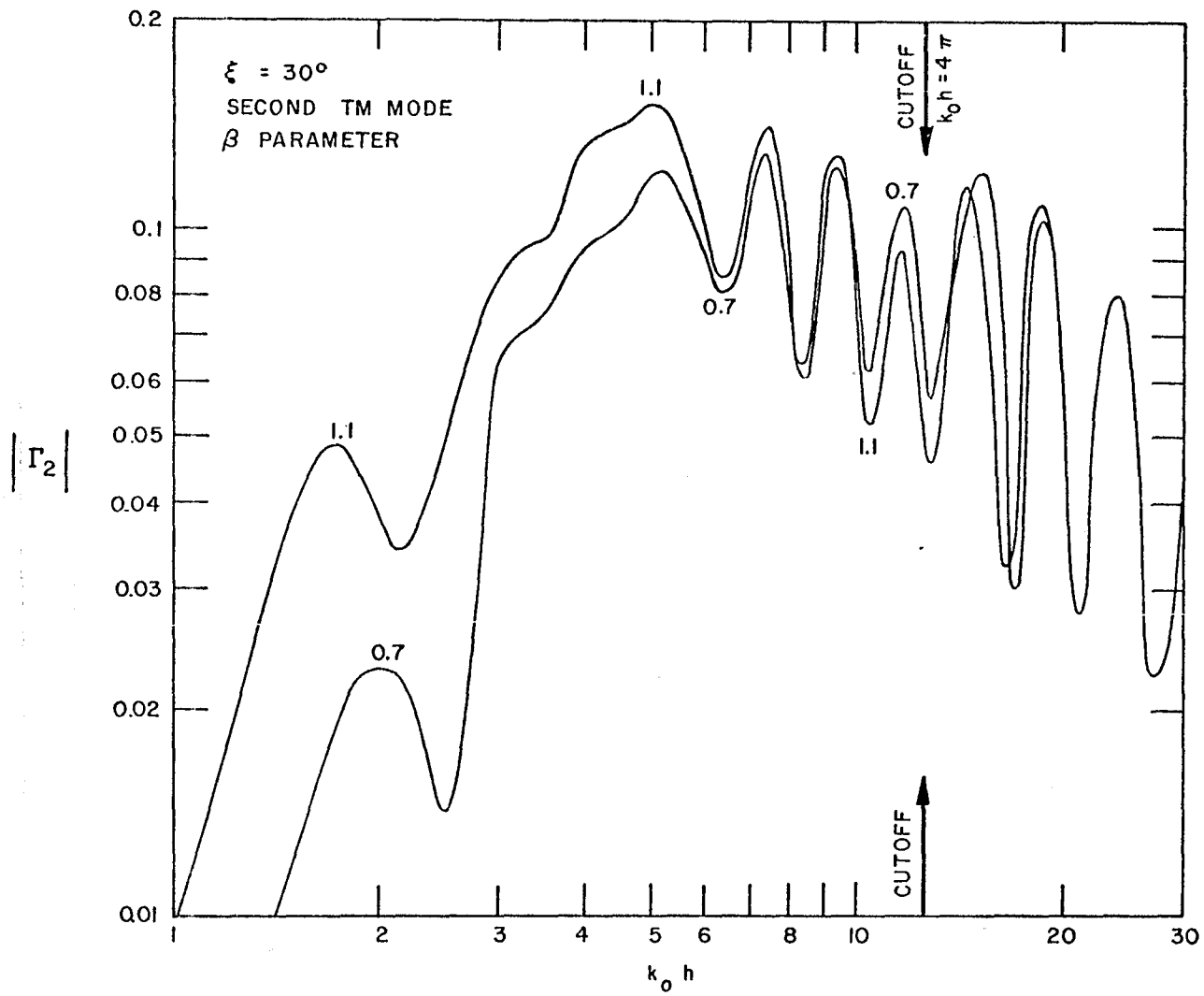
FIGURE 19
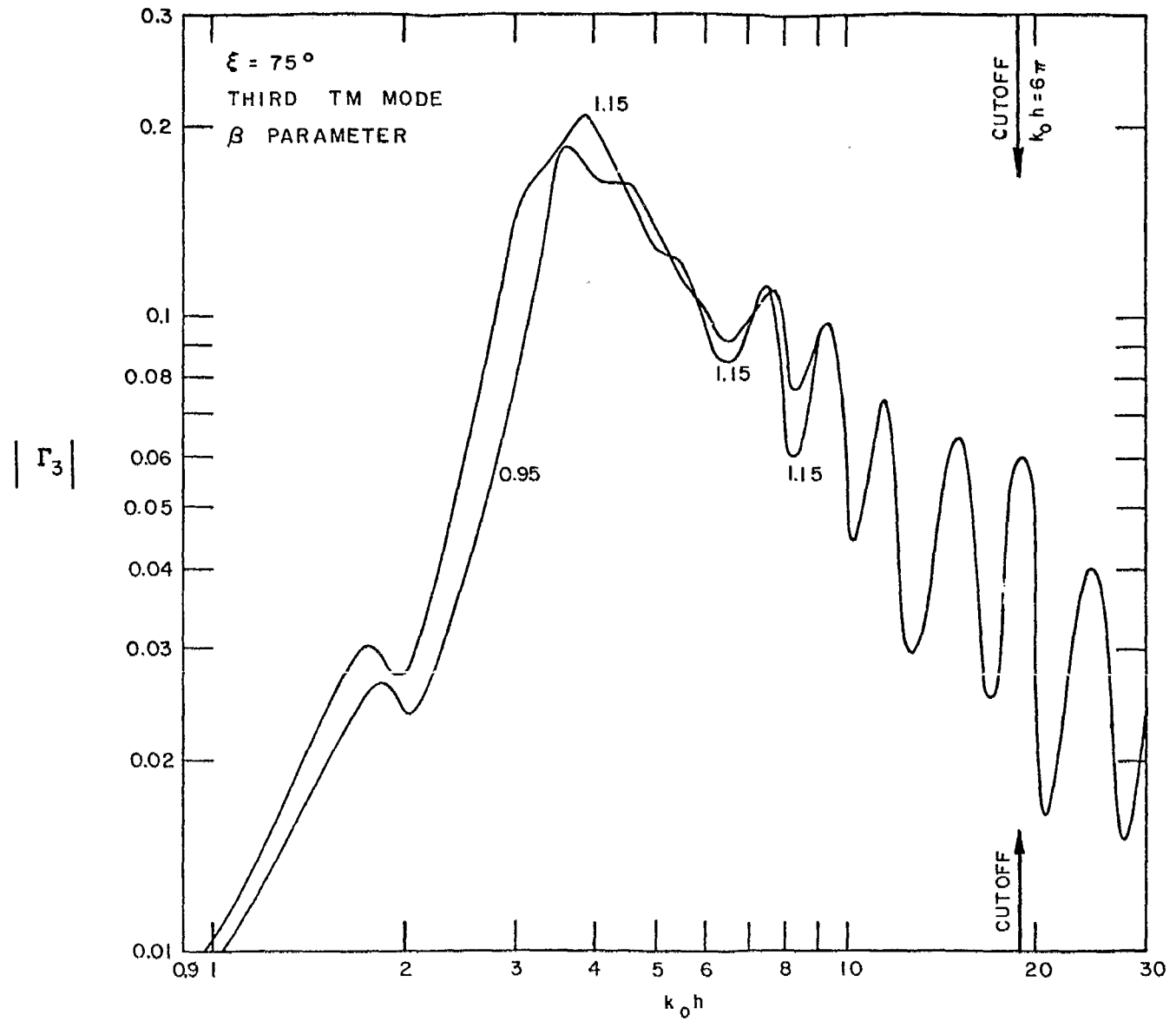
FIGURE 20
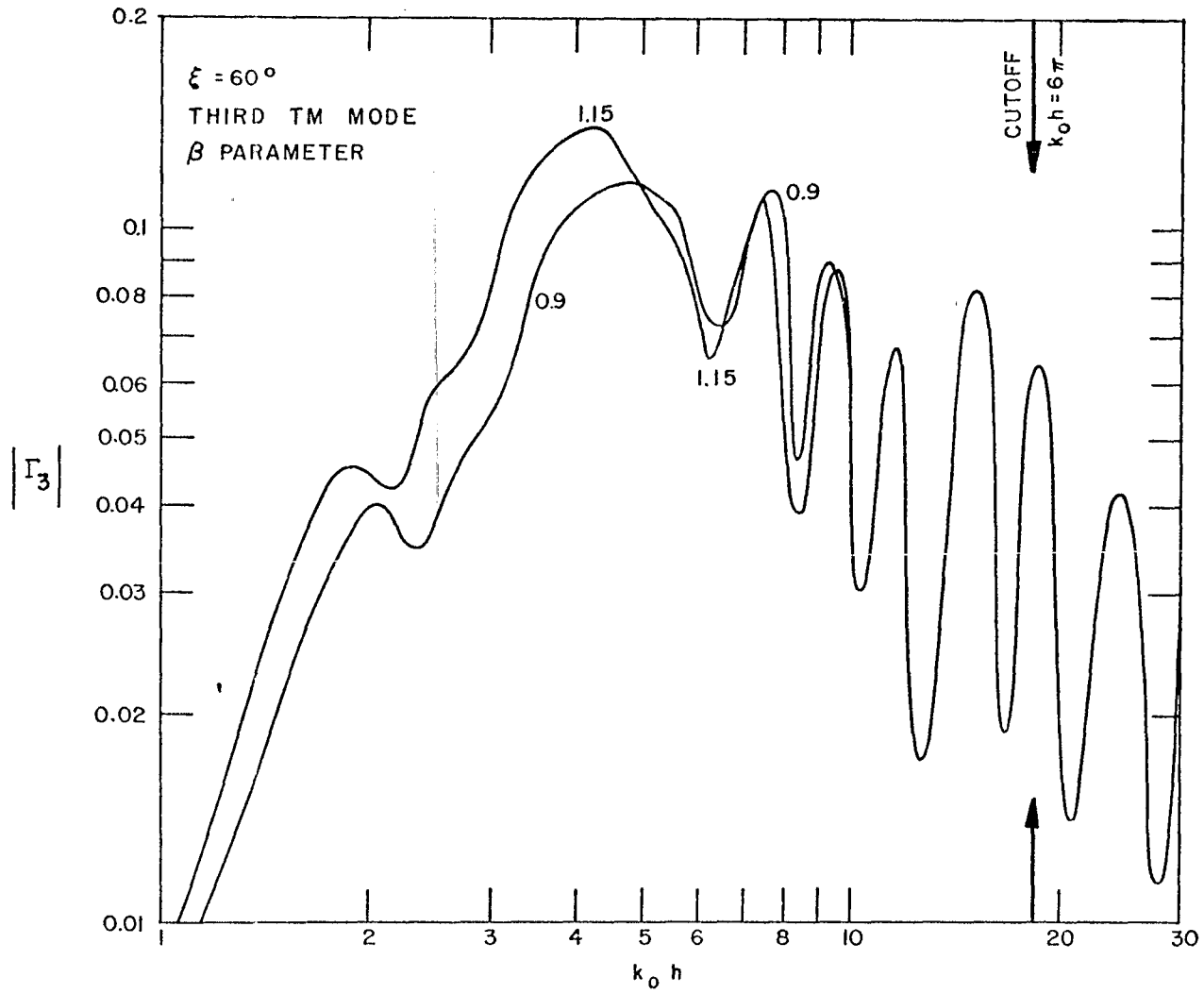
FIGURE 21
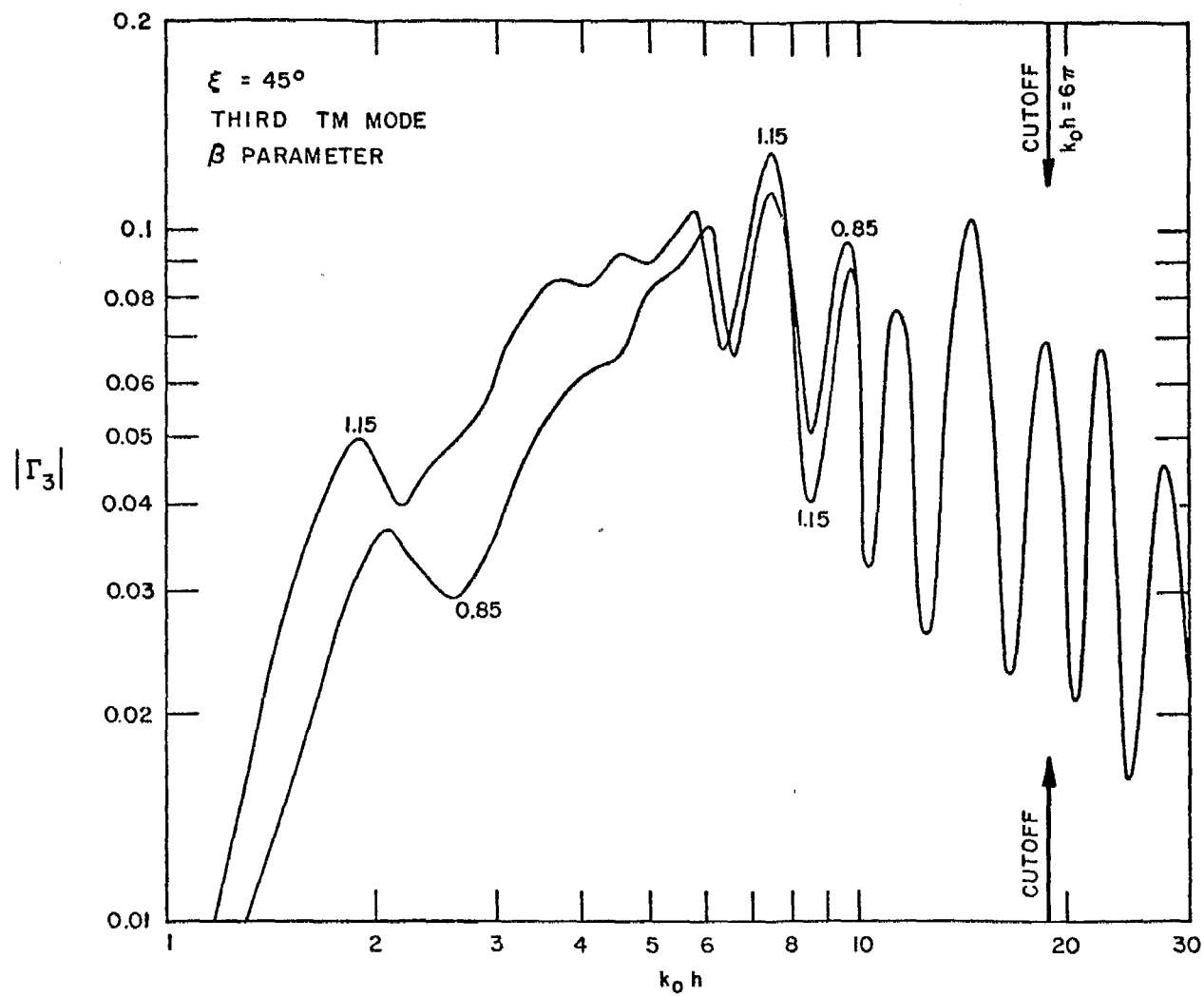
FIGURE 22
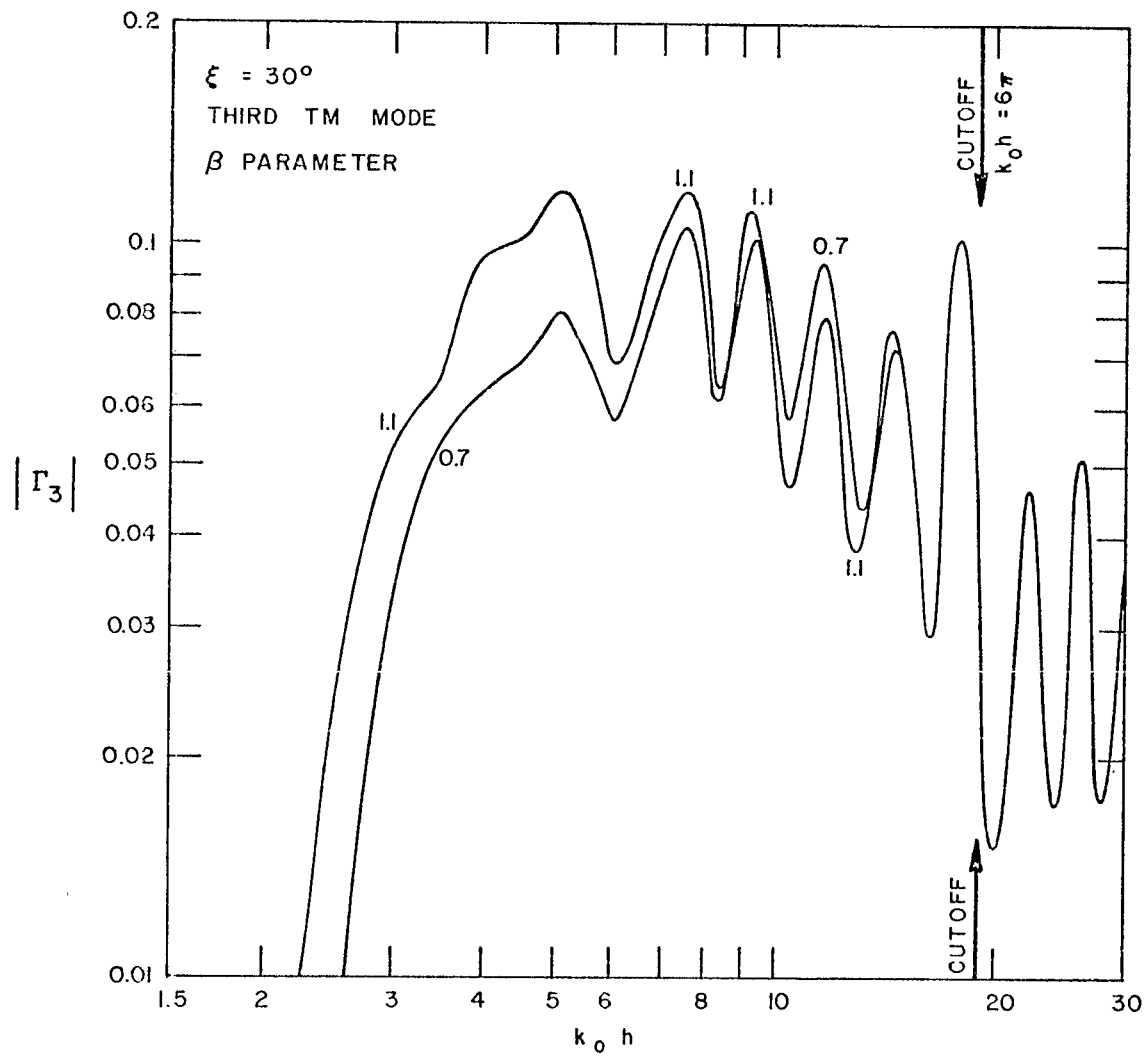
FIGURE 23
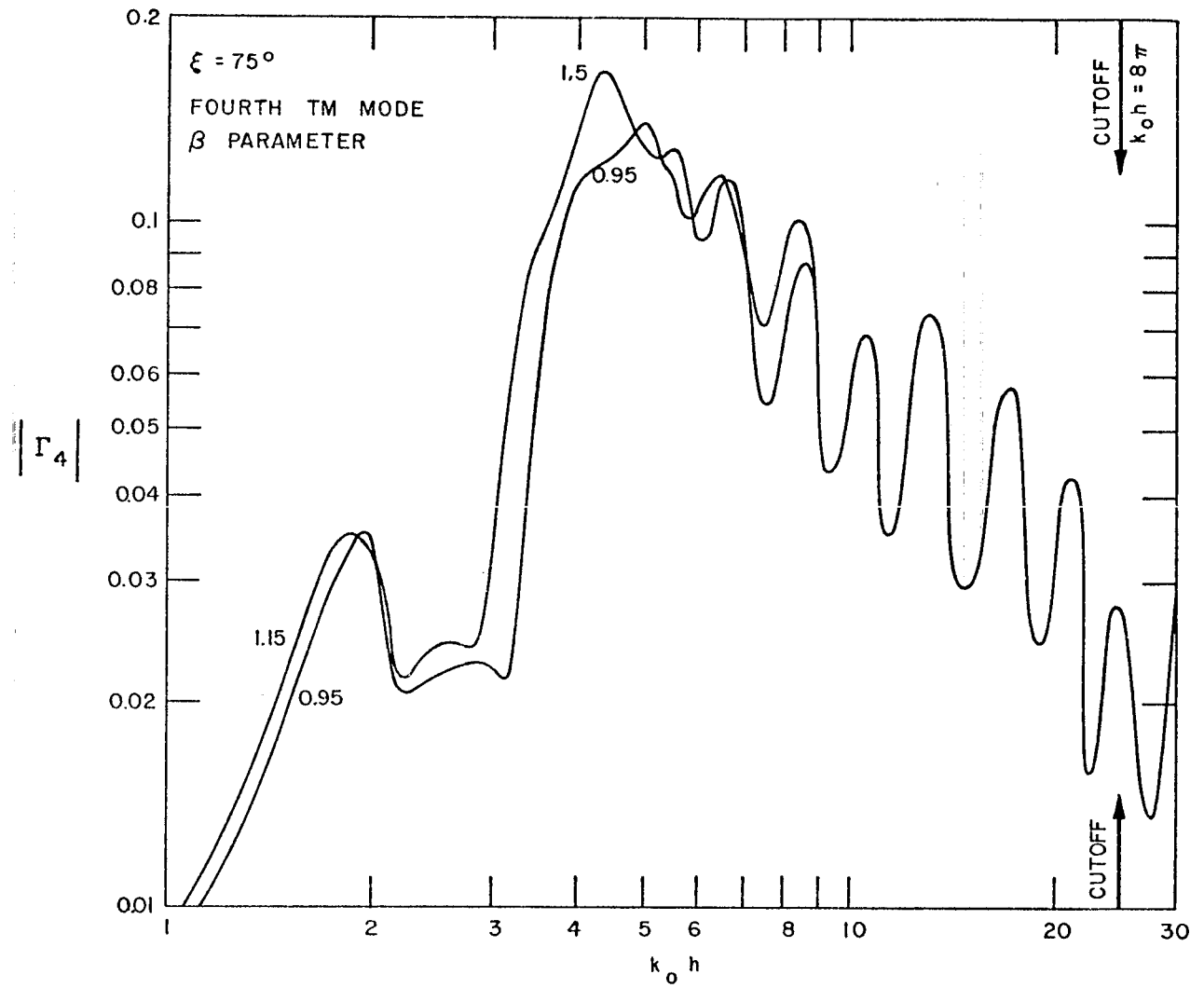
FIGURE 24
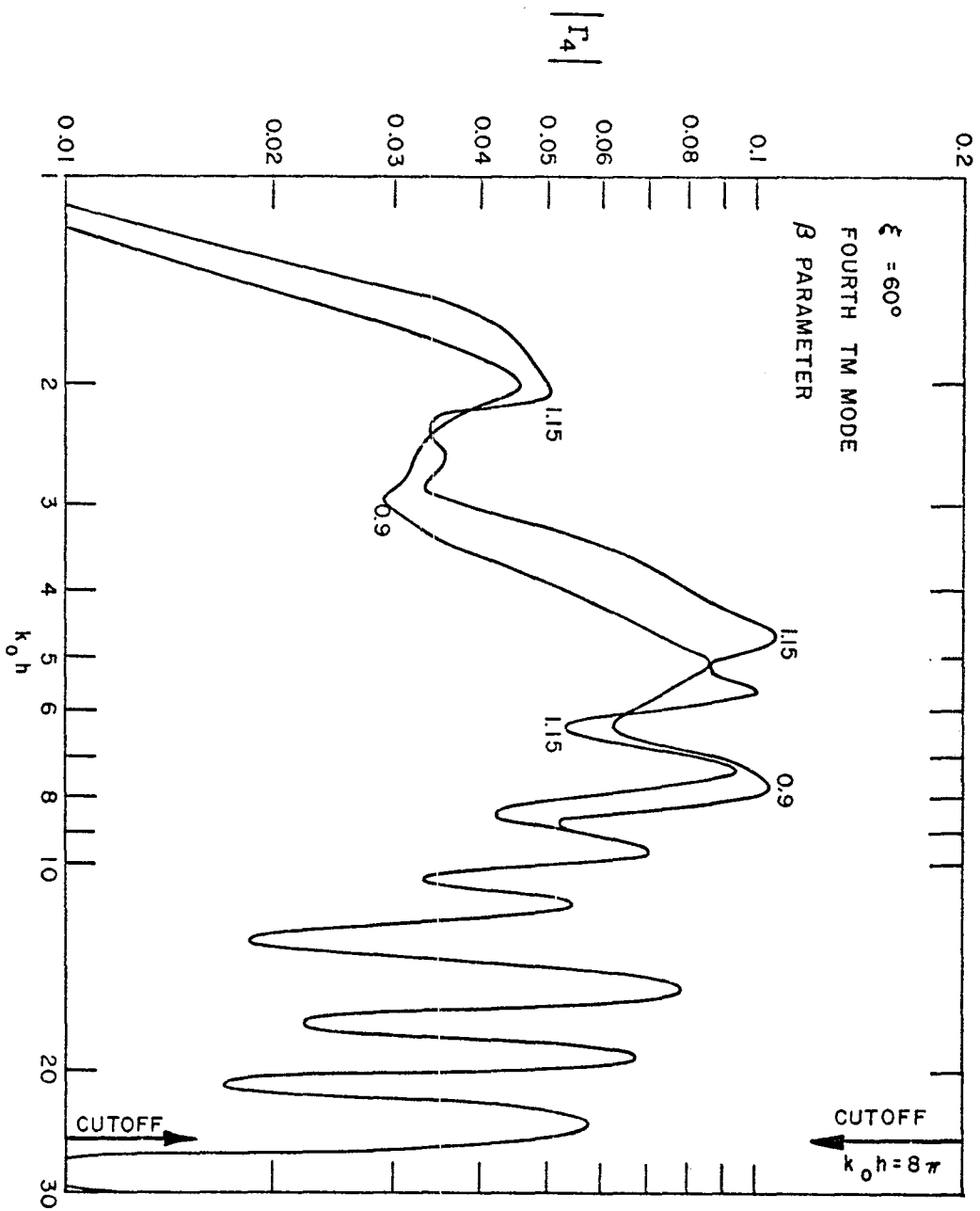
FIGURE 25

FIGURE 26

58
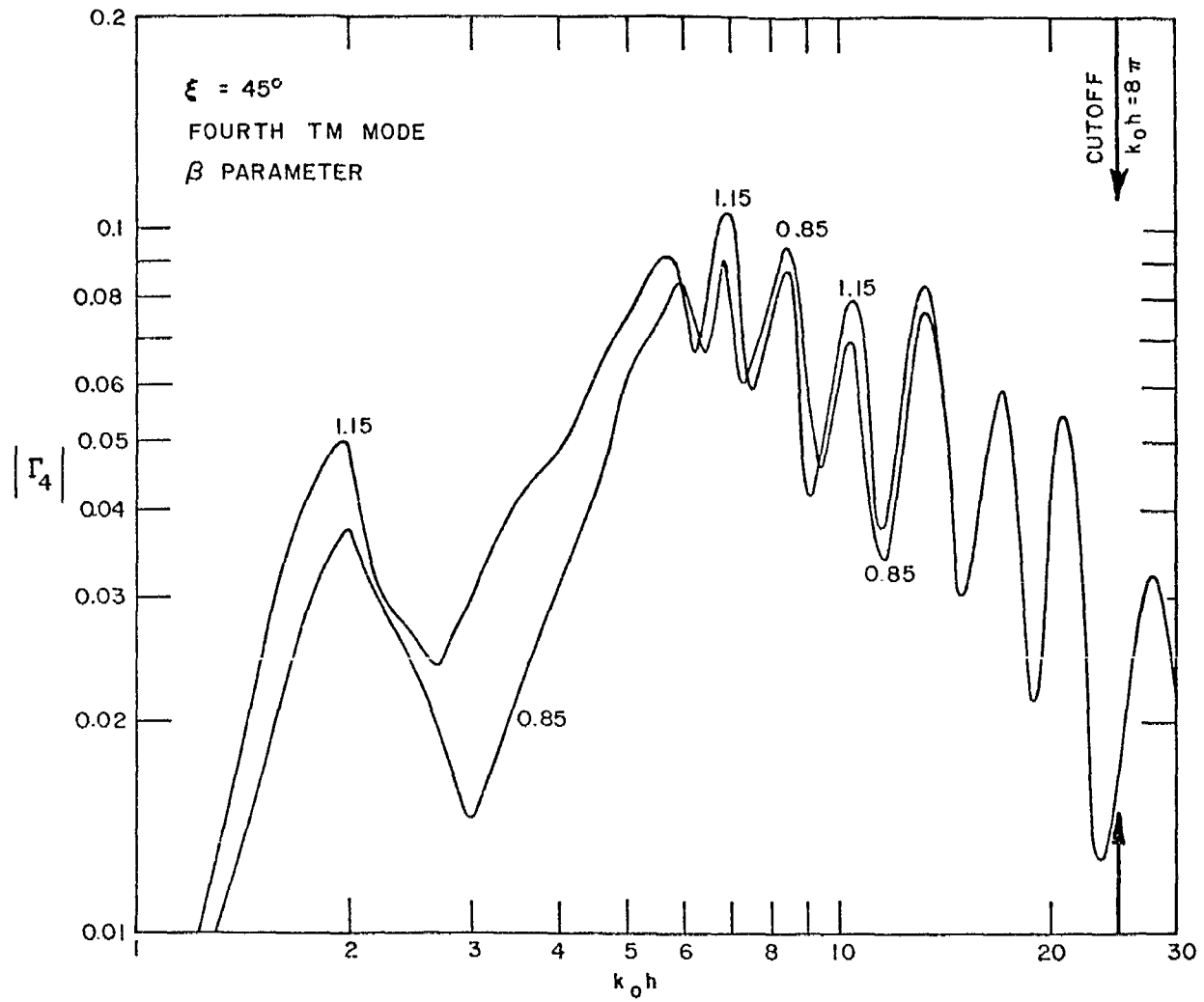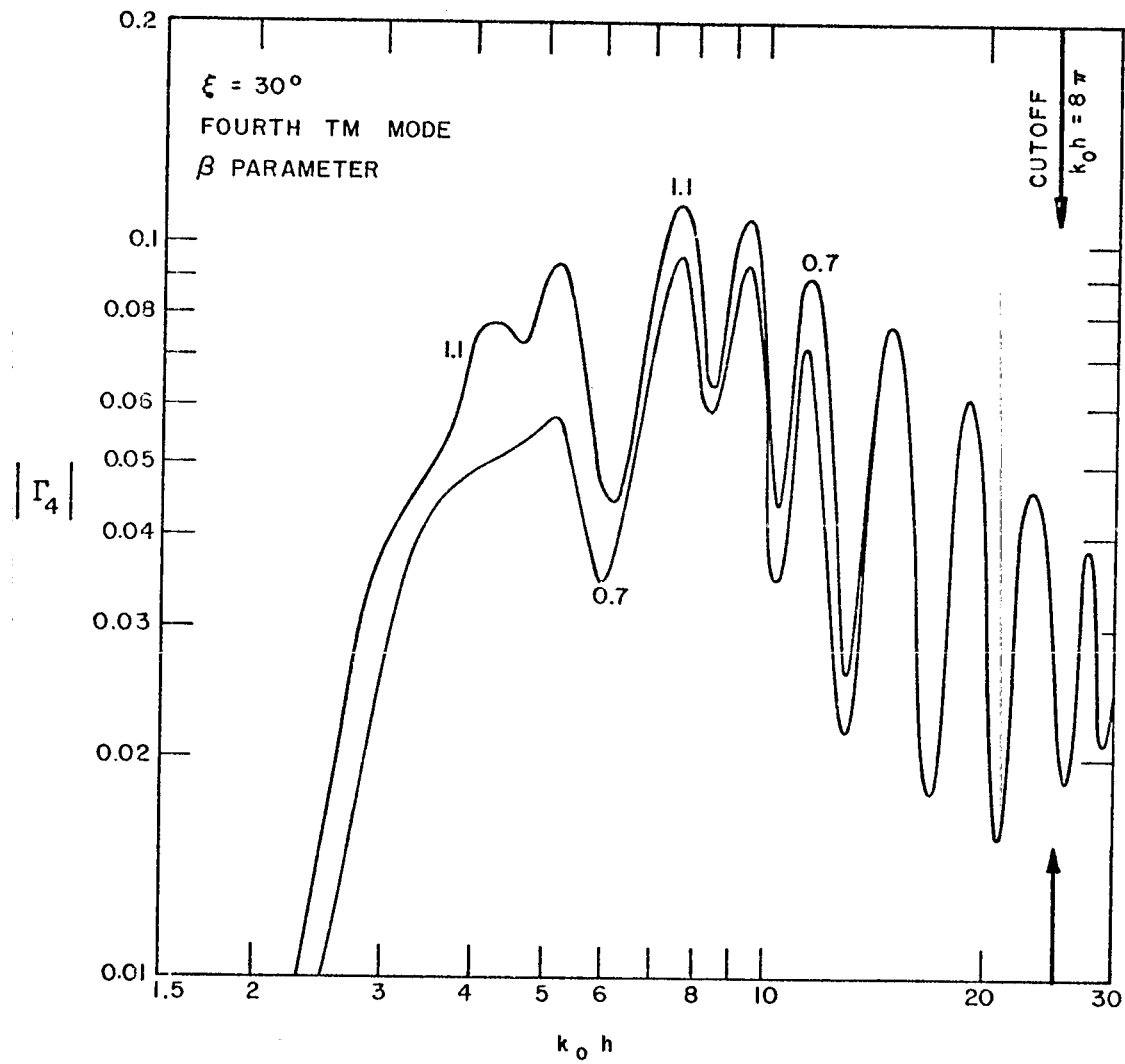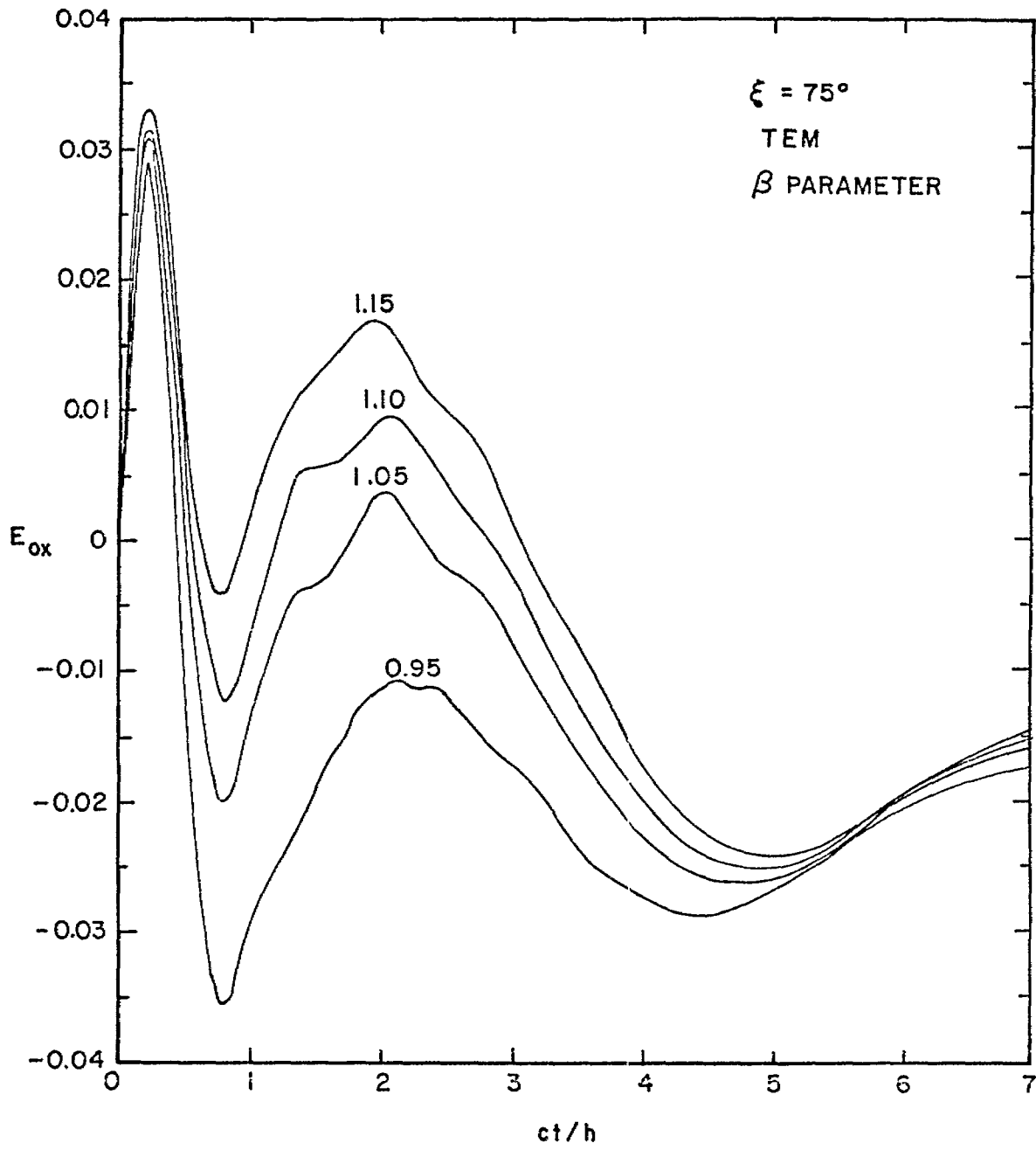
FIGURE 27

FIGURE 28
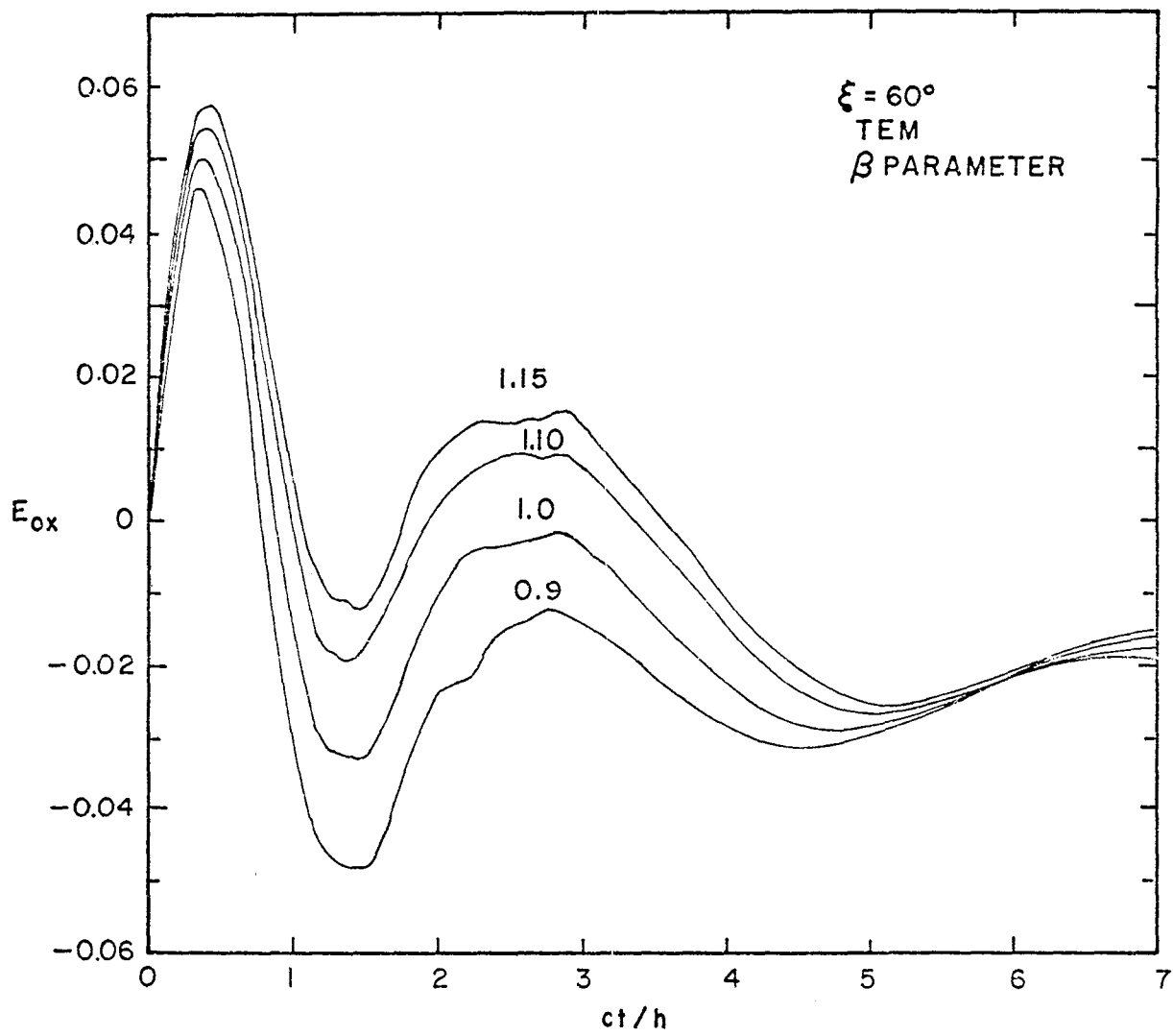
FIGURE 29
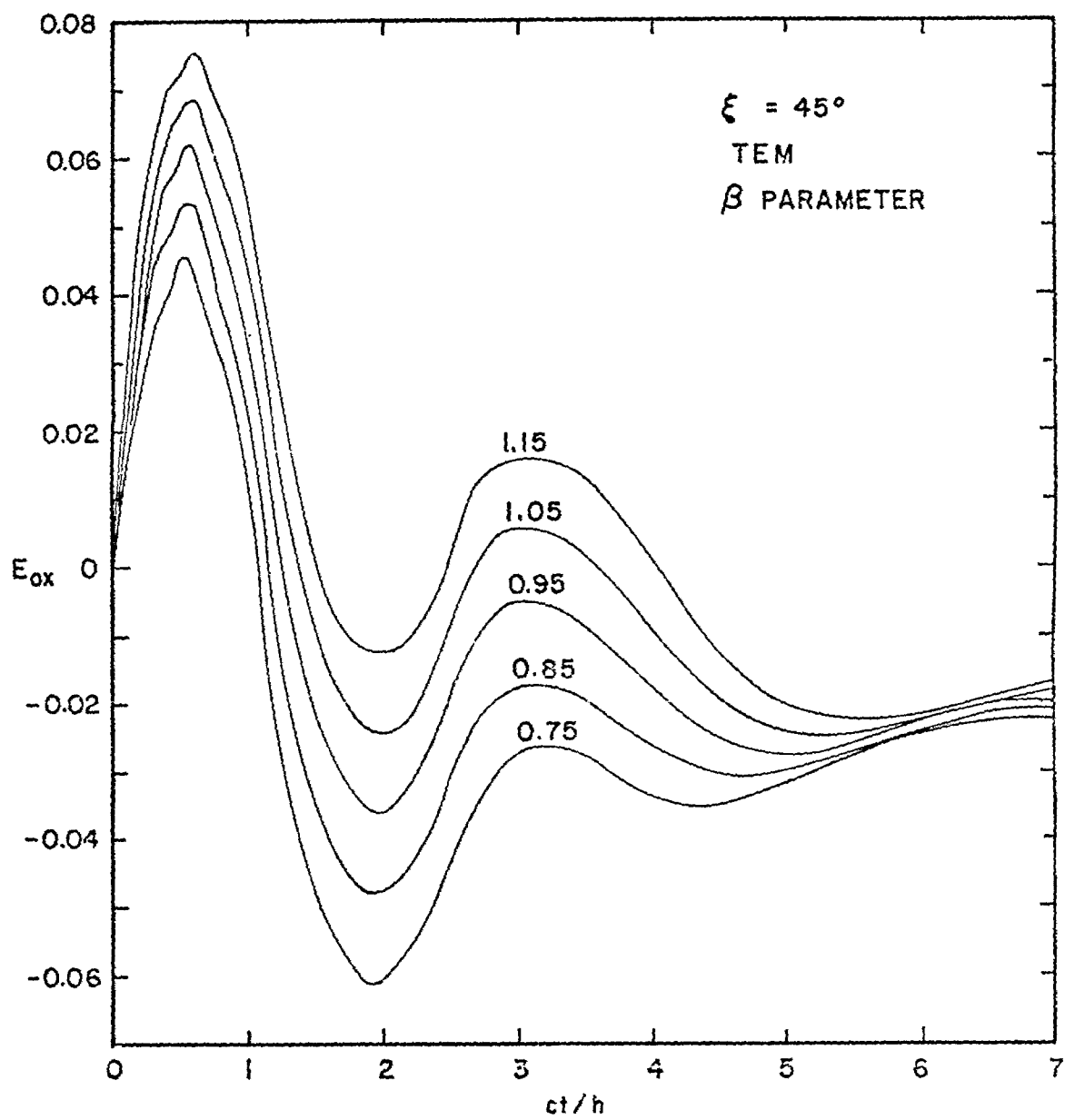
FIGURE 30
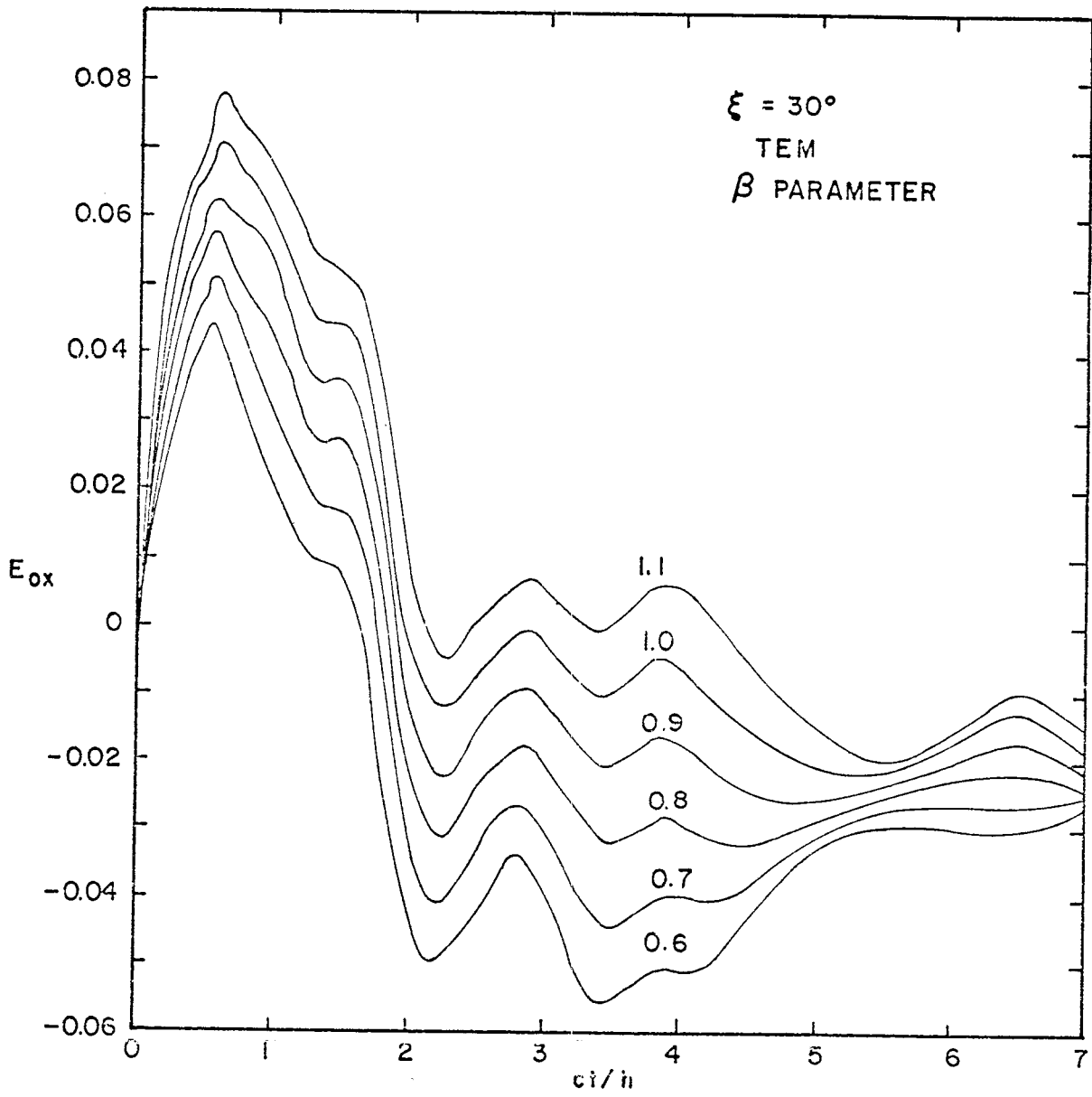
FIGURE 31
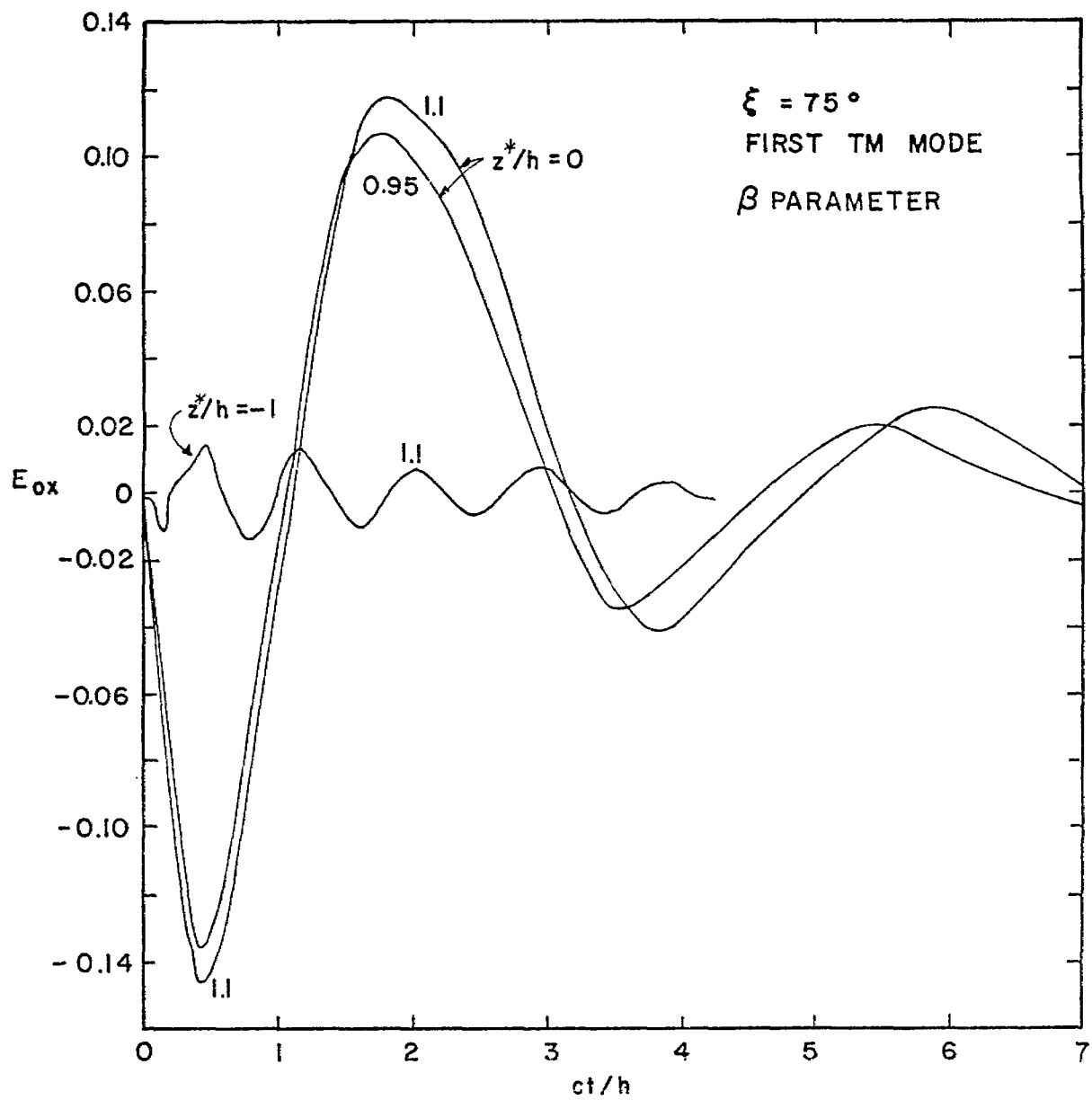
63

FIGURE 32

FIGURE 33

65

FIGURE 34

66

FIGURE 35

FIGURE 36

$\xi = 60°$
SECOND TM MODE
β PARAMETER

FIGURE 37

69

FIGURE 38

70

FIGURE 39

71
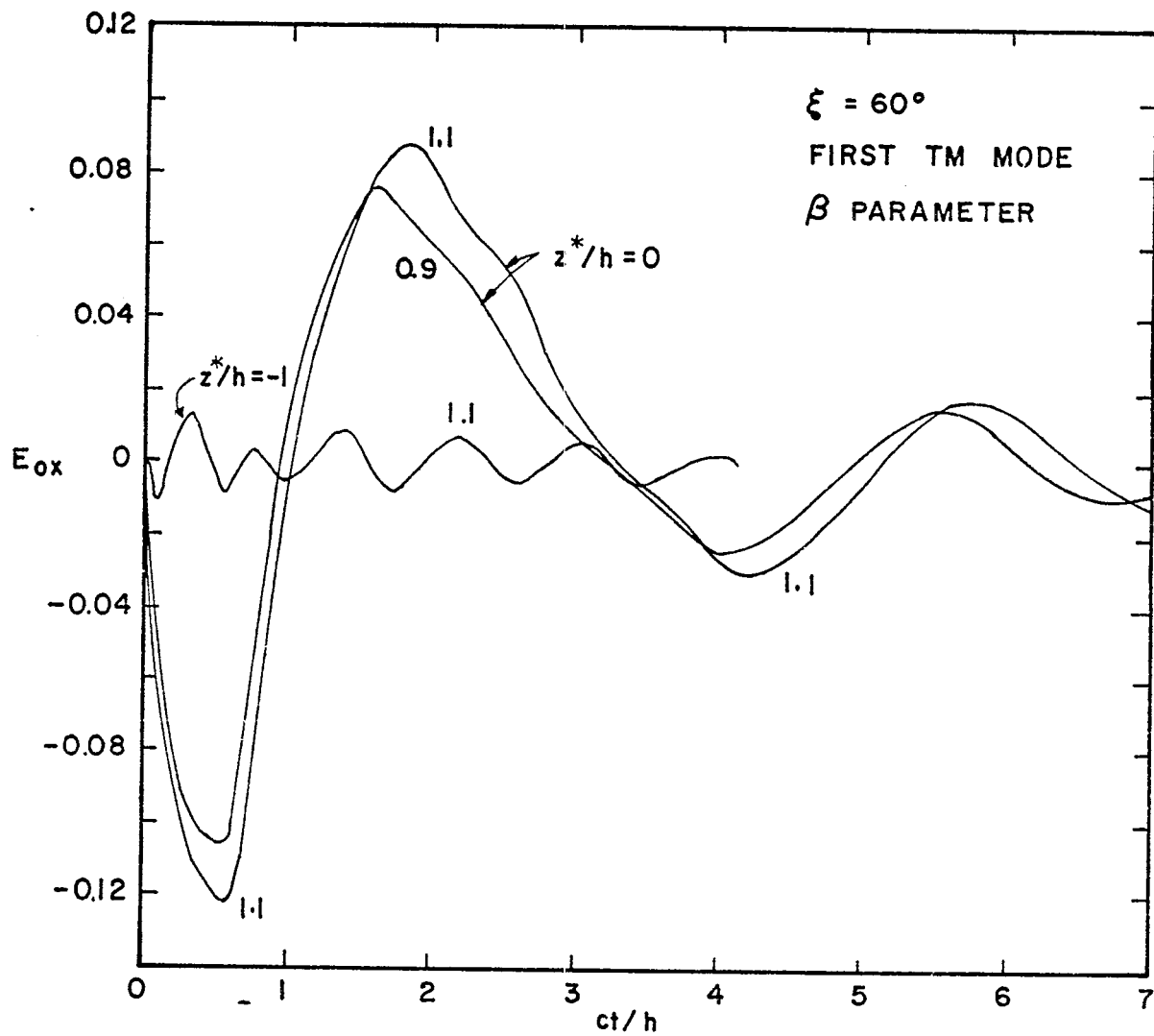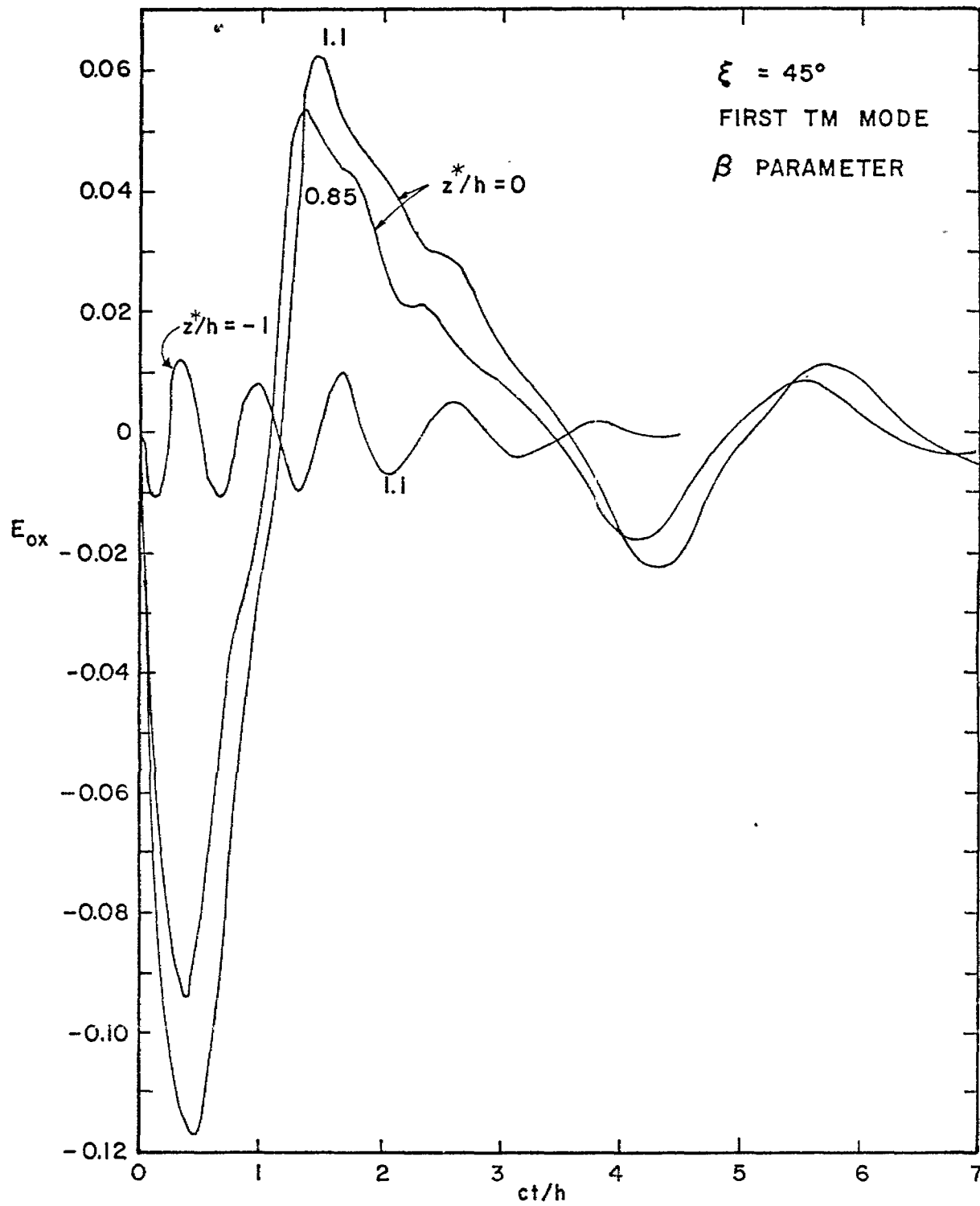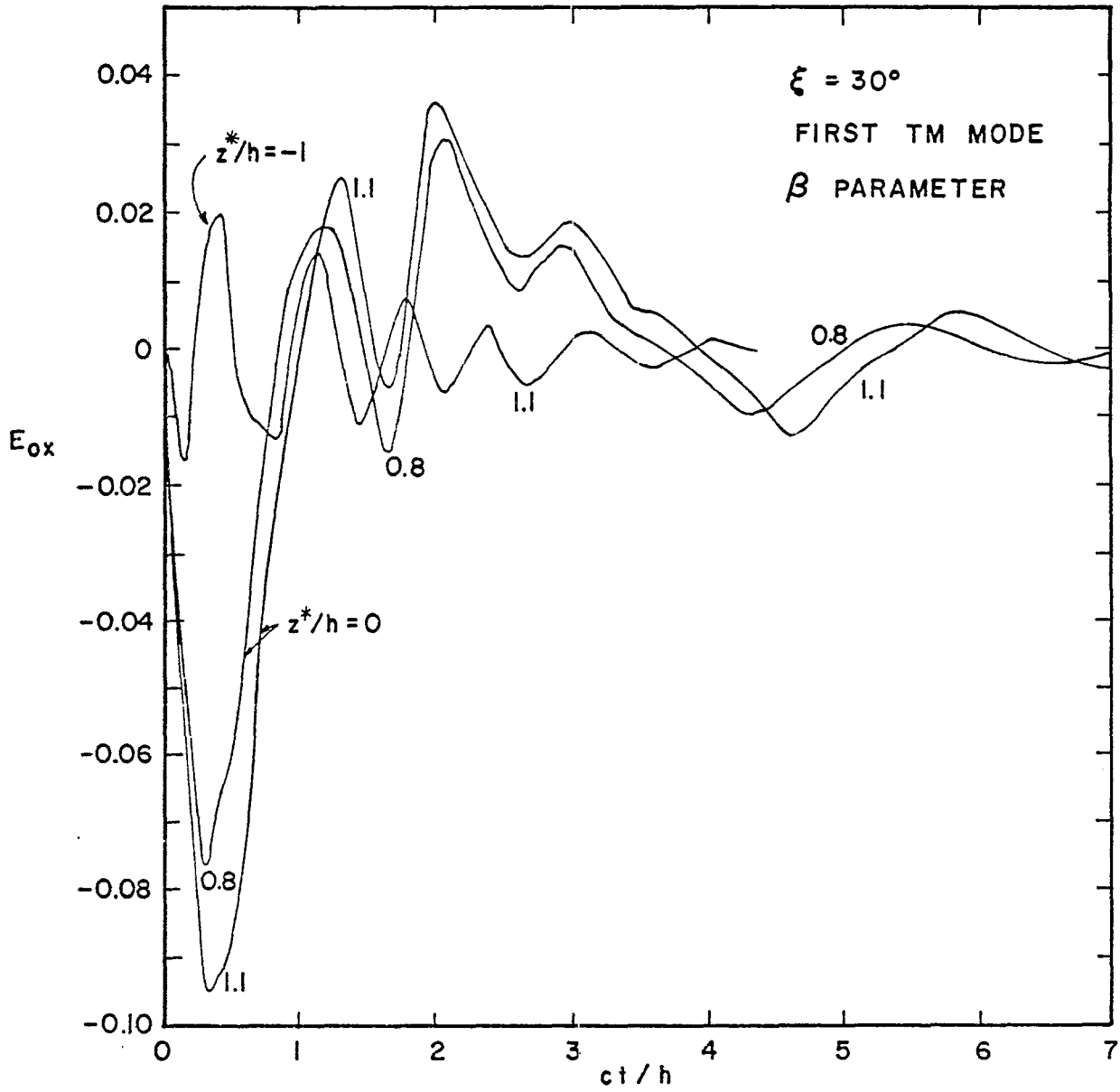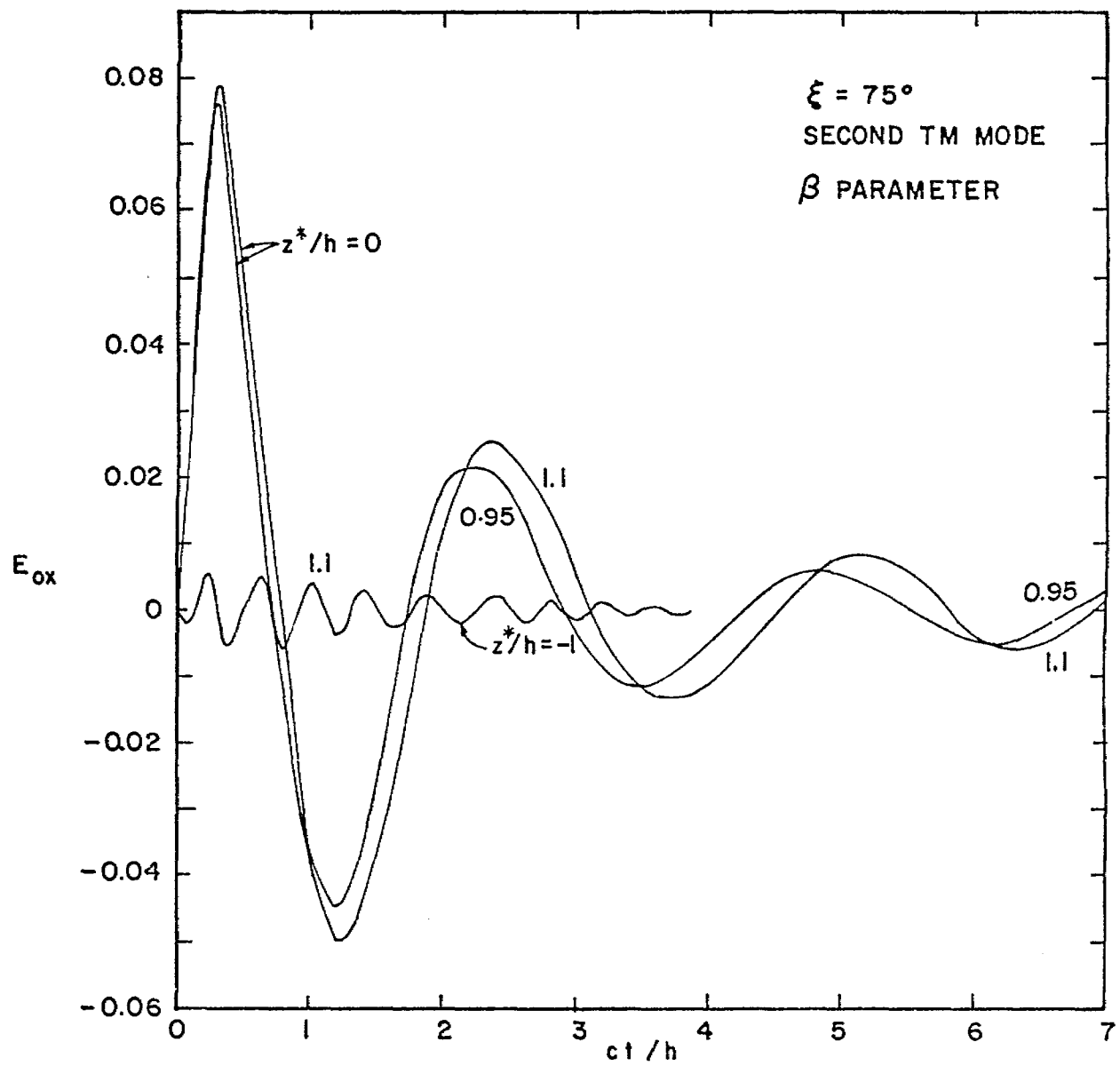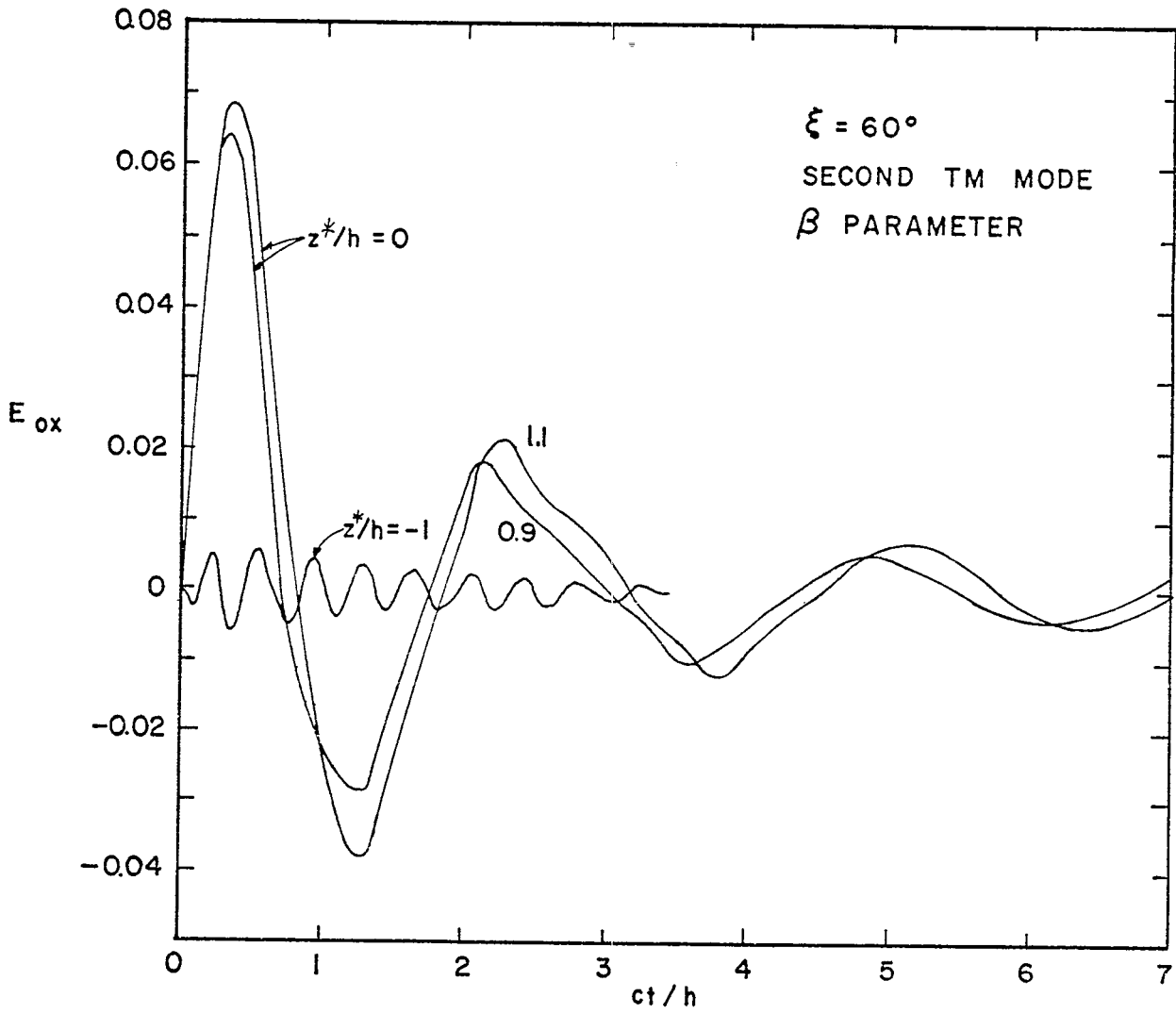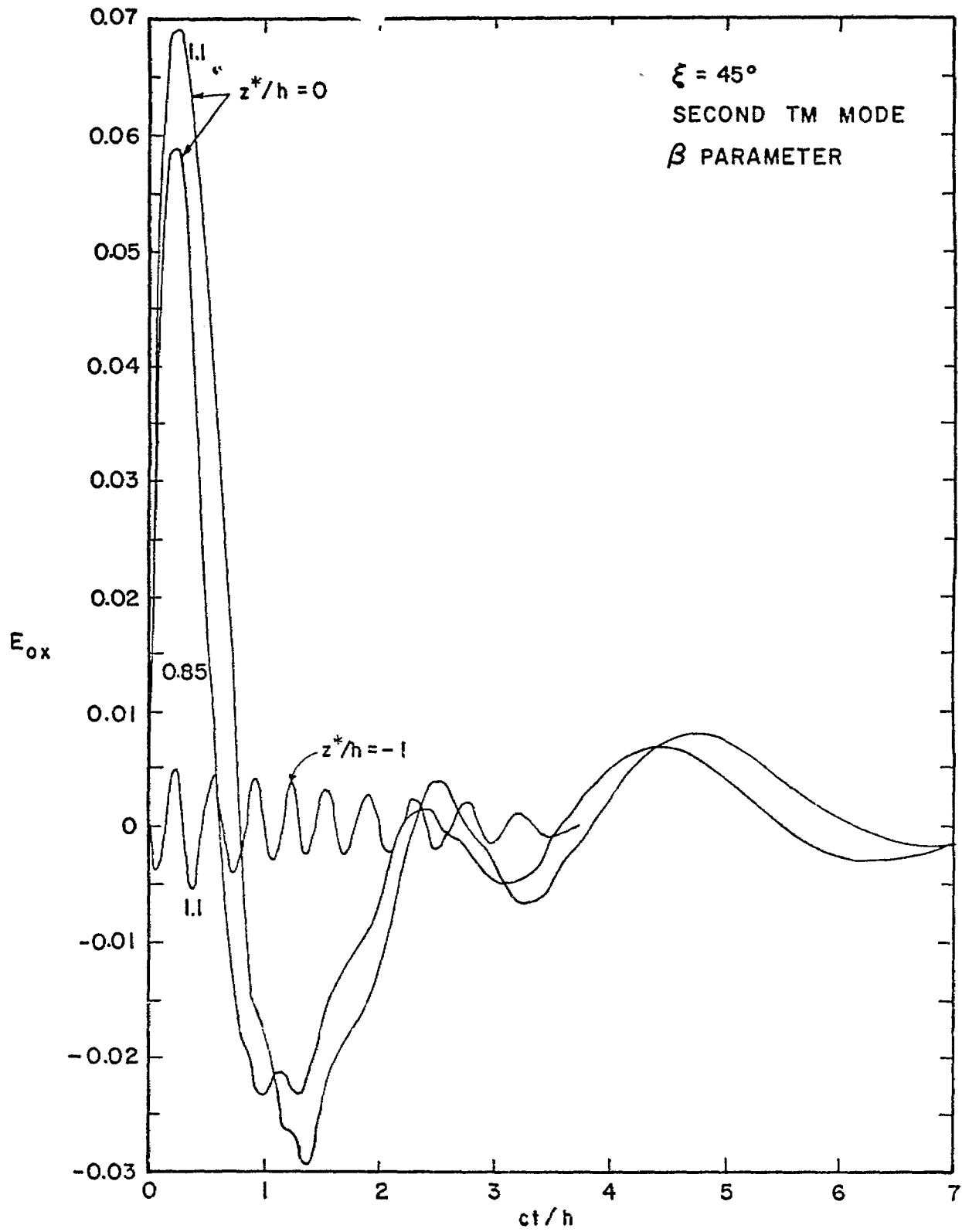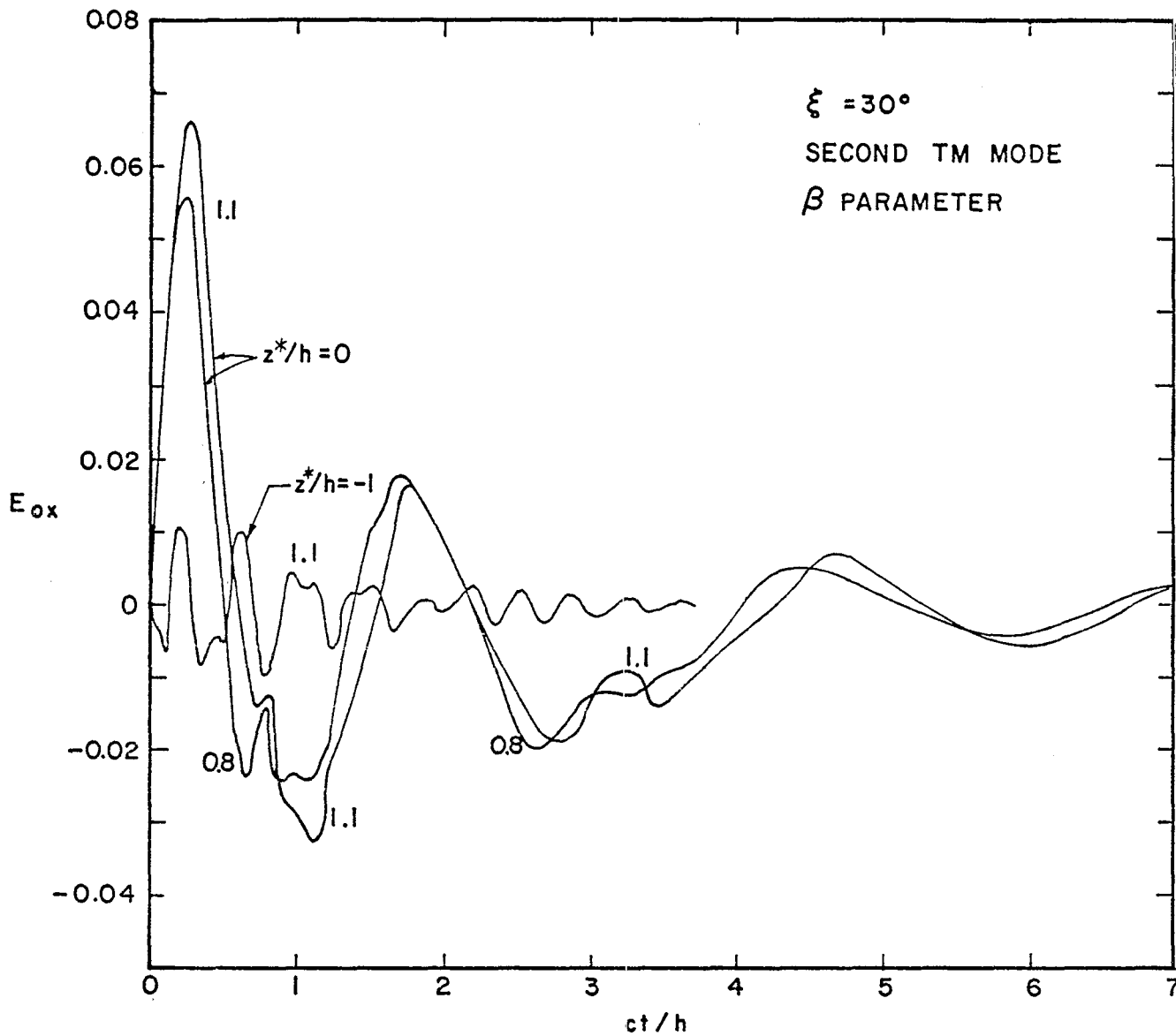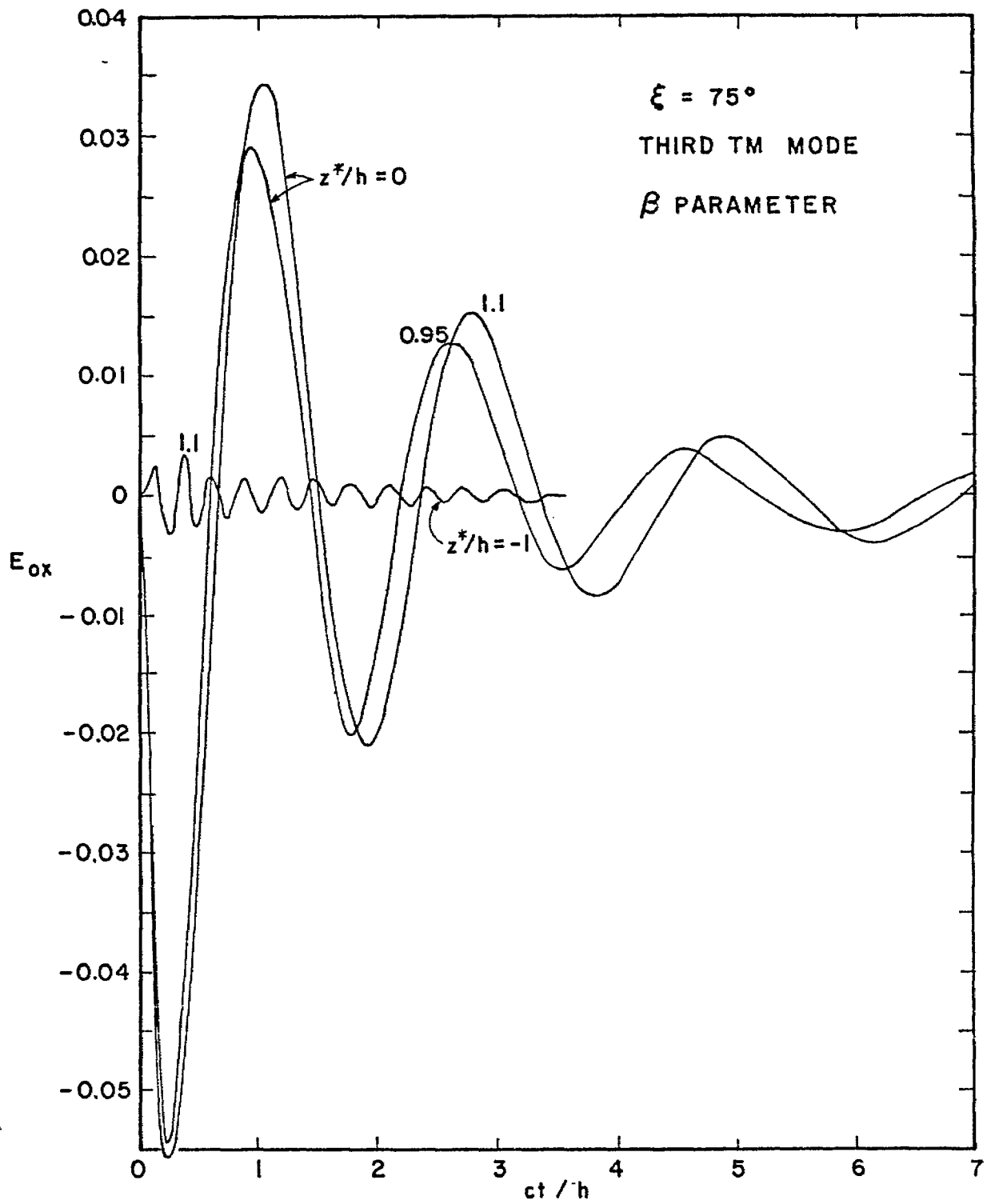
FIGURE 40

FIGURE 41

73

FIGURE 42

FIGURE 43

75
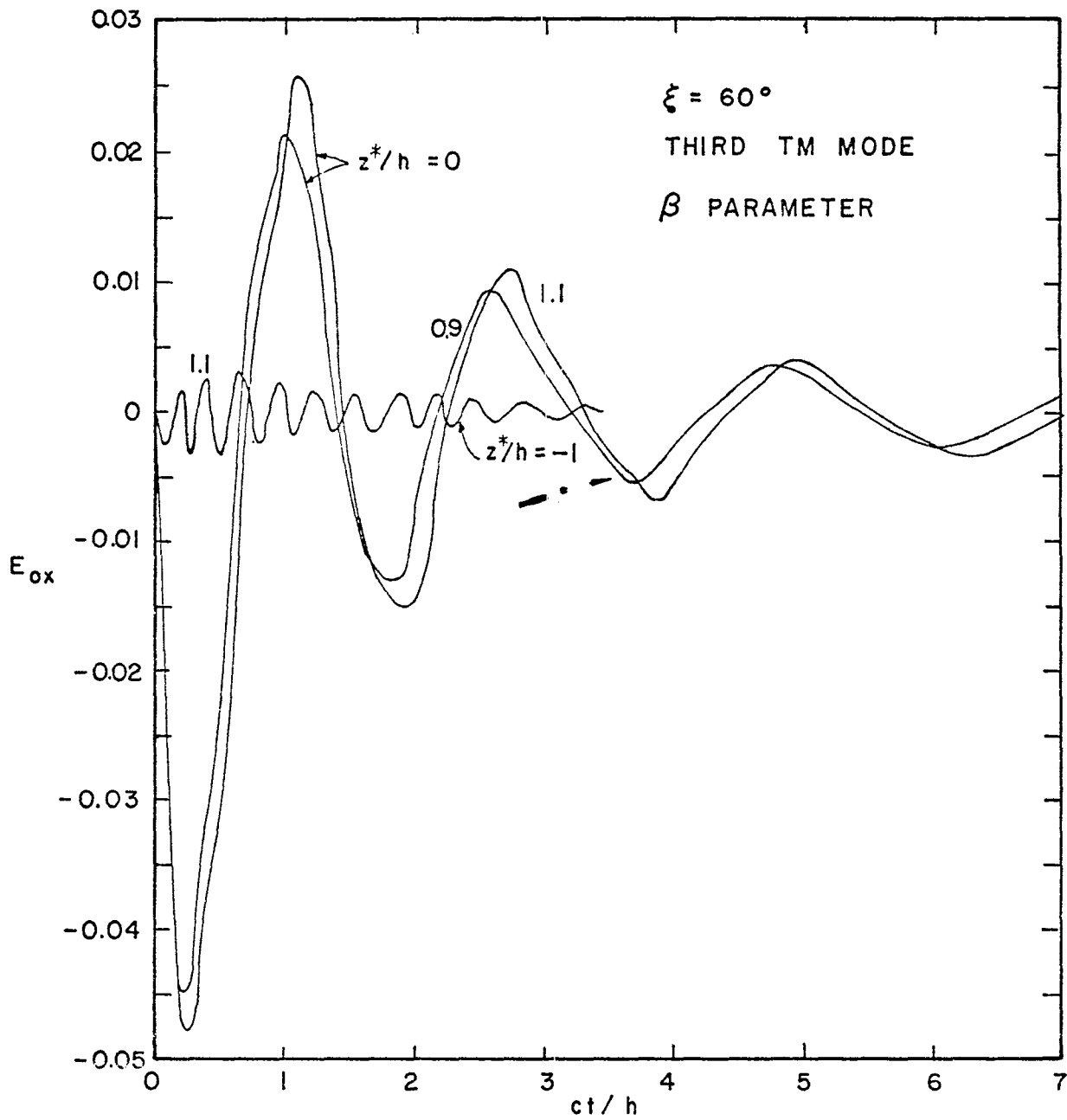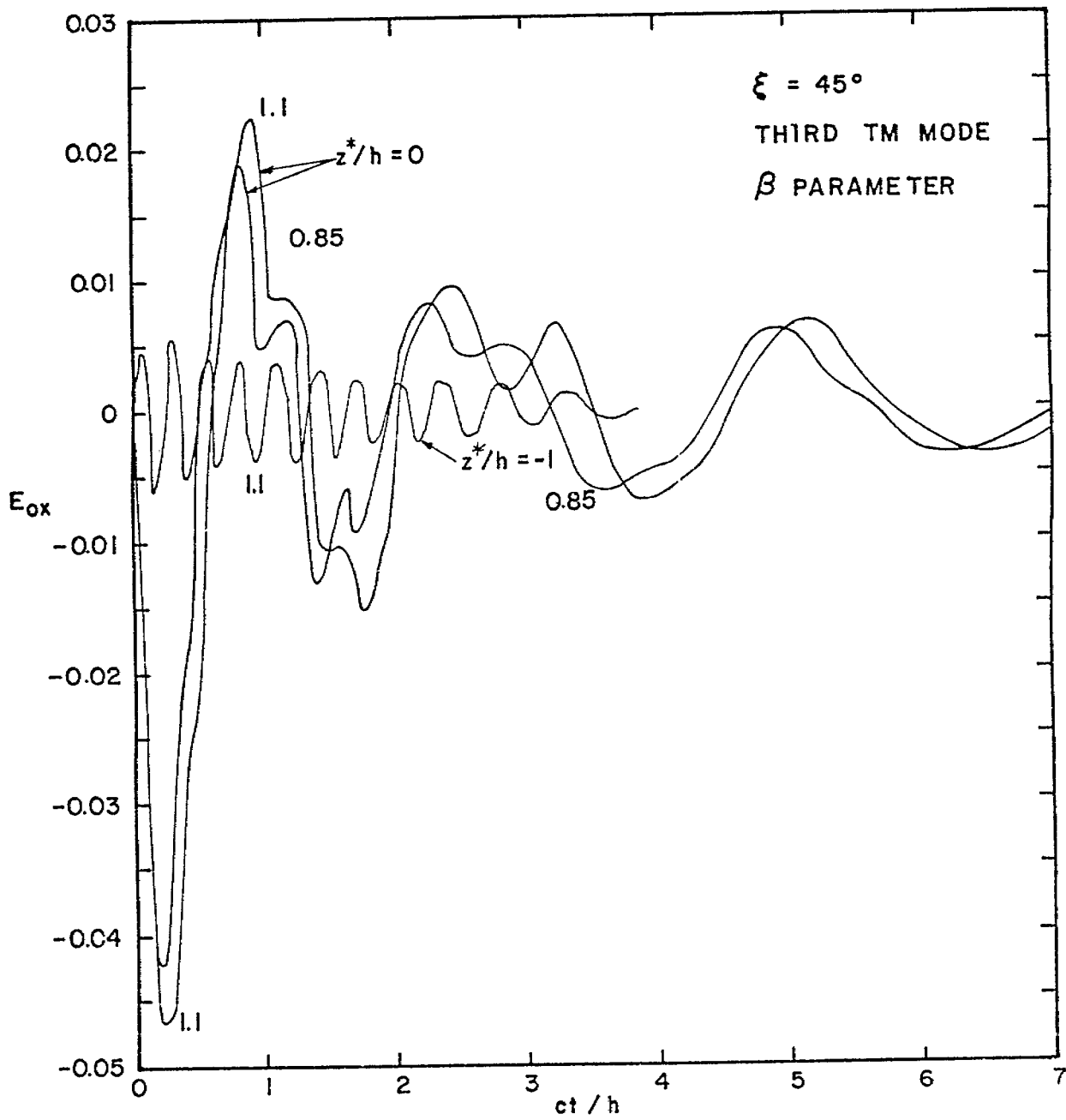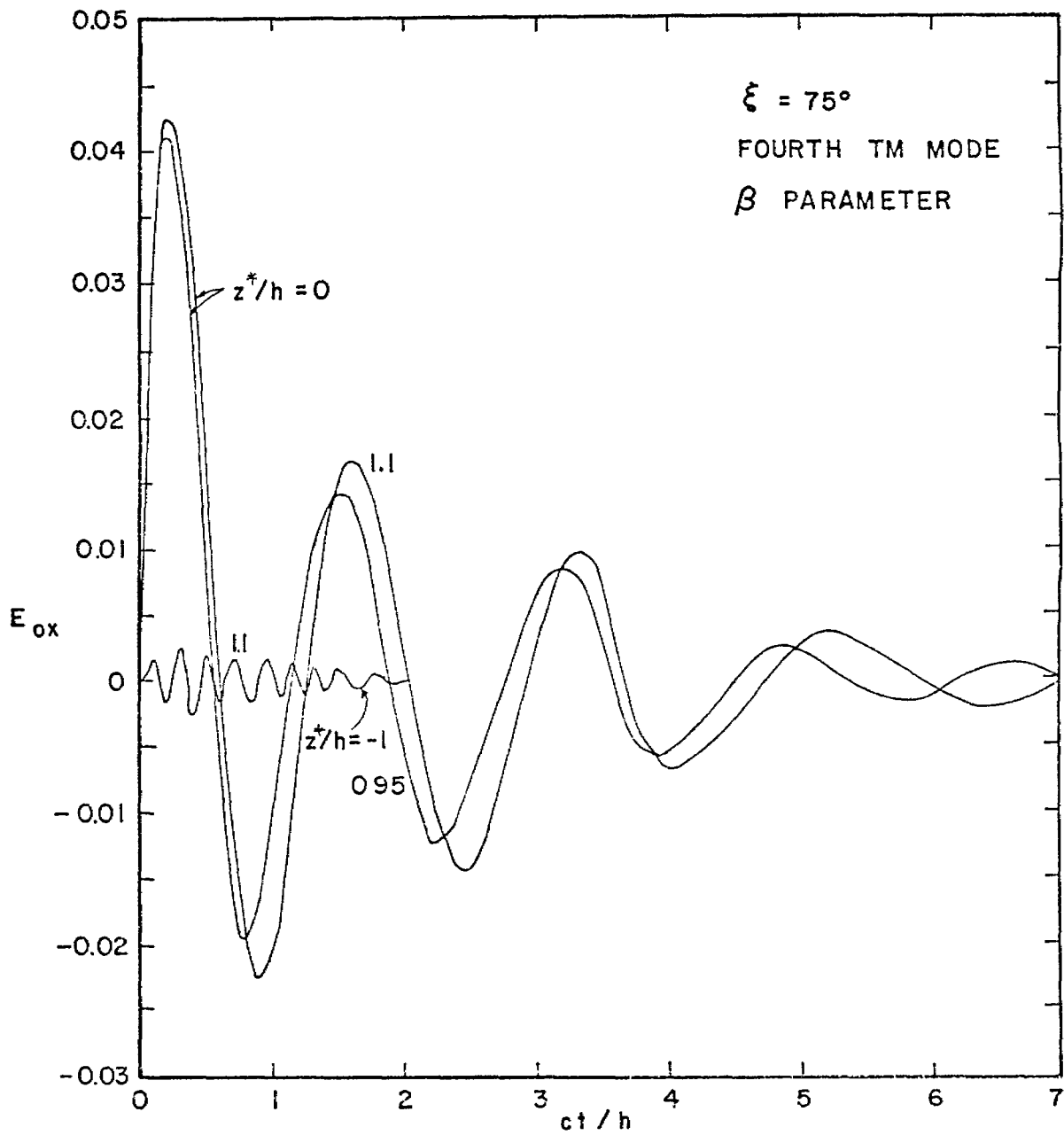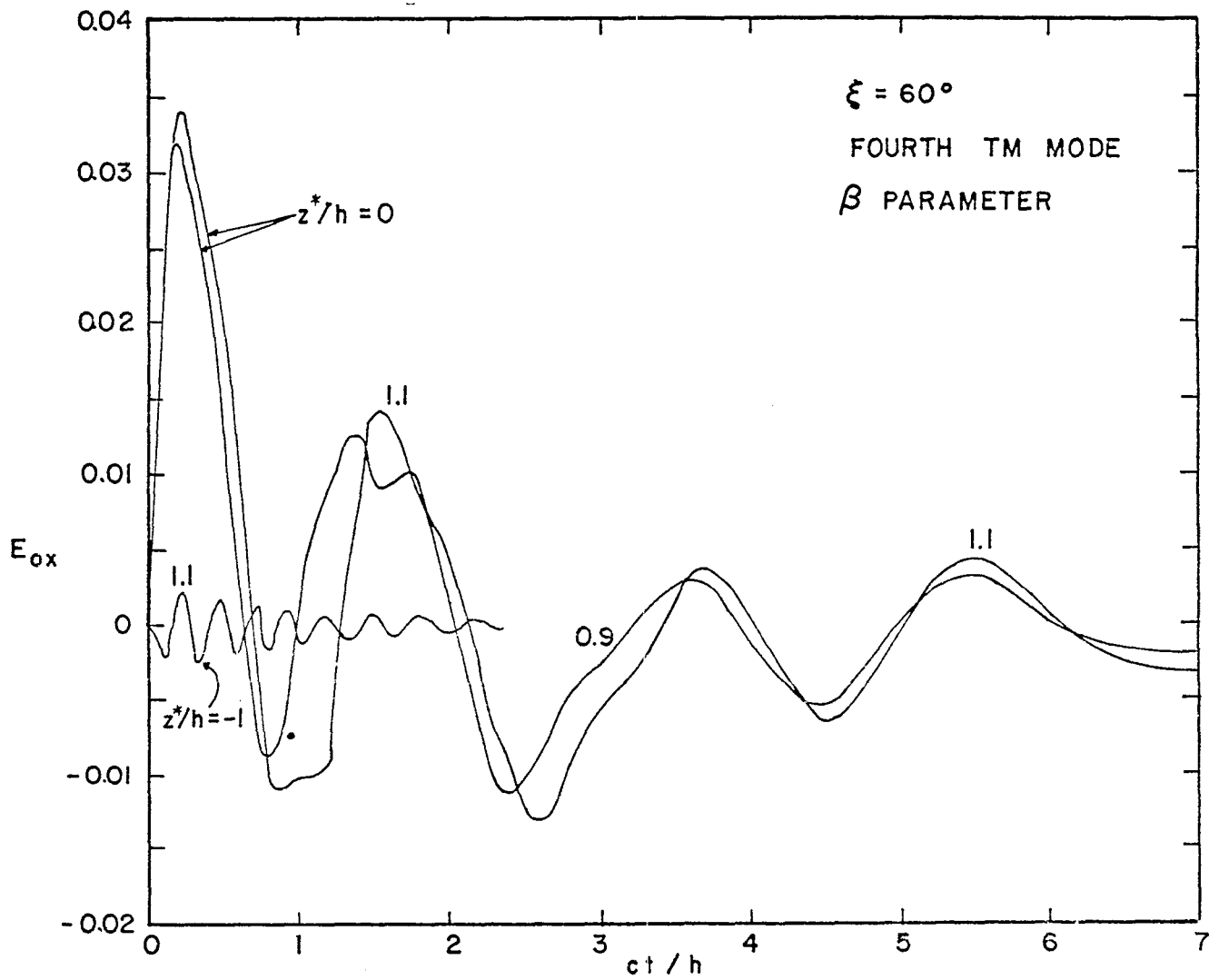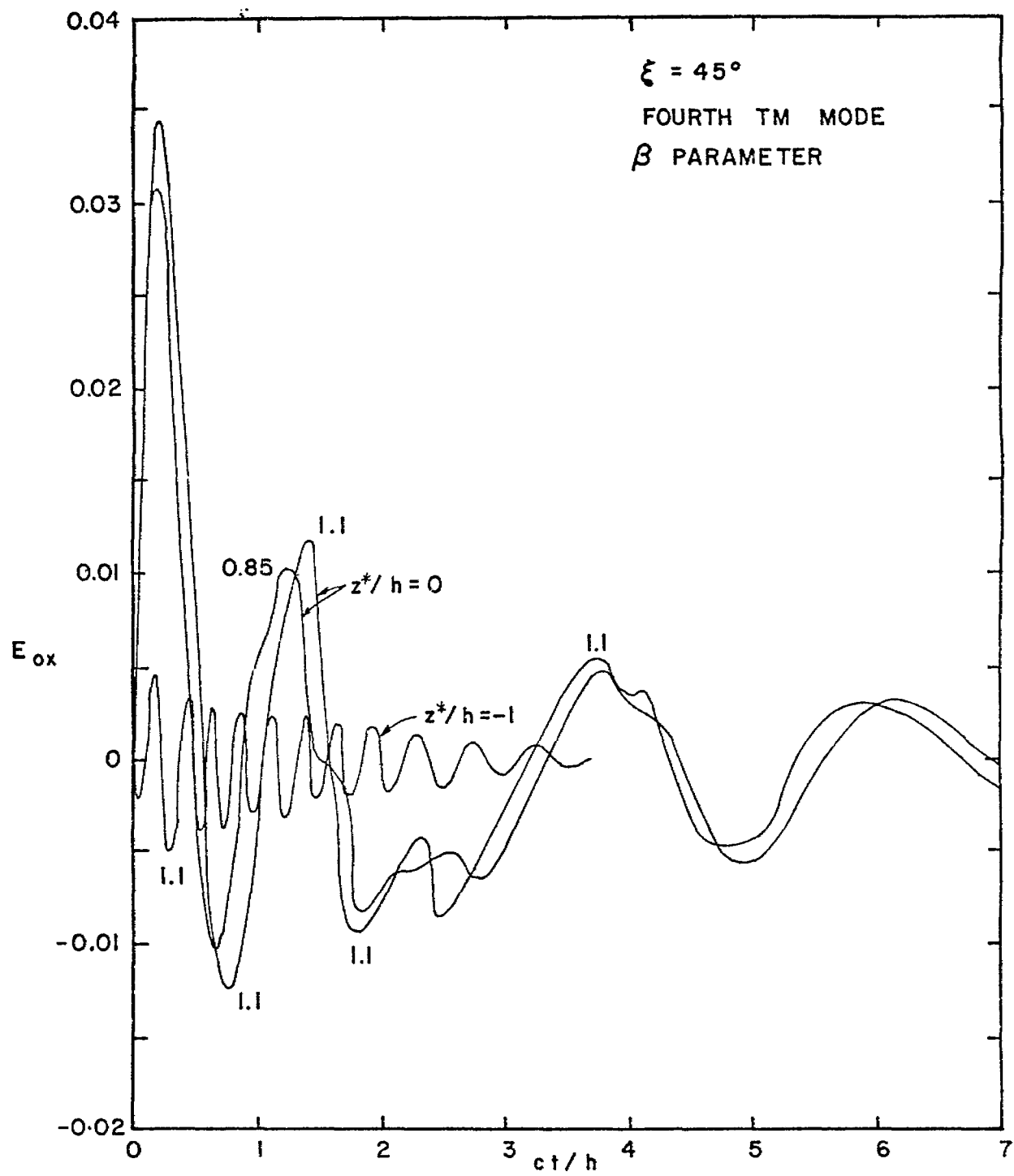
FIGURE 44

FIGURE 45

FIGURE 46
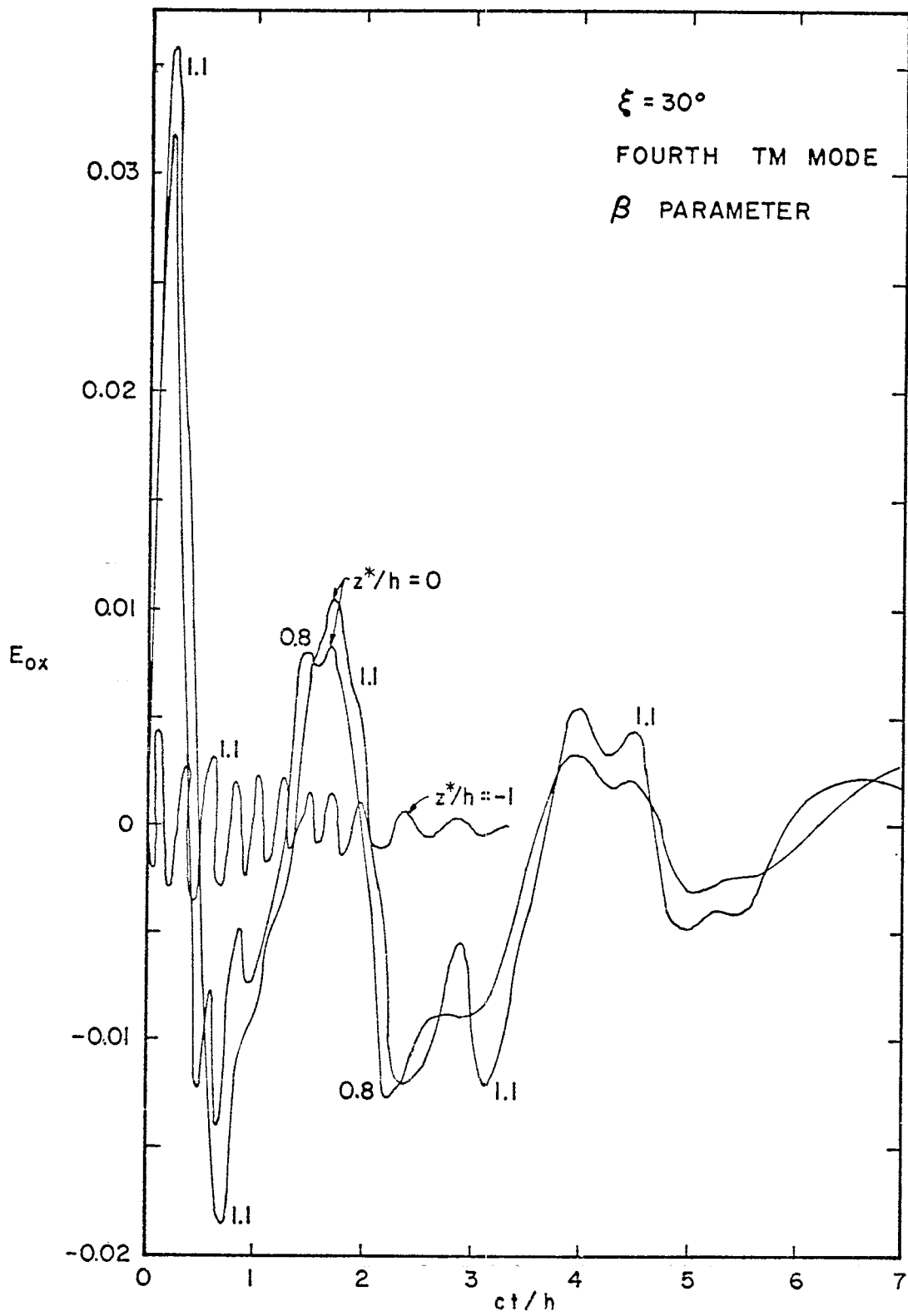
FIGURE 47

FIGURE 48

80

$$L / \mu_o h = \beta \sin \xi$$
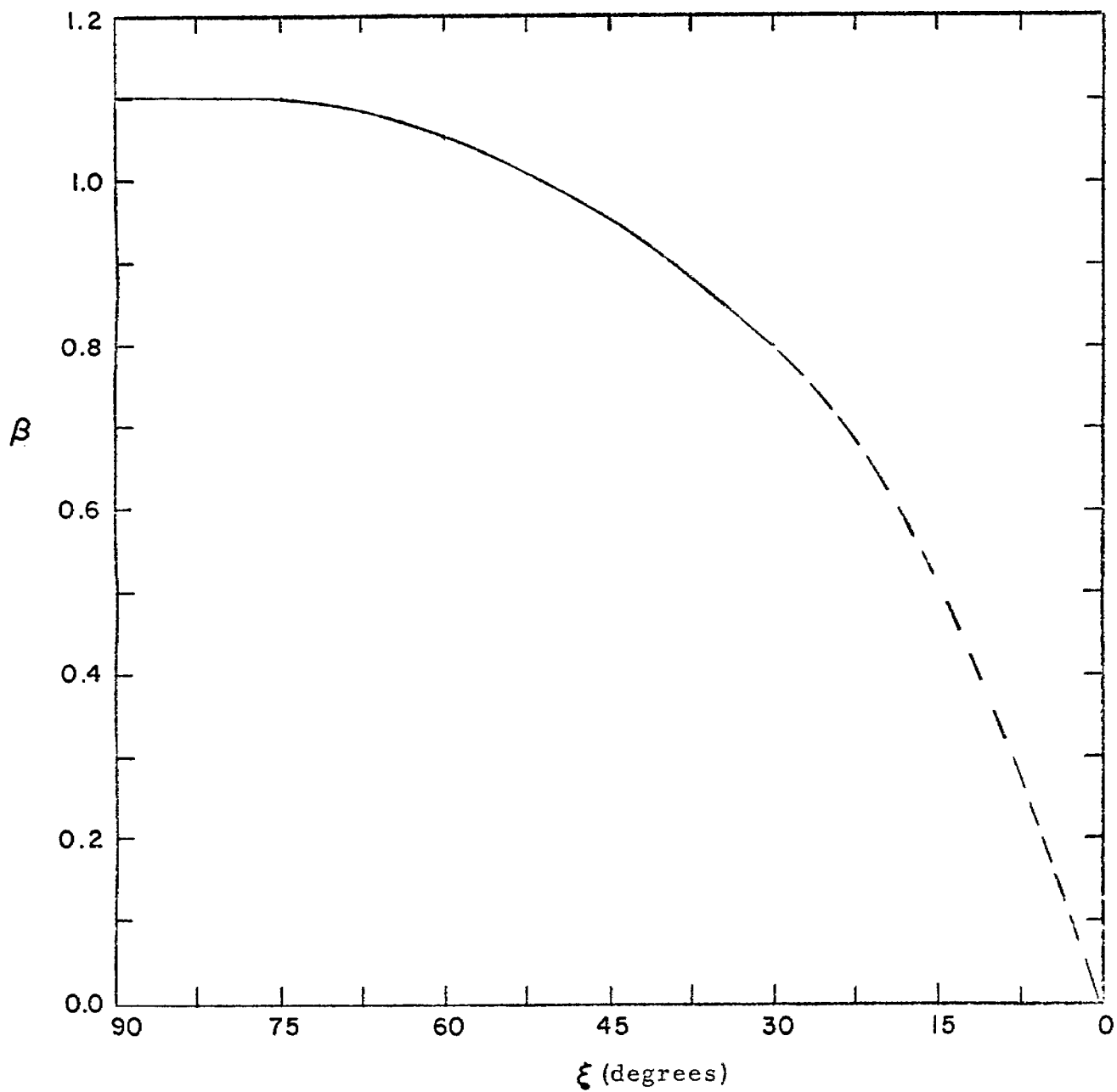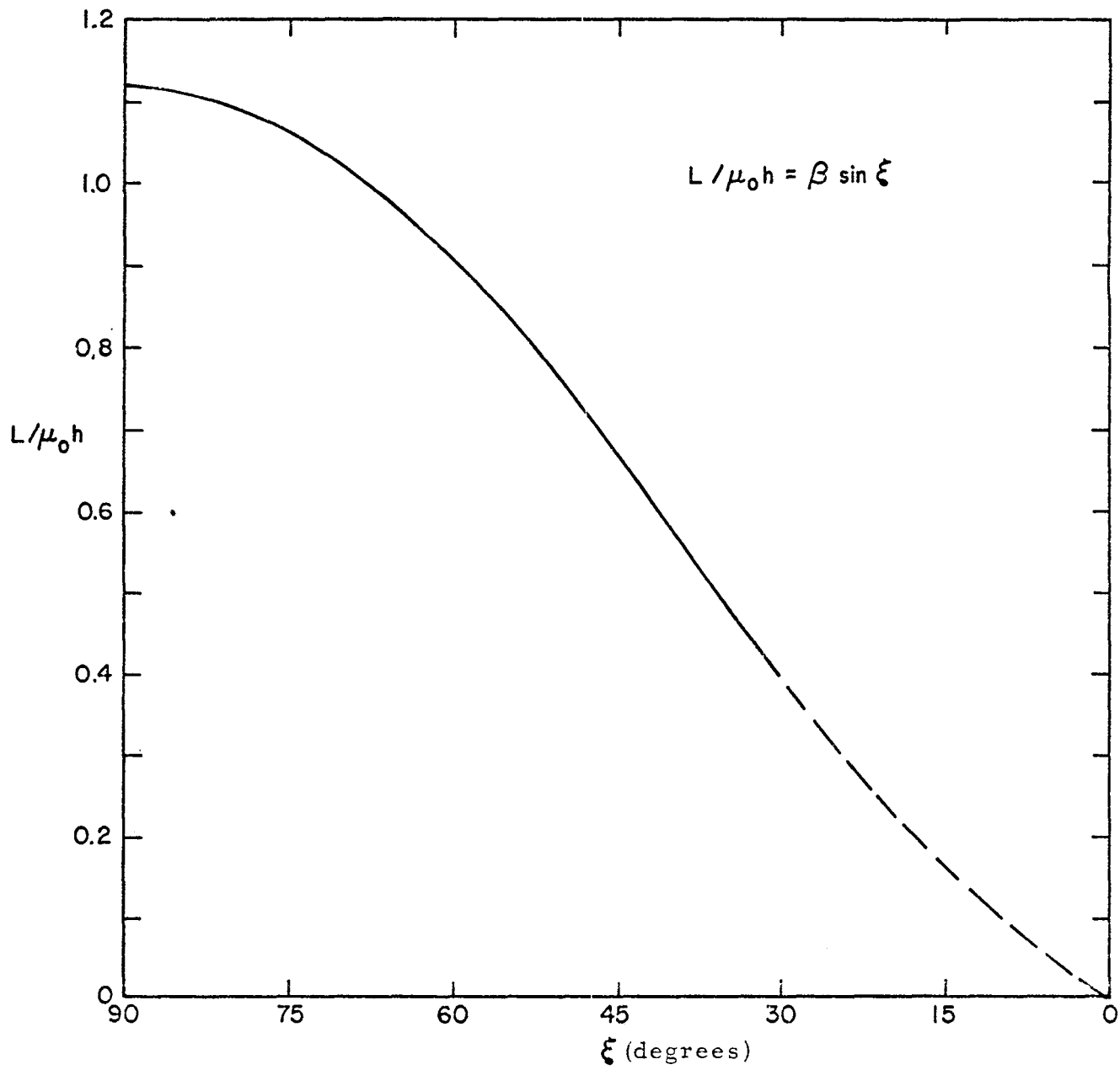
FIGURE 49

Acknowledgement

82

References

1. A. D. Varvatsis and M. I. Sancer, "Performance of an Admittance Sheet plus Coplanar Flanges as a Matched Termination of a Two-Dimensional Parallel-Plate Transmission Line, I. Perpendicular Case," Sensor and Simulation Note 163, January 1973.

2. Carl E. Baum, "A Sloped Admittance Sheet Plus Coplanar Conducting Flanges as a Matched Termination of a Two-Dimensional Parallel-Plate Transmission Line," Sensor and Simulation Note 95, December 1969.

3. R. W. Latham and K. S. H. Lee, "Termination of Two Parallel Semi-Infinite Plates by a Matched Admittance Sheet," Sensor and Simulation Note 68, January 1969.